EFFECTIVE FIELD THEORY FOR TOP QUARK PHYSICS

BY

CEN ZHANG

DISSERTATION

Submitted in partial fulfillment of the requirements
for the degree of Doctor of Philosophy in Physics
in the Graduate College of the
University of Illinois at Urbana-Champaign, 2011

Urbana, Illinois

Doctoral Committee:

Professor Tony Liss, Chair
Professor Scott Willenbrock, Director of Research
Professor John Stack
Research Associate Professor Timothy Stelzer

Abstract

The top quark plays an important role in the search for physics beyond the standard model because of its large mass. In the situation where new physics exist at an energy scale higher than the scale we can probe directly, it is desirable to have a model-independent approach, which we can use to parametrize and to constrain possible new physics. In this dissertation an effective-field-theory approach to top quark physics is suggested. In this approach, the leading effects of new physics at relatively low energy scale is parametrized by effective operators which have mass dimension six.

We first consider top-quark decay, single top production, and top-quark pair production in hadron colliders. We classify all dimension-six operators and identify 15 operators that contribute to these processes. We compute the deviation from the standard model induced by these operators. The results provide a systematic way of searching for (or obtaining bounds on) physics beyond the standard model.

We then turn to precision electroweak experiments. We study the effect of one dimension-six operator involving the top quark and the electroweak gauge bosons on precision electroweak data via a top-quark loop. We demonstrate the renormalizability, in the modern sense, of the effective field theory. We use the oblique parameter $\hat{U}$ to bound the coefficient of this operator, and compare with the bound derived from measurements on top-quark decay.

Finally, we extend this analysis to include 8 dimension-six operators which generate anomalous interactions among the electroweak gauge bosons and the top quark. We calculate their corrections to all major precision electroweak observables. The corrections are compared with data to obtain constraints on these operators.

To my parents.

Acknowledgments

First I would like to thank my advisor, Scott Willenbrock, for his direction throughout my thesis research. I also wish to thank my committee members, Tony Liss, John Stack and Timothy Stelzer, who offered guidance and support.

This project would not have been possible without the support of many people. I would like to thank Jon Thaler and Alessandro Strumia, for helpful guidance on the project. I would like to thank my colleagues, Nicolas Greiner, Harrison Mebane, and Céline Degrande, for invaluable discussion and assistance in carrying out many calculations. I am grateful for correspondence with Tim Tait, Bohdan Grzadkowski, J. Drobnak and J. Serra.

I would also like to thank the University of Illinois Graduate College for providing me with the financial means to complete this project.

This work is supported in part by the U. S. Department of Energy under contracts No. DE-FG02-91ER40677.

Table of Contents

List of Tables

List of Figures

List of Abbreviations

SM	Standard Model
VEV	Vacuum expectation value
EWSB	Electroweak symmetry breaking
LHC	Large Hadron Collider
PEWM	Precision electroweak measurements
EOM	Equation of motion

Chapter 1

Introduction

More than a century of experimental results and theoretical progress have led us to the formulation of an elegant and compact theory of the fundamental interactions among particles: the standard model (SM). It reproduces a huge amount of experimental data, spanning several orders of magnitude in energy. The electromagnetic, weak and strong forces are all described in the same mathematical framework of gauge theories. The electromagnetic and weak interactions are associated to the $SU(2)_L \times U(1)_Y$ gauge symmetry, which is then spontaneously broken by the vacuum expectation value (VEV) of the Higgs field, at the TeV scale. All massive particles acquire masses from the VEV of the Higgs boson.

The SM of particle physics, while giving an extremely economical description of the electroweak symmetry breaking (EWSB), does not explain the origin of the symmetry breaking. A common puzzle in the SM is the so-called hierarchy problem, which reduces to the question of "why is the Higgs boson so light?", because naturally one would expect that the Higgs boson would receive radiative corrections that push its mass up to the Planck scale. For this reason, it is a general belief that new states which couple to the SM states exist at the TeV scale. Fortunately, with the recent turn-on of CERN's Large Hadron Collider (LHC), searches for new physics at the TeV scale becomes possible.

1.1 Top Quark as a Probe of New Physics

Top quark physics is among the central physics topics at the Tevatron and it will remain so at the LHC in the next few years. Searching for new physics beyond the SM in observables involving the top quark is strongly motivated for several reasons:

- The top quark Yukawa coupling is expected to be enhanced compared to those of lighter fermions. In the SM, all fermions acquire mass through the Yukawa interaction, which describes the coupling between the fermions and the Higgs sector. The top quark, being the heaviest particle, is the only particle with Yukawa coupling $y \approx 1$ among all the SM fermions. This implies that any new physics which is responsible for EWSB is expected to couple strongly to the top quark, leading to many events

where top quarks are produced in association with new physics.

- The largest contribution to the quadratic divergence of the SM Higgs mass comes from the top quark loop. This implies the immediate need for new physics at the TeV scale to solve the hierarchy problem. One example is the scalar partner of the top quark in supersymmetry.

- The top quark is the only "bare" quark whose spin information can be measured from its decay products. An important property of the top is that it decays before hadronization (with a lifetime of 10^{-25}s which is an order of magnitude smaller than the hadronization lifetime of 10^{-24}s). This offers the opportunity to explore the properties of a "bare quark", such as its spin, mass, and couplings.

For the above reasons, the top quark plays a special role in searches for new physics beyond the SM.

While the current existing bounds do not forbid the existence of new degrees of freedom that are within the kinematical reach of the LHC, it is important to consider also the possibility that these states are heavier and cannot be produced on shell. In this case new degrees of freedom enter only at the virtual level to modify the interactions among the SM particles, especially the top quarks. Perhaps the most well known example for such effects is the forward-backward asymmetry ($A_{\rm FB}$) measurement at the Tevatron. In this experiment, top quark pairs produced in proton-antiproton collisions are observed to be produced preferentially in the forward hemisphere. The $A_{\rm FB}$ is predicted in the SM only from higher order QCD contributions, but the data exceed the predictions by a few standard deviations. This is possibly the first hint for new physics in the top sector.

When considering physics beyond the SM, there are often two choices. One can study a particular extension of the SM, or one can take a model-independent approach. The latter is mostly useful in the situation where the new heavy states are beyond the energy region of the LHC and reveal themselves only as anomalous interactions among the SM particles. A model-independent approach to physics beyond the SM is useful in two respects. First, it allows one to search for new physics without committing to a particular extension of the SM. Second, in the case that no new physics should appear, it allows one to quantify the accuracy with which the new physics is excluded.

A common task for anyone considering physics beyond the SM is making sure that the proposed new physics is consistent with current experimental bounds. An important subset of accurate data is the so-called precision electroweak measurements (PEWM). This contains some low-energy data such as deep inelastic scattering and atomic parity violation, a few dozens of observables at the Z pole, and the LEP2 data on e^+e^- scattering at various center-of-mass energies between the Z mass and 209 GeV. In this energy range, new heavy states could not be produced directly, and a model-independent approach is again useful. The

anomalous interactions involving top quark can have effects on the PEWM, because the top quark also plays an important role as a virtual particle in precision electroweak physics. Indeed, the correct range for the top quark mass was anticipated by precision electroweak studies. Now that the top quark mass is accurately known from direct measurements, the constrains from the PEWM can be converted into bounds on anomalous top quark couplings. In order to do this, a model-independent approach in which radiative corrections can be consistently carried out is needed.

1.2 Effective Field Theory

Having seen the need for a model-independent approach to describe new physics involving top quark, now the question is: what are the candidates for this approach?

When contempting a model-independent approach to physics beyond the SM, there are a number of desirable features that one should incorporate:

- Any extension of the standard model should satisfy the S-matrix axioms of unitary, analyticity, *etc.*.
- The symmetries of the standard model, namely Lorentz invariance and $SU(2)_L \times U(1)_Y$ gauge symmetry, should be respected.
- It should be possible to recover the standard model in an appropriate limit.
- The extended theory should be general enough to capture any physics beyond the standard model, but should give some guidance as to the most likely place to see the effects of new physics.
- It should be possible to calculate standard-model radiative corrections in the extended theory.
- It should be possible to calculate radiative corrections involving the new interactions of the extended theory.

The unique way to incorporate all of these features is via an effective quantum field theory. The first two features alone indicate a quantum field theory. The remaining features are captured by an effective quantum field theory [1, 2].

In an effective quantum field theory, heavy particles are "integrated out", leaving nonlocal interactions from virtual heavy-particle exchange. These interactions are then replaced with a set of local interactions, constructed to give the same physics at low energies. These interactions are suppressed by inverse power of the masses of the heavy particles. In this process, we have modified the high energy behavior of the theory,

so the effective theory is only a valid description of the physics at energies below the masses of the heavy particles.

An example of this approach is displayed in fig. 1.1, in the context of a Z' boson. At energies above the mass of the Z', one observes the new particle directly. At energies below the mass of the Z', one observes non-local interactions of SM fermions mediated by the exchange of a virtual Z' boson. At energies much less than the Z' mass, the leading effect appears as an effective four-fermion interaction.

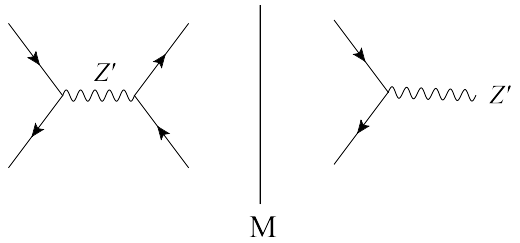

Figure 1.1: At energies greater than the Z' mass, one observes the new particle directly. At energies below the Z' mass, one observes its effects on SM particles indirectly.

Let us attach a coupling g to the Z' interaction with the SM fermions, and include the Z' propagator, proportional to $(p^2 - M^2)^{-1}$. At energies much less than the Z' mass, we can expand the propagator in p^2/M^2:

$$\frac{1}{p^2 - M^2} = -\frac{1}{M^2}\left[1 + \frac{p^2}{M^2} + \left(\frac{p^2}{M^2}\right)^2 + \cdots\right] \tag{1.1}$$

Each term in the bracket can be mimicked by a local interaction. The leading term is generated by an effective four-fermion interaction with strength g^2/M^2. Terms of higher order in p^2/M^2 can be generated by interactions involving more derivatives, with higher mass dimension. At leading order, the theory is described by the Lagrangian

$$\mathcal{L}_{\mathit{eff}} = \mathcal{L}_{\rm SM} + \frac{g^2}{M^2}\bar{\psi}\psi\bar{\psi}\psi \, . \tag{1.2}$$

This effective Lagrangian can be viewed as a description of new physics, at energy below the mass of the heavy state, M.

The principle behind the effective field theory is to take advantage of scale separation. The effects of large energy scales, or short distance scales, are suppressed by powers of the ratio between the scale of the problem and the large energy scale. This observation follows from many other fields in physics. For example, one does not worry about the sizes of planets, when studying orbital motions in the solar system. Similarly, the hydrogen spectrum can be calculated quite precisely without knowing that there are quarks and gluons inside the proton. In fact, we are so used to this idea that we can use it without thinking about it. However, in a relativistic, quantum mechanical theory, in which particles are created and destroyed, the construction

of an effective field theory is particularly useful, because among the short-distance features that can be ignored in an effective theory are all the particles too heavy to be produced. Eliminating heavy particles from the effective theory produces an enormous simplification.

Decoupling of large energy scales in field theory seems to be complicated by the fact that integration over loop momenta involves all scales. However, this is only a superficial obstacle which is straightforward to deal with in a convenient regularization scheme, for example dimensional regularization. The decoupling of large energy scales takes place in renormalizable quantum field theories whether or not techniques of effective field theory are used. In fact, the decoupling of heavy states is the reason for building high-energy accelerators. If quantum field theory were sensitive to all energy scales, it would be much more useful to increase the precision of low-energy experiments instead of building large colliders.

If we knew the complete theory of the new physics at high energy, we could work our way down to the low energy effective theory in a systematic way, by eliminating the heavy states at different energy scales from the theory. This is a "top down" approach to effective field theory. In practice, however, we do not know what the new physics is, but we do know the low energy limit of any correct theory must be the SM. It is then more useful to look at the theory from the "bottom up" view. In this view, an effective quantum field theory of the SM is constructed as follows. The SM is the most general theory of quarks, leptons, and Higgs fields interacting via an $SU(3)_C \times SU(2)_L \times U(1)_Y$ gauge symmetry, where all operators (that is, products of fields) in the Lagrangian are restricted to be of mass dimension four or less.[1] To extend the theory, add operators of higher dimension. By dimensional analysis, these operators have coefficients of inverse powers of mass, and hence are suppressed if this mass is large compared with the experimentally-accessible energies. We denote this mass scale by Λ, which is the analogue of M in Eq. (1.2), and can be regarded as the scale of the new physics. The effect of physics above scale Λ, is then described by a tower of operators, with mass dimension from two to infinity, beginning with conventional renormalizable interactions but going on to include nonrenormalizable interactions of arbitrarily high dimension.

At this point, the reader may start to worry about the renormalizability of an effective field theory. In particular, in the PEWM, the top quark enters only as a virtual particle, therefore how do we make sense of any loop calculation, if the theory contains nonrenormalizable interactions? The answer to this question is that only a finite number of terms need to be kept, because the theory only needs to reproduce experiments to finite accuracy. The higher the dimension of an operator, the smaller its contribution to low-energy experiments. Hence, obtaining results to a given accuracy requires a finite number of terms. This is the reason why nonrenormalizable theories are as good as renormalizable theories. In real calculations, only the

[1] In practice all operators, except the quadratic term in the Higgs potential, are of dimension four.

leading terms in $1/\Lambda$ are kept. Although an effective field theory is not renormalizable in the old-fashioned sense, it is renormalizable at any order in $1/\Lambda$, provided that all the pertinent operators are included [3]. In practice, one also needs to be careful when choosing a regularization scheme, because this may introduce new heavy masses which destroy the dimensional analysis. As we will see, the use of dimensional regularization with minimal subtraction ($\overline{\rm MS}$) in loop calculations will avoid such problems. A complete review on this subject may be found in [4].

All operators of higher dimension are expected to satisfy the $SU(3)_C \times SU(2)_L \times U(1)_Y$ gauge symmetry of the SM. With this requirement, there is only one dimension-five operator, and it is responsible for generating Majorana masses for neutrinos [5]. This operator is therefore irrelevant for our purpose. A complete list of dimension-six operators was first given in [6, 7, 8]. Subsequently it was found that several of this operators are not independent [9, 10]. A list of 59 independent dimension-six operators was recently given in [11].[2] In addition, we show in Appendix A that only even-dimensional operators can conserve lepton and baryon number. Therefore we can drop all the odd-dimensional operators, and the expansion parameter in an effective field theory is actually $1/\Lambda^2$.

The effective field theory of the SM can be written as

$$\mathcal{L}_{\mathit{eff}} = \mathcal{L}_{\rm SM} + \sum_i \frac{C_i}{\Lambda^2} \mathcal{O}_i^{(6)} + \cdots \tag{1.3}$$

where $\mathcal{O}_i^{(6)}$ are the dimension-six operators, and the ellipsis indicates the higher-dimension operators. The coefficients C_i are dimensionless, and parametrize the unknown interactions. Referring to our list of desirable features above, we see that the SM is recovered in the limit $\Lambda \to \infty$. Since any new physics will look like a quantum field theory at low energies, the effetive field theory is general enough to capture the low-energy effects of any physics beyond the standard model, as long as we include all possible terms consistent with the symmetries of the theory. However, by dimensional analysis we expect the dimension-six operators to be dominant, so the theory provides some guidance as to the most likely place to see the effects of new physics.[3] Finally, the extended theory can be used to calculate both tree-level and loop processes [3].

It is the dimension-six operators that we will focus on throughout this dissertation. We neglect any operators with dimension equal or higher than eight, and only keep the leading $1/\Lambda^2$ terms. Although there is a large number of dimension-six operators, typically only a few contribute to a given physical process at this order. To study the top quark physics, all operators that do not involve a top quark field can be

[2] There are 59 operators for one generation of fermions. For more generations, the number of four-fermion operators increases dramatically. For a list of four-fermion operators including three generations, see [12].

[3] For some physical processes, operators of dimension seven or greater may be dominant, and can be included.

ignored. As we will see, at leading order there are 15 operators which contribute to processes involving top quarks in hadron colliders. As for the PEWM, the number of pertinent operators is 9. Finally, because no dimension-seven operator can contribute to the leading order, the error induced by keeping only the leading correction is of order E^2/Λ^2, where E is the energy scale of the problem.

The dissertation is organized as follows: In Chapter 2, I classify the important dimension-six operators in hadron colliders, and study their effects on top quark production and decay. In Chapter 3, I focus on one operator which modifies the SM coupling between the top quark and the W boson, and study its loop effects on the PEWM. In particular, I compare the constraints on this operator obtained from hadron collider and from the PEWM. In Chapter 4, the study of PEWM is extended to include more dimension-six operators of the top quark, and constraints on 8 operators are obtained.

Chapter 2

Effective Field Theory for Top Quark Production and Decay[1]

The effective-field-theory approach to top quark production and decay is not a new approach. The effects of some dimension-six operators in certain processes are studied by different groups. This Chapter is devoted to a more complete and systematic study on this subject. We will consider the effects of all dimension-six operators on top quark interactions at hadron colliders. We focus on three different processes: top quark decay, single top production, and top pair production. The coefficients of dimension-six operators are used to parametrize the new physics. If experiments favor a non-zero coefficient, we should consider it as a hint to new physics. On the other hand, if no deviation from SM is observed experimentally, then one can place bounds on these coefficients. The effects of non-standard interactions on top-quark physics at linear colliders and photon colliders can be found in Refs. [14, 15, 16, 17].

We use the operator set introduced by Buchmuller and Wyler [6]. In their paper, they categorize all possible gauge-invariant dimension-six operators, and use the equations of motion (EOMs) to simplify them into 80 independent operators (for one generation of fermions). Subsequently it was found that several of these operators are actually not independent. A list of 59 independent dimension-six operators was recently given in [11]. We focus on the operators that have an influence on the top quark.

The leading modification to SM processes is expected to be of order $\frac{1}{\Lambda^2}$. In this dissertation we do not consider any higher order contributions. The scale Λ is larger than the scale we can probe directly, so $\frac{1}{\Lambda^4}$ contributions should be small compared to the uncertainty on top quark measurements. Hence we ignore all dimension-eight and higher operators, as well as effects involving two dimension-six operators.

For any physical observable, the $\frac{1}{\Lambda^2}$ contribution comes from the interference between dimension-six operators and the SM Lagrangian. This contribution might be suppressed for a variety reasons. For example, since all quark and lepton masses are negligible compared to the top quark mass, a new interaction that involves a right-handed quark or lepton (except for the top quark) has a very small interference with the SM charged-current weak interactions, which only involve left-handed fermions. It turns out that although there are a large number of dimension-six operators, only a few of them have significant effects at order $\frac{1}{\Lambda^2}$.

[1] The work presented in this Chapter is published in Ref. [13].

We list these operators in Tables 2.1 and 2.2.

operator	process
$O_{\phi q}^{(3)} = i(\phi^+ \tau^I D_\mu \phi)(\bar{q}\gamma^\mu \tau^I q)$	top decay, single top
$O_{tW} = (\bar{q}\sigma^{\mu\nu}\tau^I t)\tilde{\phi} W_{\mu\nu}^I$ (with real coefficient)	top decay, single top
$O_{qq}^{(1,3)} = (\bar{q}^i \gamma_\mu \tau^I q^j)(\bar{q}\gamma^\mu \tau^I q)$	single top
$O_{tG} = (\bar{q}\sigma^{\mu\nu}\lambda^A t)\tilde{\phi} G_{\mu\nu}^A$ (with real coefficient)	single top, $q\bar{q}, gg \to t\bar{t}$
$O_G = f_{ABC} G_\mu^{A\nu} G_\nu^{B\rho} G_\rho^{C\mu}$	$gg \to t\bar{t}$
$O_{\phi G} = \frac{1}{2}(\phi^+\phi) G_{\mu\nu}^A G^{A\mu\nu}$	$gg \to t\bar{t}$
7 four-quark operators	$q\bar{q} \to t\bar{t}$

Table 2.1: CP-even operators that have effects on top-quark processes at order $1/\Lambda^2$. Here q is the left-handed quark doublet, while t is the right-handed top quark. The field ϕ ($\tilde{\phi} = \epsilon\phi^*$) is the Higgs boson doublet. $D_\mu = \partial_\mu - ig_s \frac{1}{2}\lambda^A G_\mu^A - ig\frac{1}{2}\tau^I W_\mu^I - ig' Y B_\mu$ is the covariant derivative. $W_{\mu\nu}^I = \partial_\mu W_\nu^I - \partial_\nu W_\mu^I + g\epsilon_{IJK} W_\mu^J W_\nu^K$ is the W boson field strength, and $G_{\mu\nu}^A = \partial_\mu G_\nu^A - \partial_\nu G_\mu^A + g_s f^{ABC} G_\mu^B G_\nu^C$ is the gluon field strength. Because of the Hermiticity of the Lagrangian, the coefficients of these operators are real, except for O_{tW} and O_{tG}. The operator $O_{\phi q}^{(3)}$ with an imaginary coefficient can be removed using the EOM.

operator	process
$O_{tW} = (\bar{q}\sigma^{\mu\nu}\tau^I t)\tilde{\phi} W_{\mu\nu}^I$ (with imaginary coefficient)	top decay, single top
$O_{tG} = (\bar{q}\sigma^{\mu\nu}\lambda^A t)\tilde{\phi} G_{\mu\nu}^A$ (with imaginary coefficient)	single top, $q\bar{q}, gg \to t\bar{t}$
$O_{\tilde{G}} = f_{ABC} \tilde{G}_\mu^{A\nu} G_\nu^{B\rho} G_\rho^{C\mu}$	$gg \to t\bar{t}$
$O_{\phi\tilde{G}} = \frac{1}{2}(\phi^+\phi)\tilde{G}_{\mu\nu}^A G^{A\mu\nu}$	$gg \to t\bar{t}$

Table 2.2: CP-odd operators that have effects on top-quark processes at order $1/\Lambda^2$. Notations are the same as in Table 1, and $\tilde{G}_{\mu\nu} = \epsilon_{\mu\nu\rho\sigma} G^{\rho\sigma}$.

In Table 2.1, only one of the four-quark operators, $O_{qq}^{(1,3)} = (\bar{q}^i \gamma_\mu \tau^I q^j)(\bar{q}\gamma^\mu \tau^I q)$, is listed explicitly. Here the superscripts i, j denote the first two quark generations, while q without superscript denotes the third generation. In single top production, this is the only (independent) four-quark operator that contributes. However, there are many other four-quark operators with different isospin and color structures [6, 7]. In the top pair production process $q\bar{q} \to t\bar{t}$, seven such operators contribute. The details are discussed in Section 2.3.

In Table 2.2, the CP-odd operators are listed. These interactions interfere with the SM only if the spin of the top quark is taken into account. The reason is that the SM conserves CP to a good approximation (the only CP violation is in the CKM matrix), and the interference between a CP-odd operator and a CP-even operator is a CP violation effect. It was shown in Ref. [18] that, in the absence of final-state interactions, any CP violation observable can assume non-zero value only if it is T_N-odd, where T_N is the "naive" time reversal, which means to apply time reversal without interchanging the initial and final states. Thus an observable is T_N-odd if it is proportional to a term of the form $\epsilon_{\mu\nu\rho\sigma} v^\mu v^\nu v^\rho v^\sigma$. If we don't consider the top quark spin, v must be the momentum of the particles, and such a term will not be present because

the reactions we consider here involve at most three independent momenta. Therefore top polarimetry is essential for the study of CP violation. Since the top quark rapidly undergoes two-body weak decay $t \to Wb$ with a time much shorter than the time scale necessary to depolarize the spin, information on the top spin can be obtained from its decay products. CP violation will be discussed in Section 2.4.

There is an argument that can be used to neglect certain operators [8]. Some new operators can be generated at tree level from an underlying gauge theory, while others must be generated at loop order. In general the loop generated operators are suppressed by a factor of $1/16\pi^2$. However, the underlying theory may not be a weakly coupled gauge theory, or the loop diagrams could be enhanced due to the index of a fermion in a large representation. Furthermore, the underlying theory may not be a gauge theory at all. Fortunately, the effective-field-theory approach does not depend on the underlying theory. We will consider all dimension-six operators, without making any assumptions about the nature of the underlying theory.

We do not make any assumptions about the flavor structure of the dimension-six operators, although we don't consider any flavor-changing neutral currents in this paper. The charged-current weak interaction of the top quark is proportional to V_{tb}, so the SM rate for top decay and single top production is proportional to V_{tb}^2. We write all dimension-six operators in such a way that all relevant couplings derived from these operators involve fields in their mass-eigenstates, so no diagonalization of the new interactions is necessary. Hence, in charged-current weak interactions, the interference between the SM amplitude and the new interaction is proportional to $V_{tb}C_i$, where C_i is the (real) coefficient of the dimension-six Hermitian operator O_i (also recall that V_{tb} itself is purely real in the standard parameterization [19]). If the operator is not Hermitian, the coefficient C_i is complex; CP-conserving processes are proportional to $V_{tb}\mathrm{Re}C_i$, while CP-violating processes are instead proportional to $V_{tb}\mathrm{Im}C_i$.

Deviations of top-quark processes from SM predictions have often been discussed using a vertex-function approach, where the Wtb vertex is parameterized in terms of four unknown form factors [20]. Given our precision knowledge of the electroweak interaction, this approach is too crude. The effective field theory approach is well motivated; it takes into consideration the unbroken $SU(3)_C \times SU(2)_L \times U(1)_Y$ gauge symmetry; it includes contact interactions as well as vertex corrections; it is valid for both on-shell and off-shell quarks; and it can be used for loop processes [3]. None of these virtues are shared by the vertex function approach [21].

The remainder of this Chapter is organized as follows. In Section 2.1 we discuss top-quark decay. In Section 2.2 we discuss single top production. Top pair production is discussed in Section 2.3. The CP-odd operators are considered in Section 2.4. Section 2.5 is conclusion.

2.1 Top Quark Decay

When the fermion masses (except for the top quark) are ignored, there are only two independent dimension-six operators in [11] that contribute to top-quark decay at leading order:

$$O_{\phi q}^{(3)} = i(\phi^+ \tau^I D_\mu \phi)(\bar{q}\gamma^\mu \tau^I q) \quad (2.1)$$

$$O_{tW} = (\bar{q}\sigma^{\mu\nu}\tau^I t)\tilde{\phi} W_{\mu\nu}^I \quad (2.2)$$

The operators $O_{\phi q}^{(3)}$ and O_{tW} modify the SM Wtb interaction. Upon symmetry breaking, they generate the following terms in the Lagrangian:

$$L_{eff} = \frac{C_{\phi q}^{(3)}}{\Lambda^2}\frac{gv^2}{\sqrt{2}}\bar{b}\gamma^\mu P_L t W_\mu^- + h.c. \quad (2.3)$$

$$L_{eff} = -2\frac{C_{tW}}{\Lambda^2} v\bar{b}\sigma^{\mu\nu} P_R t \partial_\nu W_\mu^- + h.c. \quad (2.4)$$

where $v = 246$ GeV is the vacuum expectation value (VEV) of ϕ. The operator $O_{\phi q}^{(3)}$ simply leads to a rescaling of the SM Wtb vertex by a factor of $(1 + \frac{C_{\phi q}^{(3)} v^2}{\Lambda^2 V_{tb}})$, so it does not affect any distributions, and is therefore impossible to detect in angular distributions of top-quark decays. The vertex-function approach to top-quark decay is pursued in Refs. [22, 23].

These operators interfere with the SM amplitude, as is shown in Figure 2.1. We can compute their correction to the SM amplitude. The $t \to be^+\nu$ squared amplitude is:

$$\frac{1}{2}\Sigma|M|^2 = \frac{V_{tb}^2 g^4 u(m_t^2 - u)}{2(s - m_W^2)^2} + \frac{C_{\phi q}^{(3)} V_{tb} v^2}{\Lambda^2}\frac{g^4 u(m_t^2 - u)}{(s - m_W^2)^2} + \frac{4\sqrt{2}\mathrm{Re}C_{tW} V_{tb} m_t m_W}{\Lambda^2}\frac{g^2 su}{(s - m_W^2)^2} \quad (2.5)$$

where C_i is the coefficient of operator O_i, and s, t, u are generalizations of the usual Mandelstam variables $(s = (p_t - p_b)^2, \quad t = (p_t - p_\nu)^2, \quad u = (p_t - p_{e^+})^2)$. $C_{\phi q}^{(3)}$ is real.

Using the narrow width approximation for the W boson, the differential decay rate is

$$\frac{d\Gamma}{d\cos\theta} = \left(V_{tb}^2 + \frac{2C_{\phi q}^{(3)} V_{tb} v^2}{\Lambda^2}\right)\frac{g^4}{4096\pi^2 m_t^3 m_W \Gamma_W}(m_t^2 - m_W^2)^2[m_t^2 + m_W^2 + (m_t^2 - m_W^2)\cos\theta](1 - \cos\theta)$$
$$+\frac{\mathrm{Re}C_{tW} V_{tb} g^2}{128\sqrt{2}\pi^2\Lambda^2 m_t^2 \Gamma_W} m_W^2 (m_t^2 - m_W^2)^2(1 - \cos\theta) \quad (2.6)$$

Here θ is the angle between the momenta of top quark and the neutrino in the W rest frame, and Γ_W is the

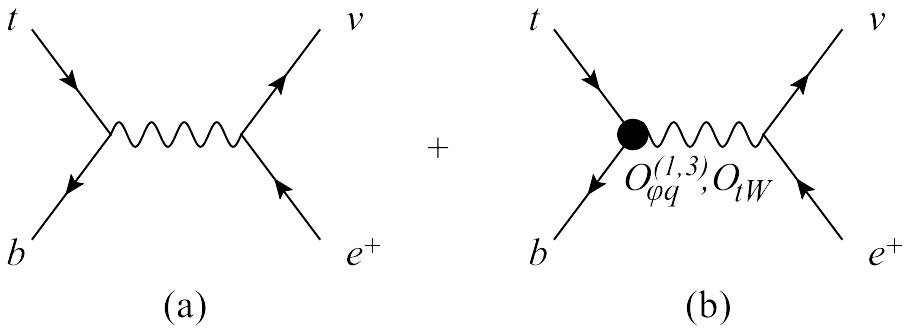

Figure 2.1: The Feynman diagrams for $t \to be^+\nu$. (a) is the SM amplitude; (b) represents the vertex correction induced by the operator $O_{\phi q}^{(3)}$ and O_{tW}.

width of the W boson. In the SM, at tree level Γ_W is given by:

$$\Gamma_W = \frac{3\alpha_W}{4} m_W \ . \tag{2.7}$$

The angular dependence is shown in Figure 2.2. The curves are normalized to have equal areas. The contribution from $O_{\phi q}^{(3)}$ is the same as the SM contribution, because $O_{\phi q}^{(3)}$ simply rescales the SM Wtb vertex. It therefore does not affect angular distributions. The angular dependence of the contribution from O_{tW} is not dramatically different from the SM.

The partial width is given by

$$\Gamma = \left(V_{tb}^2 + \frac{2C_{\phi q}^{(3)} V_{tb} v^2}{\Lambda^2} \right) \frac{g^4 (m_t^6 - 3m_W^4 m_t^2 + 2m_W^6)}{3072\pi^2 \Gamma_W m_t^3 m_W} + \mathrm{Re}C_{tW} V_{tb} \frac{g^2 m_W^2 (m_t^2 - m_W^2)^2}{64\sqrt{2}\pi^2 \Lambda^2 \Gamma_W m_t^2} \ . \tag{2.8}$$

Both dimension-six operators affect the partial width. The total width is given by the above expression times a factor of nine. Unfortunately, it is not known how to measure the partial or total widths in a hadron collider environment.

We also consider the energy dependence of the leptons in the top quark rest frame. The SM computation can be found in [24, 25]. The correction from dimension-six operators at leading order is:

$$\begin{aligned}
\frac{d\Gamma}{dE_{e^+}} &= \left(V_{tb}^2 + \frac{2C_{\phi q}^{(3)} V_{tb} v^2}{\Lambda^2} \right) \frac{g^4 E_{e^+} (m_t - 2E_{e^+})}{128\pi^2 m_W \Gamma_W} + \frac{\mathrm{Re}C_{tW} V_{tb} g^2 m_W^2 (m_t - 2E_{e^+})}{16\sqrt{2}\pi^2 \Lambda^2 \Gamma_W} \\
\frac{d\Gamma}{dE_\nu} &= \left(V_{tb}^2 + \frac{2C_{\phi q}^{(3)} V_{tb} v^2}{\Lambda^2} \right) \frac{g^4 (-4E_\nu^2 m_t^2 + 2E_\nu (m_t^3 + 2m_W^2 m_t) - m_W^2 (m_t^2 + m_W^2))}{256\pi^2 m_t^2 m_W \Gamma_W} \\
&\quad + \frac{\mathrm{Re}C_{tW} V_{tb} g^2 m_W^2 (2E_\nu m_t - m_W^2)}{16\sqrt{2}\pi^2 \Lambda^2 m_t \Gamma_W}
\end{aligned} \tag{2.9}$$

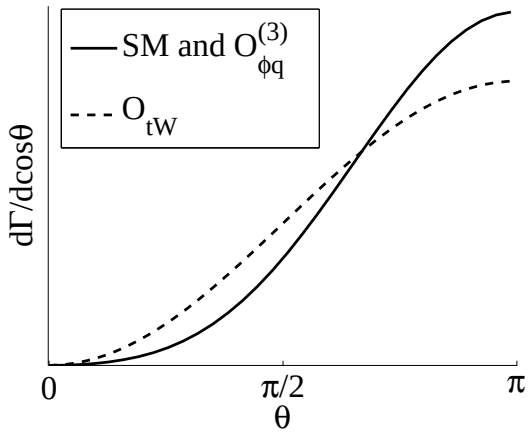

Figure 2.2: The differential decay rate induced by different operators. The curves are normalized so that the area is the same.

where $m_W^2/2m_t < E_{e^+}, E_\nu < m_t/2$ are the energies of the electron and neutrino, respectively. We do not list the energy dependence of the bottom quark, because the narrow width approximation for the W boson is used and the energy of the bottom quark is given by $E_b = (m_t^2 - m_W^2)/2m_t$. These results are shown in Figure 2.3 and 2.4. Again the curves are normalized so that the areas are the same. Compared to Figure 2.2, the two curves are more distinct, which implies the effect of O_{tW} would be more apparent in the energy distribution of the leptons.

The angular distribution and the energy distribution are not independent. The energy of the leptons are fixed in the W rest frame. Therefore their energy in the top quark rest frame is given by a boost, which only depends on the angle θ:

$$E_\nu = \frac{1}{2}(E + |q|\cos\theta) \tag{2.10}$$

$$E_{e^+} = \frac{1}{2}(E - |q|\cos\theta) \tag{2.11}$$

where $E = (m_t^2 + m_W^2)/2m_t$ and $|q| = (m_t^2 - m_W^2)/2m_t$ are the energy and momentum of the W boson in the top quark rest frame. Furthermore, both the angular distribution and energy distribution can be expressed using the W helicity fractions [22]:

$$\frac{1}{\Gamma}\frac{d\Gamma}{d\cos\theta} = \frac{3}{8}(1+\cos\theta)^2 f_+ + \frac{3}{8}(1-\cos\theta)^2 f_- + \frac{3}{4}\sin^2\theta f_0 \tag{2.12}$$

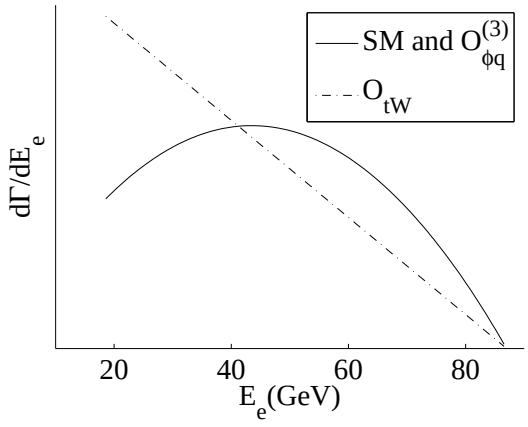

Figure 2.3: The energy dependence of the electron.

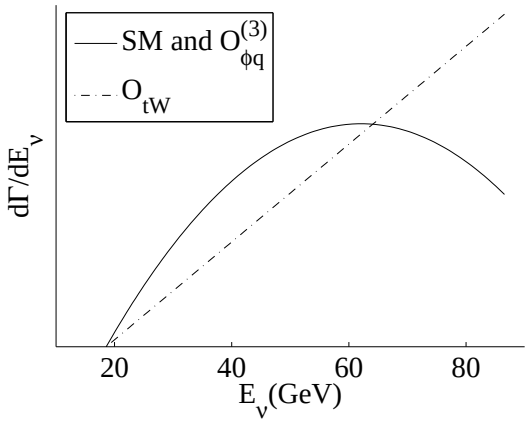

Figure 2.4: The energy dependence of the neutrino.

and

$$\frac{1}{\Gamma}\frac{d\Gamma}{dE_{e^+}} = \frac{1}{(E_{max}-E_{min})^3}\left(3(E_{e^+}-E_{min})^2 f_+ + 3(E_{max}-E_{e^+})^2 f_- + 6(E_{max}-E_{e^+})(E_{e^+}-E_{min})f_0\right) \tag{2.13}$$

where $E_{max} = m_t/2$ and $E_{min} = m_W^2/2m_t$, $f_i = \Gamma_i/\Gamma$ are the W boson helicity fractions, corresponding to positive (+), negative (-), or zero (0) helicity. The helicity fraction is affected by the operator O_{tW}:

$$\begin{aligned} f_0 &= \frac{m_t^2}{m_t^2+2m_W^2} - \frac{4\sqrt{2}\mathrm{Re}C_{tW}v^2}{\Lambda^2 V_{tb}}\frac{m_t m_W(m_t^2-m_W^2)}{(m_t^2+2m_W^2)^2} \\ f_- &= \frac{2m_W^2}{m_t^2+2m_W^2} + \frac{4\sqrt{2}\mathrm{Re}C_{tW}v^2}{\Lambda^2 V_{tb}}\frac{m_t m_W(m_t^2-m_W^2)}{(m_t^2+2m_W^2)^2} \\ f_+ &= 0 \end{aligned} \tag{2.14}$$

These equations make manifest the earlier observation that the operator $O_{\phi q}^{(3)}$, which simply rescales the SM vertex, cannot affect any distributions. Thus top-quark decay is sensitive only to the operator O_{tW}, and can be used to measure (or bound) its coefficient.

Finally, we investigate the polarized differential decay rate. In the rest frame of the top quark, the angular distribution of any top quark decay product is given by [24, 25]

$$\frac{1}{\Gamma}\frac{d\Gamma}{d\cos\theta_i} = \frac{1+\alpha_i\cos\theta_i}{2} \tag{2.15}$$

where $\theta_i = \theta_b, \theta_\nu, \theta_{e^+}$ is the angle between the spin axis of the top quark and the momentum of the bottom quark, neutrino or positron. The "analyzing power" α_i measures the degree to which the direction of the decay product i is correlated with the top spin. If dimension-six operators are added, the relation still

holds, but the coefficient α_i will be affected by the new operators. Since $O_{\phi q}^{(3)}$ is just a rescaling of the SM interaction, the only correction is from O_{tW}. This could be an independent way to determine the coefficient $\mathrm{Re}C_{tW}$. At leading order, the correction is given by:

$$\begin{aligned}
\alpha_b &= -\frac{m_t^2-2m_W^2}{m_t^2+2m_W^2}+\frac{\mathrm{Re}C_{tW}v^2}{\Lambda^2 V_{tb}}\frac{8\sqrt{2}m_t m_W(m_t^2-m_W^2)}{(m_t^2+2m_W^2)^2} \\
\alpha_v &= \frac{m_t^6-12m_t^4m_W^2+3m_t^2m_W^4(3+8\ln(m_t/m_W))+2m_W^6}{m_t^6-3m_t^2m_W^4+2m_W^6} \\
&\quad -\frac{\mathrm{Re}C_{tW}v^2}{\Lambda^2 V_{tb}}\frac{12\sqrt{2}m_t m_W(m_t^6-6m_t^4m_W^2+3m_t^2m_W^4(1+4\ln(m_t/m_W))+2m_W^6)}{(m_t^2+2m_W^2)^2(m_t^2-m_W^2)^2} \\
\alpha_{e^+} &= 1
\end{aligned} \tag{2.16}$$

The same equations hold for hadronic top decay, with $\alpha_u = \alpha_\nu$, $\alpha_{\bar{d}} = \alpha_{e^+}$. The coefficient α_{e^+} is not affected by dimension-six operators. This is consistent with the results in Ref. [26].

The measurement of these coefficients requires a source of polarized top quarks. This is addressed in the next section.

2.2 Single Top Production

Single top quarks are produced through the electroweak interaction. There are three separate processes: s-channel [27], t-channel [28, 29, 30], and Wt production [31]. An effective field theory approach to the s- and t-channel processes was advocated in Ref. [32]. We update that analysis by including an additional operator, which was neglected in that study because it is loop-suppressed if the underlying theory is a gauge theory. We also perform an effective field theory analysis of the Wt process. The vertex-function approach to single-top production is pursued in Refs. [33, 34, 35].

Single top production contains four distinct channels: the s-channel process $u\bar{d} \to t\bar{b}$, the t-channel processes $ub \to dt$ and $\bar{d}b \to \bar{u}t$, and the Wt associated production channel $gb \to Wt$. We first consider the s and t channels. The following operators contribute [32]:

$$O_{\phi q}^{(3)} = i(\phi^+\tau^I D_\mu \phi)(\bar{q}\gamma^\mu\tau^I q) \tag{2.17}$$

$$O_{tW} = (\bar{q}\sigma^{\mu\nu}\tau^I t)\tilde{\phi}W_{\mu\nu}^I \tag{2.18}$$

$$O_{qq}^{(1,3)} = (\bar{q}^i\gamma_\mu\tau^I q^j)(\bar{q}\gamma^\mu\tau^I q) \tag{2.19}$$

For the four-quark operator $O_{qq}^{(1,3)}$, the superscripts i, j denote the first two quark generations. Another four-quark operator that could contribute is $(\bar{q}^i\gamma_\mu q)(\bar{q}\gamma^\mu q^j)$. However, using the Fierz identity, this can

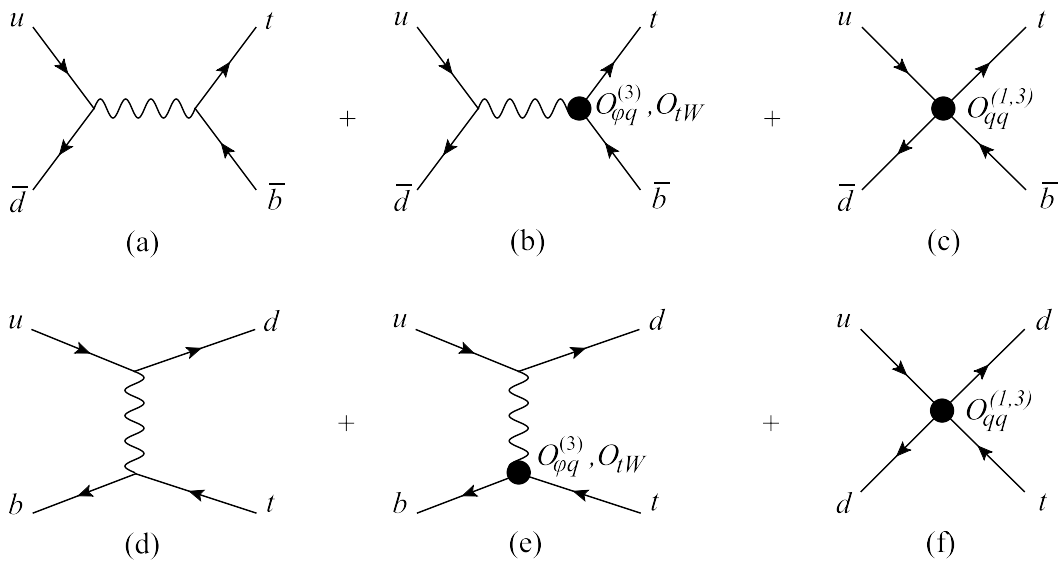

Figure 2.5: Feynman diagrams for the s- and t-channel single top production. (a-c) are the s-channel diagrams, while (d-f) are the t-channel diagrams. (a,d) are the SM amplitude, (b,e) are the correction from $O_{\phi q}^{(3)}$ and O_{tW}, and (c,f) are the four-fermion interaction from $O_{qq}^{(1,3)}$. The diagrams for the t-channel process $\bar{d}b \to \bar{u}t$ can be obtained by interchanging u and d quarks in (d-f).

be turned into a linear combination of $O_{qq}^{(1,3)}$ and some other four-quark operators with different isospin and color structures which do not contribute to this process. Four-quark operators are neglected in the vertex-function approach to the Wtb vertex.

The Feynman diagrams are shown in Figure 2.5. Since the operator O_{tW} will be measured (or bounded) from studies of top-quark decay, the s- and t-channel production of single top quarks can be used to measure (or bound) the operators $O_{\phi q}^{(3)}$ and $O_{qq}^{(1,3)}$.

Now we turn to consider the $gb \to Wt$ process. The contributing operators are

$$O_{\phi q}^{(3)} = i(\phi^+ \tau^I D_\mu \phi)(\bar{q}\gamma^\mu \tau^I q) \tag{2.20}$$

$$O_{tW} = (\bar{q}\sigma^{\mu\nu}\tau^I t)\tilde{\phi} W_{\mu\nu}^I \tag{2.21}$$

$$O_{tG} = (\bar{q}\sigma^{\mu\nu}\lambda^A t)\tilde{\phi} G_{\mu\nu}^A \tag{2.22}$$

Again, the first two operators $O_{\phi q}^{(3)}$ and O_{tW} will affect the Wtb coupling. The "chromomagnetic moment" operator O_{tG} modifies the gtt coupling:

$$L_{eff} = \frac{\mathrm{Re}C_{tG}}{\sqrt{2}\Lambda^2} v \left(\bar{t}\sigma^{\mu\nu}\lambda^A t\right) G_{\mu\nu}^A \tag{2.23}$$

This interaction is neglected in the vertex-function approach to the Wtb vertex.

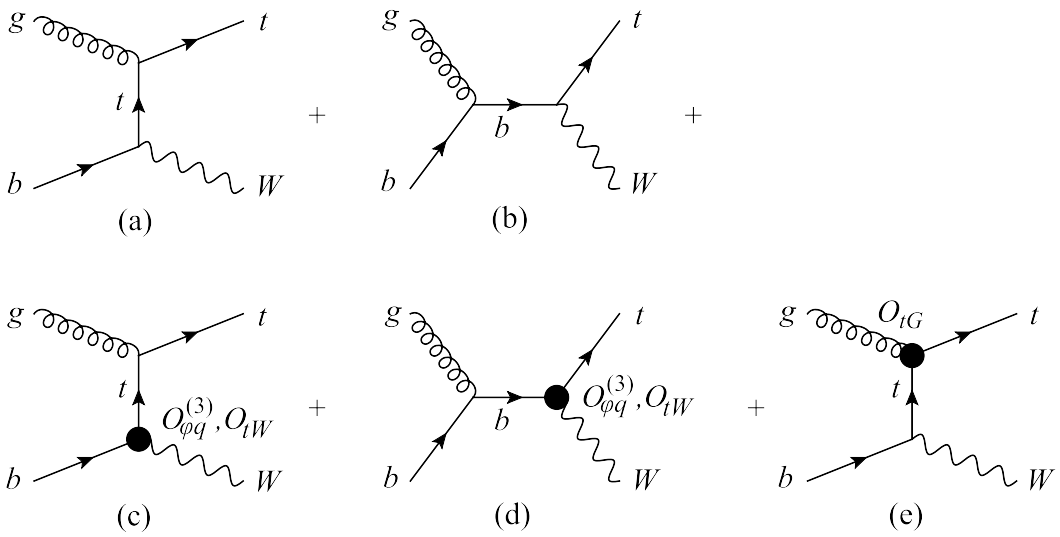

Figure 2.6: The Feynman diagrams for Wt associated production process. (a,b) are the SM amplitude. (c,d) are corrections due to the operator $O^{(3)}_{\phi q}$ and O_{tW}. (e) is a modification on the gtt vertex.

The Feynman diagrams are shown in Figure 2.6. Since the operators $O^{(3)}_{\phi q}$ and O_{tW} will be measured (or bounded) from single-top production and top-quark decay, respectively, the Wt associated production process can be used to measure (or bound) the operator O_{tG}, which is also present in $t\bar{t}$ production (see Section 2.3).

Here we list all the corrections to the SM amplitudes and cross sections. The squared amplitude of the three channels are:

s-channel:

$$\begin{aligned}\frac{1}{4}\Sigma|M_{u\bar{d}\to t\bar{b}}|^2 = &\left(V_{tb}^2 + \frac{2C^{(3)}_{\phi q}V_{tb}v^2}{\Lambda^2}\right)\frac{g^4u(u-m_t^2)}{4(s-m_W^2)^2}\\ &- \frac{2\sqrt{2}\mathrm{Re}C_{tW}V_{tb}m_tm_W}{\Lambda^2}\frac{g^2su}{(s-m_W^2)^2} + \frac{2C^{(1,3)}_{qq}V_{tb}}{\Lambda^2}\frac{g^2u(u-m_t^2)}{s-m_W^2}\end{aligned} \tag{2.24}$$

t-channel:

$$\begin{aligned}\frac{1}{4}\Sigma|M_{ub\to dt}|^2 = &\left(V_{tb}^2 + \frac{2C^{(3)}_{\phi q}V_{tb}v^2}{\Lambda^2}\right)\frac{g^4s(s-m_t^2)}{4(t-m_W^2)^2}\\ &- \frac{2\sqrt{2}\mathrm{Re}C_{tW}V_{tb}m_tm_W}{\Lambda^2}\frac{g^2st}{(t-m_W^2)^2} + \frac{2C^{(1,3)}_{qq}V_{tb}}{\Lambda^2}\frac{g^2s(s-m_t^2)}{t-m_W^2}\end{aligned} \tag{2.25}$$

$$\begin{aligned}\frac{1}{4}\Sigma|M_{\bar{d}b\to\bar{u}t}|^2 = &\left(V_{tb}^2 + \frac{2C^{(3)}_{\phi q}V_{tb}v^2}{\Lambda^2}\right)\frac{g^4u(u-m_t^2)}{4(t-m_W^2)^2}\\ &- \frac{2\sqrt{2}\mathrm{Re}C_{tW}V_{tb}m_tm_W}{\Lambda^2}\frac{g^2ut}{(t-m_W^2)^2} + \frac{2C^{(1,3)}_{qq}V_{tb}}{\Lambda^2}\frac{g^2u(u-m_t^2)}{t-m_W^2}\end{aligned} \tag{2.26}$$

Wt associated production:

$$\frac{1}{96}\Sigma|M_{gb\to Wt}|^2 = \left(V_{tb}^2 + \frac{2C_{\phi q}^{(3)}V_{tb}v^2}{\Lambda^2}\right)\frac{g^2g_s^2}{24m_W^2s(t-m_t^2)^2}\left(m_t^8-(2s+t)m_t^6+((s+t)^2-2tm_W^2-2m_W^4)m_t^4\right.$$
$$-(t(s+t)^2-2(s^2-st+2t^2)m_W^2+2tm_W^4-4m_W^6)m_t^2$$
$$\left.-2tm_W^2(s^2+t^2-2(s+t)m_W^2+2m_W^4)\right)$$
$$+\frac{2\mathrm{Re}C_{tW}V_{tb}g_s^2m_tm_W}{3\sqrt{2}\Lambda^2s(t-m_t^2)^2}\left(3m_t^6-(2s+3t+6m_W^2)m_t^4\right.$$
$$\left.-(s^2+2st-3t^2-6m_W^4)m_t^2+t(s^2-2st-3t^2+6(s+t)m_W^2-6m_W^4)\right)$$
$$+\frac{\mathrm{Re}C_{tG}V_{tb}^2g^2g_sm_tv}{3\sqrt{2}\Lambda^2(m_t^2-t)}(m_t^2+2s-t) \tag{2.27}$$

As before, C_i is the coefficient of operator O_i and s,t,u are the usual Mandelstam variables. We have set $V_{ud}=1$ for simplicity. The differential cross sections are as follows:

$$\begin{aligned}\frac{d\sigma_{u\bar{d}\to t\bar{b}}}{d\cos\theta} &= \left(V_{tb}^2+\frac{2C_{\phi q}^{(3)}V_{tb}v^2}{\Lambda^2}\right)\frac{g^4(s-m_t^2)^2}{512\pi s^2(s-m_W^2)^2}(1+\cos\theta)\left(s+m_t^2+(s-m_t^2)\cos\theta\right)\\ &+\mathrm{Re}C_{tW}V_{tb}\frac{g^2m_tm_W(s-m_t^2)^2}{16\sqrt{2}\pi\Lambda^2s(s-m_W^2)^2}(1+\cos\theta)\\ &+C_{qq}^{(1,3)}V_{tb}\frac{g^2(s-m_t^2)^2}{64\pi\Lambda^2s^2(s-m_W^2)}(1+\cos\theta)(s+m_t^2+(s-m_t^2)\cos\theta)\end{aligned} \tag{2.28}$$

with θ the angle between up quark and top quark momenta in the center of mass frame;

$$\begin{aligned}\frac{d\sigma_{ub\to dt}}{d\cos\theta} &= \left(V_{tb}^2+\frac{2C_{\phi q}^{(3)}V_{tb}v^2}{\Lambda^2}\right)\frac{g^4(s-m_t^2)^2}{32\pi s(2m_W^2+(s-m_t^2)(1-\cos\theta))^2}\\ &+\mathrm{Re}C_{tW}V_{tb}\frac{g^2m_tm_W(s-m_t^2)^2(1-\cos\theta)}{4\sqrt{2}\pi\Lambda^2s(2m_W^2+(s-m_t^2)(1-\cos\theta))^2}\\ &-C_{qq}^{(1,3)}V_{tb}\frac{g^2(s-m_t^2)^2}{8\pi\Lambda^2s(2m_W^2+(s-m_t^2)(1-\cos\theta))}\end{aligned} \tag{2.29}$$

$$\begin{aligned}\frac{d\sigma_{\bar{d}b\to\bar{u}t}}{d\cos\theta} &= \left(V_{tb}^2+\frac{2C_{\phi q}^{(3)}V_{tb}v^2}{\Lambda^2}\right)\frac{g^4(s-m_t^2)^2(1+\cos\theta)(s+m_t^2+(s-m_t^2)\cos\theta)}{128\pi s^2(2m_W^2+(s-m_t^2)(1-\cos\theta))^2}\\ &-\mathrm{Re}C_{tW}V_{tb}\frac{g^2m_tm_W(s-m_t^2)^3\sin^2\theta}{8\sqrt{2}\pi\Lambda^2s^2(2m_W^2+(s-m_t^2)(1-\cos\theta))^2}\\ &-C_{qq}^{(1,3)}V_{tb}\frac{g^2(s-m_t^2)^2(1+\cos\theta)(s+m_t^2+(s-m_t^2)\cos\theta)}{32\pi\Lambda^2s^2(2m_W^2+(s-m_t^2)(1-\cos\theta))}\end{aligned} \tag{2.30}$$

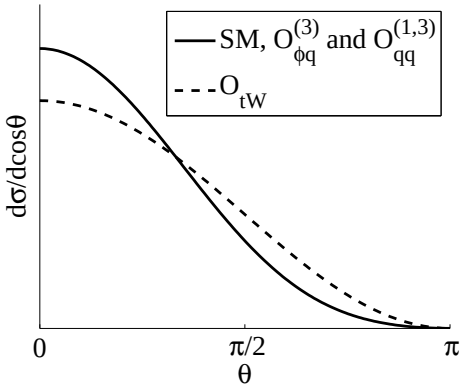

Figure 2.7: The s-channel differential cross section at $\sqrt{s} = 2m_t$.

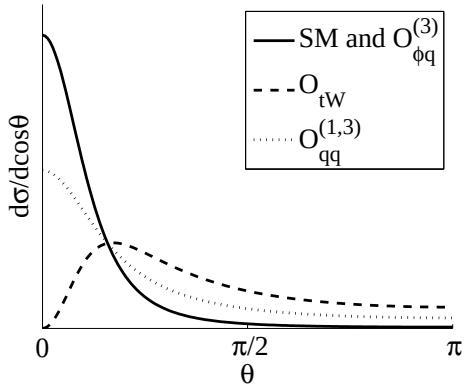

Figure 2.8: The t-channel ($ub \to dt$) differential cross section at $\sqrt{s} = 2m_t$.

with θ the angle between bottom quark and top quark momenta in the center of mass frame;

$$
\begin{aligned}
\frac{d\sigma_{gb\to Wt}}{d\cos\theta} = &\left(V_{tb}^2 + \frac{2C_{\phi q}^{(3)} V_{tb} v^2}{\Lambda^2}\right) \frac{g^2 g_s^2 \lambda^{1/2}}{1536\pi s^3 m_W^2 (s + m_t^2 - m_W^2 - \lambda^{1/2}\cos\theta)^2} \Big[(m_t^2 + 10m_W^2)s^3 \\
&+(3m_t^4 + 19m_t^2 m_W^2 - 22m_W^4)s^2 - (9m_t^6 + 8m_t^4 m_W^2 + 5m_t^2 m_W^4 - 22m_W^6)s \\
&+5(m_t^2 - m_W^2)^3(m_t^2 + 2m_W^2) - (m_t^2 + 2m_W^2)\lambda^{3/2}\cos^3\theta \\
&+\left((6m_W^2 - m_t^2)s - m_t^4 - m_t^2 m_W^2 + 2m_W^4\right)\lambda\cos^2\theta \\
&-\left((14m_W^2 - m_t^2)s^2 - 2(m_t^4 - 7m_t^2 m_W^2 + 6m_W^4)s + 3(m_t^6 - 3m_t^2 m_W^4 + 2m_W^6)\right)\lambda^{1/2}\cos\theta\Big] \\
&- \mathrm{Re}C_{tW} V_{tb} \frac{g_s^2 m_t m_W \lambda^{1/2}}{96\sqrt{2}\pi\Lambda^2 s^3 \left(s + m_t^2 - m_W^2 - \lambda^{1/2}\cos\theta\right)^2} \Big[5s^3 - 9(m_t^2 - m_W^2)s^2 \\
&+(19m_t^4 + 10m_t^2 m_W^2 - 29m_W^4)s - 15(m_t^2 - m_W^2)^3 + 3\lambda^{3/2}\cos^3\theta - (5s - 3m_t^2 + 3m_W^2)\lambda\cos^2\theta \\
&-\left(3s^2 - 10(m_t^2 - m_W^2)s - 9(m_t^2 - m_W^2)^2\right)\lambda^{1/2}\cos\theta\Big] \\
&+ \mathrm{Re}C_{tG} V_{tb}^2 \frac{g^2 g_s v m_t \lambda^{1/2}\left(m_t^2 - m_W^2 + 5s - \lambda^{1/2}\cos\theta\right)}{96\sqrt{2}\pi\Lambda^2 s^2\left(m_t^2 - m_W^2 + s - \lambda^{1/2}\cos\theta\right)}
\end{aligned}
\tag{2.31}
$$

with θ the angle between gluon and top quark momenta in the center of mass frame, and $\lambda = s^2 + m_t^4 + m_W^4 - 2sm_t^2 - 2sm_W^2 - 2m_t^2 m_W^2$. The angular dependence at $\sqrt{s} = 2m_t$ (recall that the kinematic threshold is $\sqrt{s} = m_t$) is shown in Figures 2.7-2.10 (areas are normalized).

The total cross sections are:

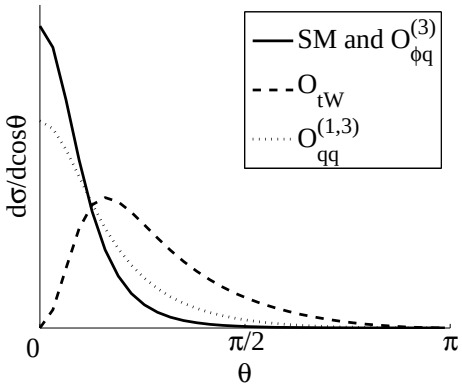

Figure 2.9: The t-channel ($\bar{d}b \to \bar{u}t$) differential cross section at $\sqrt{s} = 2m_t$.

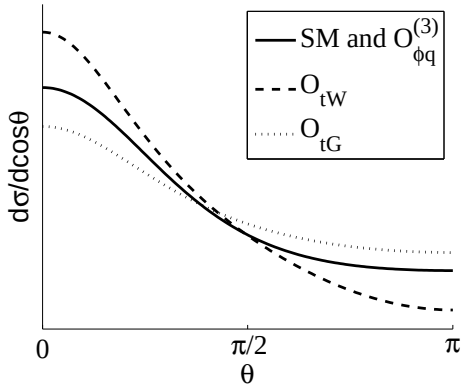

Figure 2.10: The $gb \to Wt$ channel differential cross section at $\sqrt{s} = 2m_t$.

$$\sigma_{u\bar{d}\to t\bar{b}} = \left(V_{tb}^2 + \frac{2C_{\phi q}^{(3)} V_{tb} v^2}{\Lambda^2}\right) \frac{g^4 (s-m_t^2)^2 (2s+m_t^2)}{384\pi\Lambda^2 s^2 (s-m_W^2)^2} + \mathrm{Re}C_{tW} V_{tb} \frac{g^2 m_t m_W (s-m_t^2)^2}{8\sqrt{2}\pi\Lambda^2 s (s-m_W^2)^2} + C_{qq}^{(1,3)} V_{tb} \frac{g^2 (s-m_t^2)^2 (2s+m_t^2)}{48\pi\Lambda^2 s^2 (s-m_W^2)} \tag{2.32}$$

$$\sigma_{ub\to dt} = \left(V_{tb}^2 + \frac{2C_{\phi q}^{(3)} V_{tb} v^2}{\Lambda^2}\right) \frac{g^4 (s-m_t^2)^2}{64\pi\Lambda^2 s m_W^2 (s-m_t^2+m_W^2)} - \mathrm{Re}C_{tW} V_{tb} \frac{g^2 m_t m_W \left(s - m_t^2 - (s-m_t^2+m_W^2)\ln\frac{s-m_t^2+m_W^2}{m_W^2}\right)}{4\sqrt{2}\pi\Lambda^2 s (s-m_t^2+m_W^2)} - C_{qq}^{(1,3)} V_{tb} \frac{g^2 (s-m_t^2)\ln\frac{s-m_t^2+m_W^2}{m_W^2}}{8\pi\Lambda^2 s} \tag{2.33}$$

$$\sigma_{\bar{d}b\to\bar{u}t} = \left(V_{tb}^2 + \frac{2C_{\phi q}^{(3)} V_{tb} v^2}{\Lambda^2}\right) \frac{g^4 \left((s+2m_W^2)(s-m_t^2) - m_W^2 (2s+2m_W^2-m_t^2)\ln\frac{s+m_W^2-m_t^2}{m_W^2}\right)}{64\pi s^2 m_W^2} - \mathrm{Re}C_{tW} V_{tb} \frac{g^2 m_t m_W \left((s+2m_W^2-m_t^2)\ln\frac{s+m_W^2-m_t^2}{m_W^2} - 2(s-m_t^2)\right)}{4\sqrt{2}\pi\Lambda^2 s^2} - C_{qq}^{(1,3)} V_{tb} \frac{g^2 \left(2(s+m_W^2-m_t^2)(s+m_W^2)\ln\frac{s+m_W^2-m_t^2}{m_W^2} - (s-m_t^2)(3s+2m_W^2-m_t^2)\right)}{16\pi\Lambda^2 s^2} \tag{2.34}$$

$$\sigma_{gb\to Wt} = \left(V_{tb}^2 + \frac{2C_{\phi q}^{(3)} V_{tb} v^2}{\Lambda^2}\right) \frac{g^2 g_s^2}{384 s^3 m_W^2} \Bigg(- \left((3m_t^2 - 2m_W^2)s + 7(m_t^2 - m_W^2)(m_t^2 + 2m_W^2)\right) \lambda^{1/2}$$
$$+2(m_t^2 + 2m_W^2)(s^2 + 2(m_t^2 - m_W^2)s + 2(m_t^2 - m_W^2)^2) \ln\left(\frac{s + m_t^2 - m_W^2 + \lambda^{1/2}}{s + m_t^2 - m_W^2 - \lambda^{1/2}}\right)\Bigg)$$
$$- \mathrm{Re}C_{tW} V_{tb} \frac{g_s^2 m_t m_W}{24\sqrt{2}\Lambda^2 s^3} \Bigg(\left(s + 21(m_t^2 - m_W^2)\right) \lambda^{1/2}$$
$$+2\left(s^2 - 6(m_t^2 - m_W^2)s - 6(m_t^2 - m_W^2)^2\right) \ln\left(\frac{s + m_t^2 - m_W^2 + \lambda^{1/2}}{s + m_t^2 - m_W^2 - \lambda^{1/2}}\right)\Bigg)$$
$$+ \mathrm{Re}C_{tG} V_{tb}^2 \frac{g^2 g_s v m_t}{24\sqrt{2}\Lambda^2 s^2} \left(2s \ln\left(\frac{s + m_t^2 - m_W^2 + \lambda^{1/2}}{s + m_t^2 - m_W^2 - \lambda^{1/2}}\right) + \lambda^{1/2}\right) \tag{2.35}$$

The operators $O_{\phi q}^{(3)}$ and $O_{qq}^{(1,3)}$ will be measured (or bounded) by single top production. Because they enter with the opposite relative sign in s- and $t-$ channel production (see Eqs. (2.28),(2.29)), it will be valuable to measure these two processes separately.

The operator O_{tW} also has an effect on the produced top quark spin. In the SM $s-$ and $t-$channel single top production, the top quark is always polarized in the direction of d or $\bar{d}$ three-momentum in the top rest frame [36]. When O_{tW} is present, the top quark spin deviates from its original direction, but is still in the production plane. For example, in the $s-$channel process, the top spin deviates away from the three-momentum of the $\bar{b}$, with an angle (in the top rest frame)

$$\delta\theta = \mathrm{Re}C_{tW} \frac{2\sqrt{2}v^2}{\Lambda^2} \frac{\sqrt{s}}{m_W} \frac{(s - m_t^2)\sin\theta}{s + m_t^2 + (s - m_t^2)\cos\theta} \tag{2.36}$$

where θ is the scattering angle in the W rest frame. Similarly, in the $t-$channel process $b\bar{d} \to t\bar{u}$, the top spin deviates toward the three-momentum of $\bar{u}$, with the same angle. In the $t-$channel process $bu \to td$, the top spin deviates toward the three-momentum of the incoming b quark, with an angle

$$\delta\theta = \mathrm{Re}C_{tW} \frac{\sqrt{2}v^2}{\Lambda^2} \frac{\sqrt{s}}{m_W} \sin\theta \tag{2.37}$$

In Eq. (2.16) we reported the effect of the operator O_{tW} on the analyzing power of top decay. Let $\hat{\mathbf{s}}$ be the unit vector in the top quark spin direction and $\hat{\mathbf{p}}_i$ be the unit vector in the direction of the three-momentum of the decay product i in the top rest frame, we have

$$\alpha_i = 3 < \hat{\mathbf{s}} \cdot \hat{\mathbf{p}}_i > \tag{2.38}$$

In practice, we can use the $s-$ and $t-$channel single top production as a source of polarized top quark. To measure the analyzing power, we can replace $\hat{\mathbf{s}}$ with $\hat{\mathbf{p}}_{d,\bar{d}}$, the unit vector in the direction of three-momentum of d or $\bar{d}$, depending on the production channel:

$$\alpha_i = 3 < \hat{\mathbf{p}}_{d,\bar{d}} \cdot \hat{\mathbf{p}}_i > \tag{2.39}$$

In single top production the top quark spin is affected by O_{tW}, so $\hat{\mathbf{s}}$ and $\hat{\mathbf{p}}_{d,\bar{d}}$ are not exactly aligned. However, the direction in which the top quark spin deviates from the three-momentum of d or $\bar{d}$ is independent of the $\hat{\mathbf{p}}_i$, i.e.

$$< (\hat{\mathbf{p}}_{d,\bar{d}} - \hat{\mathbf{s}}) \cdot \hat{\mathbf{p}}_i >= 0 \tag{2.40}$$

Therefore Eq. (2.39) still holds. In other words, the effect of O_{tW} on the production vertex doesn't affect the measurement of the analyzing power.

2.3 Top Pair Production

The effect of higher dimension operators on top quark pair production is studied in [37, 38, 39]. In Ref. [37], two dimension-six operators, the chromomagnetic moment operator, O_{tG}, and the triple gluon field strength operator, O_G, are considered:

$$O_{tG} = (\bar{q}\sigma^{\mu\nu}\lambda^A t)\tilde{\phi}G^A_{\mu\nu} \tag{2.41}$$

$$O_G = f_{ABC}G^{A\nu}_{\mu}G^{B\rho}_{\nu}G^{C\mu}_{\rho} \tag{2.42}$$

It is shown that O_G will generate observable cross section deviations from QCD at the LHC even for relatively small values of its coefficient.

Here we redo the leading order calculation, and also take into account the operator $O_{\phi G}$:

$$O_{\phi G} = \frac{1}{2}(\phi^+\phi)G^A_{\mu\nu}G^{A\mu\nu} \tag{2.43}$$

which is a Higgs-gluon interaction. Its effect on the Higgs production rate and branching ratios has been discussed in [40]. We include this operator because it contributes to top pair production through $gg \to h \to t\bar{t}$,

$$L_{eff} = \frac{1}{2}\frac{C_{\phi G}}{\Lambda^2}vhG^A_{\mu\nu}G^{A\mu\nu} \tag{2.44}$$

which could be significant because the top quark has a large Yukawa coupling.

Top quark pair production proceeds at the tree level through the parton reactions $gg \to t\bar{t}$ and $q\bar{q} \to t\bar{t}$. We first consider the gluon channel. The Feynman diagrams are shown in Figure 2.11. The operator O_{tG} changes the SM gtt coupling, and also generates a new $ggtt$ interaction. O_G affects the three-point gluon vertex in QCD. $O_{\phi G}$ generates a new diagram with an s-channel Higgs boson.

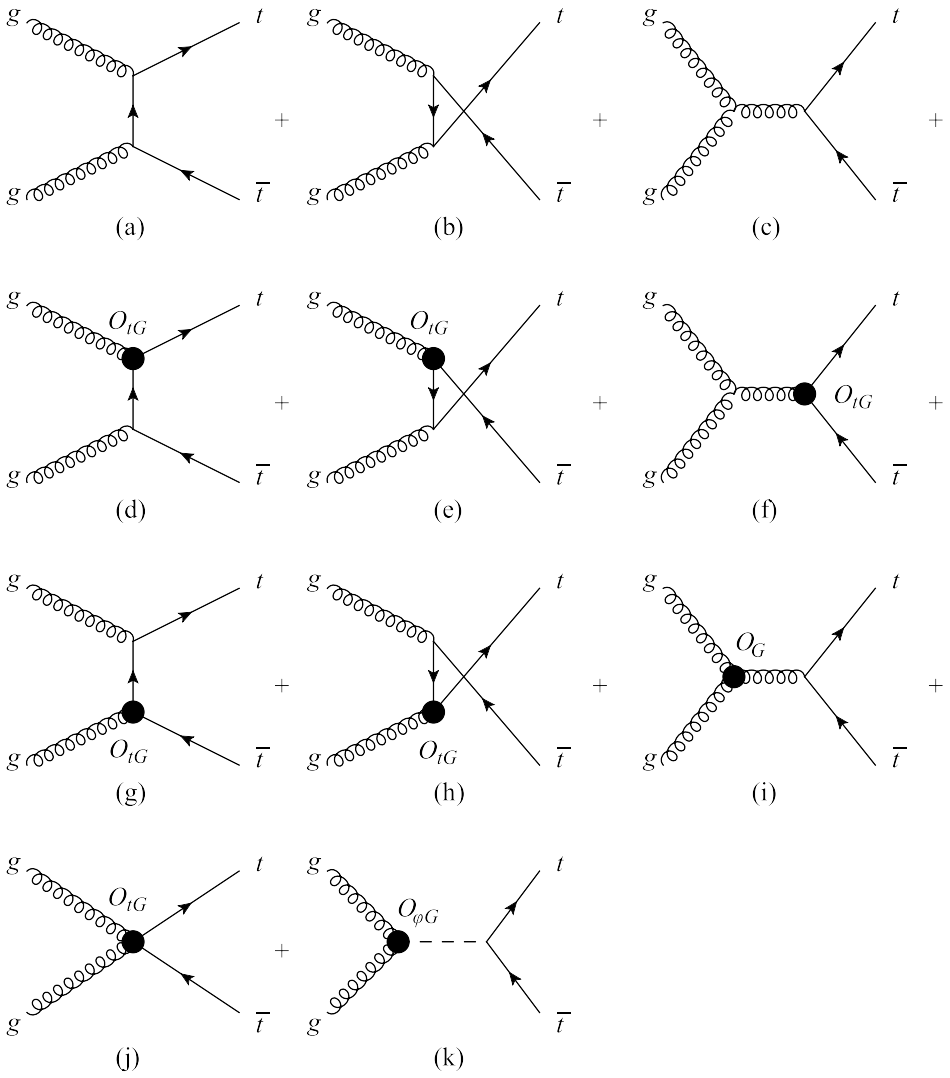

Figure 2.11: The Feynman diagrams for $gg \to t\bar{t}$ process. Diagram (a-c) are the SM amplitude. (d-h) are the gtt vertex correction induced by O_{tG}. (i) is the g^3 vertex correction induced by O_G. (j) is a $ggtt$ interaction from O_{tG}, and (k) is a $gg \to h \to tt$ process, induced by $O_{\phi G}$.

The squared amplitude is:

$$\begin{aligned}\frac{1}{256}|M|^2 &= \frac{3g_s^4}{4}\frac{(m^2-t)(m^2-u)}{s^2} - \frac{g_s^4}{24}\frac{m^2(s-4m^2)}{(m^2-t)(m^2-u)} + \frac{g_s^4}{6}\frac{tu-m^2(3t+u)-m^4}{(m^2-t)^2} \\ &+\frac{g_s^4}{6}\frac{tu-m^2(t+3u)-m^4}{(m^2-u)^2} - \frac{3g_s^4}{8}\frac{tu-2m^2t+m^4}{s(m^2-t)} - \frac{3g_s^4}{8}\frac{tu-2m^2u+m^4}{s(m^2-u)} \\ &+\frac{\sqrt{2}\mathrm{Re}C_{tG}g_s^3vm}{3\Lambda^2}\frac{4s^2-9tu-9m^2s+9m^4}{(m^2-t)(m^2-u)} + \frac{9C_Gg_s^3}{8\Lambda^2}\frac{m^2(t-u)^2}{(m^2-t)(m^2-u)} \\ &-\frac{C_{\phi G}g_s^2m^2}{8\Lambda^2}\frac{s^2(s-4m^2)}{(s-m_h^2)(t-m^2)(u-m^2)}\end{aligned} \tag{2.45}$$

where m is the mass of the top quark and m_h is the mass of the Higgs boson.

The differential and total cross sections are

$$\begin{aligned}\frac{d\sigma}{d\cos\theta} &= \frac{g_s^4\beta}{1536\pi s(1-\beta^2\cos^2\theta)^2} \\ &\left(7(1+2\beta^2-2\beta^4)-\beta^2(5-32\beta^2+18\beta^4)\cos^2\theta-(25\beta^4-18\beta^6)\cos^4\theta-9\beta^6\cos^6\theta\right) \\ &+\mathrm{Re}C_{tG}\frac{g_s^3v\beta\sqrt{1-\beta^2}(7+9\beta^2\cos^2\theta)}{96\sqrt{2}\pi\Lambda^2\sqrt{s}(1-\beta^2\cos^2\theta)} + C_G\frac{9g_s^3\beta^3(1-\beta^2)\cos^2\theta}{256\pi\Lambda^2(1-\beta^2\cos^2\theta)} \\ &-C_{\phi G}\frac{g_s^2s\beta^3(1-\beta^2)}{256\pi\Lambda^2(s-m_h^2)(1-\beta^2\cos^2\theta)}\end{aligned} \tag{2.46}$$

$$\begin{aligned}\sigma &= \frac{g_s^4}{768\pi s}\left(31\beta^3-59\beta+(33-18\beta^2+\beta^4)\ln\frac{1+\beta}{1-\beta}\right) + \mathrm{Re}C_{tG}\frac{g_s^3v\sqrt{1-\beta^2}}{48\sqrt{2}\pi\Lambda^2\sqrt{s}}\left(8\ln\frac{1+\beta}{1-\beta}-9\beta\right) \\ &+C_G\frac{9g_s^3(1-\beta^2)}{256\pi\Lambda^2}\left(\ln\frac{1+\beta}{1-\beta}-2\beta\right) - C_{\phi G}\frac{g_s^2s\beta^2(1-\beta^2)}{256\pi\Lambda^2(s-m_h^2)}\ln\frac{1+\beta}{1-\beta}\end{aligned} \tag{2.47}$$

Here θ is the angle between the gluon and top quark momenta in the center of mass frame; $\beta \equiv \sqrt{1-\frac{4m^2}{s}}$ is the velocity of the top quark. Top quark pair production can be used to measure (or bound) the coefficients of the operators O_{tG}, O_G and $O_{\phi G}$. The operator O_{tG} is also probed by Wt associated production, as discussed above, and the operator $O_{\phi G}$ is probed by Higgs production [40].

Now we turn to consider the quark process $q\bar{q} \to t\bar{t}$. There are a large number of four-quark operators with different chiral and flavor structures [7, 6, 37]. Here we consider all possible chirality and color structures. In Ref. [6], only one generation is considered. When there are three generations, the quark field in these operators can be of any generation. For example, $(\bar{q}^i\gamma_\mu q^j)(\bar{q}\gamma^\mu q)$ and $(\bar{q}^i\gamma_\mu q)(\bar{q}\gamma^\mu q^j)$ (superscripts i, j are used to denote the first two generations) should be considered as different operators. The effect of some of these operators are suppressed by the color structure or by the small quark mass. For example, $(\bar{q}^i\gamma_\mu q^j)(\bar{q}\gamma^\mu q)$

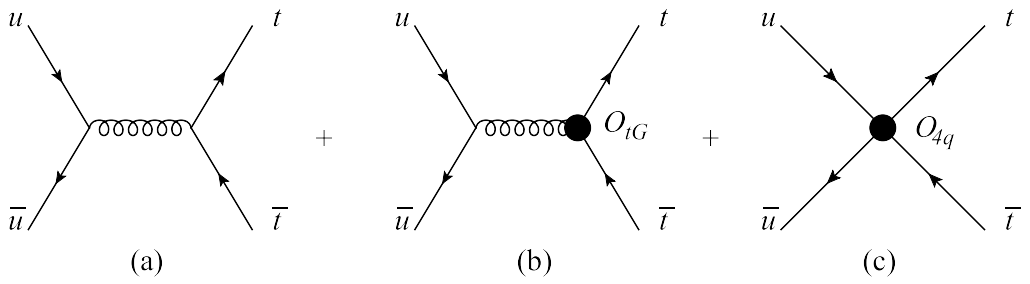

Figure 2.12: The Feynman diagrams for $u\bar{u} \to t\bar{t}$ process. (a) is the SM amplitude, (b) is the correction on gtt coupling induced by O_{tG}, and (c) is the four-fermion interactions. The $d\bar{d} \to t\bar{t}$ process has the same diagrams.

doesn't interfere with the SM, because the t and $\bar{t}$ form a color singlet; an operator like $(\bar{q}t)\epsilon(\bar{q}^i d^j)$ doesn't interfere either, because it involves a left-handed and a right-handed down quark while the SM $gd\bar{d}$ coupling doesn't change chirality.

Using the Fierz transformation and the following SU(2) and SU(3) identities

$$\begin{aligned} \tau^I_{ab}\tau^I_{cd} &= -\delta_{ab}\delta_{cd} + 2\delta_{ad}\delta_{bc} \\ t^A_{ij}t^A_{kl} &= -\frac{1}{6}\delta_{ij}\delta_{kl} + \frac{1}{2}\delta_{il}\delta_{jk} \end{aligned} \tag{2.48}$$

we find that only the following four-quark operators contribute to the $u\bar{u}, d\bar{d} \to t\bar{t}$ reaction:

$$\begin{aligned} &O^{(8,1)}_{qq} = \tfrac{1}{4}(\bar{q}^i\gamma_\mu\lambda^A q^j)(\bar{q}\gamma^\mu\lambda^A q) && O^{(8,3)}_{qq} = \tfrac{1}{4}(\bar{q}^i\gamma_\mu\tau^I\lambda^A q^j)(\bar{q}\gamma^\mu\tau^I\lambda^A q) \\ &O^{(8)}_{ut} = \tfrac{1}{4}(\bar{u}^i\gamma_\mu\lambda^A u^j)(\bar{t}\gamma^\mu\lambda^A t) && O^{(8)}_{dt} = \tfrac{1}{4}(\bar{d}^i\gamma_\mu\lambda^A d^j)(\bar{t}\gamma^\mu\lambda^A t) \\ &O^{(1)}_{qu} = (\bar{q}u^i)(\bar{u}^j q) && O^{(1)}_{qd} = (\bar{q}d^i)(\bar{d}^j q) \\ &O^{(1)}_{qt} = (\bar{q}^i t)(\bar{t}q^j) \end{aligned} \tag{2.49}$$

We do not include the operators that have the form $(\bar{q}\lambda^A u^i)(\bar{u}^j\lambda^A q)$. This operator can be turned into a linear combination of $O^{(1)}_{qu}$, which is already considered, and another operator $(\bar{q}_c u^i_b)(\bar{u}^j_a q_d)\delta_{ab}\delta_{cd}$ (a, b, c, d denote color indices), which does not contribute because the t and $\bar{t}$ form a color singlet. In addition, we also need to consider the operator O_{tG}, whose effect is to change the gtt coupling. The diagrams are shown in Figure 2.12. The result is

$$\begin{aligned} \frac{1}{36}|M_{\bar{u}u\to\bar{t}t}|^2 &= g_s^2(M_1^2 + M_2^2) + \frac{32\sqrt{2}\mathrm{Re}C_{tG}g_s^3 vm}{9\Lambda^2} + C_u^1\frac{s}{\Lambda^2}M_1^2 + C_u^2\frac{s}{\Lambda^2}M_2^2 \\ \frac{1}{36}|M_{\bar{d}d\to\bar{t}t}|^2 &= g_s^2(M_1^2 + M_2^2) + \frac{32\sqrt{2}\mathrm{Re}C_{tG}g_s^3 vm}{9\Lambda^2} + C_d^1\frac{s}{\Lambda^2}M_1^2 + C_d^2\frac{s}{\Lambda^2}M_2^2 \end{aligned} \tag{2.50}$$

where

$$
\begin{aligned}
C_u^1 &= C_{qq}^{(8,1)} + C_{qq}^{(8,3)} + C_{ut}^{(8)} && (2.51)\\
C_u^2 &= C_{qu}^{(1)} + C_{qt}^{(1)} && (2.52)\\
C_d^1 &= C_{qq}^{(8,1)} - C_{qq}^{(8,3)} + C_{dt}^{(8)} && (2.53)\\
C_d^2 &= C_{qd}^{(1)} + C_{qt}^{(1)} && (2.54)\\
M_1^2 &= \frac{4g_s^2}{9s^2}(3m^4 - m^2(t+3u) + u^2) && (2.55)\\
M_2^2 &= \frac{4g_s^2}{9s^2}(3m^4 - m^2(3t+u) + t^2) && (2.56)
\end{aligned}
$$

The cross section is

$$
\begin{aligned}
\frac{d\sigma_{\bar{u}u,\bar{d}d\to\bar{t}t}}{d\cos\theta} &= \frac{g_s^4}{144\pi s}\beta(2-\beta^2\sin^2\theta) + \mathrm{Re}C_{tG}\frac{g_s^3 v\beta\sqrt{1-\beta^2}}{9\sqrt{2}\pi\Lambda^2\sqrt{s}}\\
&\quad + C_{u,d}^1\frac{g_s^2}{288\pi\Lambda^2}\beta(2+2\beta\cos\theta-\beta^2\sin^2\theta)\\
&\quad + C_{u,d}^2\frac{g_s^2}{288\pi\Lambda^2}\beta(2-2\beta\cos\theta-\beta^2\sin^2\theta) \qquad (2.57)
\end{aligned}
$$

where θ is the angle between up or down quark and the top quark momenta, in the center of mass frame. The total cross section is

$$
\sigma_{\bar{u}u,\bar{d}d\to\bar{t}t} = \frac{g_s^4}{108\pi s}\beta(3-\beta^2) + \mathrm{Re}C_{tG}\frac{\sqrt{2}g_s^3 v}{9\pi\Lambda^2\sqrt{s}}\beta\sqrt{1-\beta^2} + (C_{u,d}^1 + C_{u,d}^2)\frac{g_s^2}{216\pi\Lambda^2}\beta(3-\beta^2) \quad (2.58)
$$

Although there are seven four-fermion operators, their effects on top-quark pair production are summarized by only four coefficients $C_{u,d}^{1,2}$. Thus top-quark pair production can be used to bound four linear combinations of the four-quark operators as well as the operator O_{tG}.

If $C_{u,d}^1$ and $C_{u,d}^2$ are distinct, they will generate a forward-backward asymmetry:

$$
\begin{aligned}
A_{FB}^t &= \frac{N(\cos\theta>0) - N(\cos\theta<0)}{N(\cos\theta>0) + N(\cos\theta<0)}\\
&= (C_{u,d}^1 - C_{u,d}^2)\frac{3s\beta}{4g_s^2\Lambda^2(3-\beta^2)} \qquad (2.59)
\end{aligned}
$$

The recent measurements of the top quark forward-backward asymmetry from the CDF and the D0 experiments can be found in [41, 42, 43, 44, 45]. The SM prediction is dominated by $O(\alpha_S^3)$ QCD interference effects and is 5% in the lab frame [46, 47, 48, 49]. There is a discrepancy of about 2σ between theory and

experiment. It is interesting to ask whether this discrepancy can be accommodated within the effective field theory framework. The challenge is to avoid too large a modification of the $t\bar{t}$ production cross section, since the current measurement is in good agreement with the SM prediction [50]. In the effective field theory approach, this can be done if $C^1_{u,d}$ and $C^2_{u,d}$ have similar non-zero values but with opposite sign, i.e. $C^1_{u,d} \approx -C^2_{u,d}$.

2.4 CP Violation

Violations of the CP symmetry are of great interest in particle physics especially since its origin is still unclear. Better understanding of this rare phenomenon can lead to new physics which may explain both the origin of mass and the preponderance of matter over anti-matter in the present universe.

The SM predicts that CP-violating effects in top physics are very small. This is primarily due to the fact that its large mass renders the Glashow-Iliopoulos-Maiani (GIM) [51] cancellation particularly effective [52, 53]. Therefore, the study of CP-violation effects in top physics is important because any observation of such effects would be a clear evidence of physics beyond the SM.

Effective field theory is a complete and model-independent approach to physics beyond the SM. Its CP-odd operators can be used to describe the CP-violation effects in top quark physics. We find that there are four CP-odd operators that can have significant contribution to top quark production and decay processes, as listed in Table 2. In this section we will consider the effects of these four operators.

2.4.1 Polarized Top Quark Decay

In top quark decay, the momenta of the four particles, t,b,e^+ and ν are not independent because of the energy-momentum conservation. However, if we define the top quark spin vector (in the top rest frame):

$$s = (0, \hat{\mathbf{s}}) \tag{2.60}$$

where the unit vector $\hat{\mathbf{s}}$ is the direction of the top quark spin, then a term proportional to $\epsilon_{\mu\nu\rho\sigma} p_t^\mu p_b^\nu p_{e^+}^\rho s^\sigma$ is T_N-odd. Thus it becomes possible to observe CP violation effects.

In the top quark decay process, there is only one operator that contributes at leading order:

$$O_{tW} = (\bar{q}\sigma^{\mu\nu}\tau^I t)\tilde{\phi} W^I_{\mu\nu} \tag{2.61}$$

This operator is CP-odd if its coefficient is imaginary.

To investigate the effect of O_{tW}, we choose the coordinate axes in the top rest frame such that the positron momentum is in the z-direction, and the bottom momentum is in the xz plane, with a positive x component. The top quark spin is $\hat{\mathbf{s}} = (\sin\theta\cos\phi, \sin\theta\sin\phi, \cos\theta)$. The decay rate is given by:

$$\frac{d\Gamma}{d\cos\theta d\phi} = \frac{V_{tb}^2 g^4 (m_t^6 - 3m_W^4 m_t^2 + 2m_W^6)}{12288\pi^3 m_t^3 m_W \Gamma_W}(1+\cos\theta) - \frac{\mathrm{Im}C_{tW} V_{tb} g^2 m_W (m_t^2 - m_W^2)^3}{2048\sqrt{2}\pi^2 \Lambda^2 \Gamma_W m_t^3}\sin\theta\sin\phi \qquad (2.62)$$

The CP-odd contribution is proportional to $\sin\phi$, so it doesn't affect the total decay rate and the analyzing power α_i defined in Eq. (2.15).

We now define the following triple-product and evaluate it in the top rest frame:

$$T = -\frac{1}{m_t}\epsilon_{\mu\nu\rho\sigma} p_t^\mu p_b^\nu p_{e^+}^\rho s^\sigma = (\mathbf{p}_b \times \mathbf{p}_{e^+}) \cdot \hat{\mathbf{s}} \qquad (2.63)$$

which corresponds to the projection of the top spin onto the direction perpendicular to the plane formed by the bottom quark and the positron. This leads to an asymmetry:

$$\begin{aligned} A_{t\to Wb} &= \frac{N(T>0) - N(T<0)}{N(T>0) + N(T<0)} \\ &= \mathrm{Im}C_{tW} \frac{3\pi v^2 (m_t^2 - m_W^2)}{4\sqrt{2}\Lambda^2 V_{tb}(m_t^2 + 2m_W^2)} \end{aligned} \qquad (2.64)$$

Such an asymmetry is a sign of CP violation. To observe such an asymmetry requires a source of polarized top quarks. This is addressed in the next section.

2.4.2 Spin Asymmetry in Single Top Production

In single top production, we can construct CP-odd observables in a similar way. In the s- and t-channel processes, O_{tW} (with imaginary coefficient) is the only CP-odd operator that contributes. Consider the s-channel process $u\bar{d} \to t\bar{b}$. We can define the following triple-product in the top rest frame

$$T = -\frac{1}{m_t}\epsilon_{\mu\nu\rho\sigma} p_t^\mu p_u^\nu p_{\bar{d}}^\rho s^\sigma = (\mathbf{p}_u \times \mathbf{p}_{\bar{d}}) \cdot \hat{\mathbf{s}} \qquad (2.65)$$

In the SM, the top spin in its rest frame is in the direction of the $\bar{d}$ three-momentum [36], therefore $T = 0$. When the CP-odd operator is added, the direction of the top quark spin can be computed. It deviates from the production plane, with an angle (in the top rest frame)

$$\theta = \mathrm{Im}C_{tW} \frac{2\sqrt{2} v^2 \sqrt{s}(s - m_t^2)\sin\theta_W}{\Lambda^2 V_{tb} m_W (s + m_t^2 + (s - m_t^2)\cos\theta_W)} \qquad (2.66)$$

where θ_W is the angle between the momenta of the up quark and the top quark in the W rest frame. The value of T is then given by

$$T = -\frac{\sqrt{2}\mathrm{Im}C_{tW}v^2 s(s-m_t^2)^2\sin^2\theta_W}{2\Lambda^2 V_{tb}m_W m_t[s+m_t^2+(s-m_t^2)\cos\theta_W]} \tag{2.67}$$

In practice, assume the top spin $\hat{\mathbf{s}}$ is measured in the direction perpendicular to the production plane, i.e. $\mathbf{s}_\perp$ takes either 1 or -1, then this will lead to an asymmetry:

$$\begin{aligned} A_{u\bar{d}\to t\bar{b}} &= \frac{N(\mathbf{s}_\perp=1)-N(\mathbf{s}_\perp=-1)}{N(\mathbf{s}_\perp=1)+N(\mathbf{s}_\perp=-1)} \\ &= \mathrm{Im}C_{tW}\frac{3\pi v^2\sqrt{s}(s-m_t^2)}{2\sqrt{2}\Lambda^2 V_{tb}m_W(2s+m_t^2)} \end{aligned} \tag{2.68}$$

Similarly, for the t-channel process $bu\to td$, we find

$$T = (\mathbf{p}_b\times\mathbf{p}_u)\cdot\hat{\mathbf{s}} = \frac{\mathrm{Im}C_{tW}v^2 s(s-m_t^2)\sin^2\theta_W}{2\sqrt{2}\Lambda^2 V_{tb}m_W m_t} \tag{2.69}$$

and for the process $b\bar{d}\to t\bar{u}$,

$$T = (\mathbf{p}_b\times\mathbf{p}_{\bar{d}})\cdot\hat{\mathbf{s}} = \frac{\sqrt{2}\mathrm{Im}C_{tW}v^2 s(s-m_t^2)^2\sin^2\theta_W}{2\Lambda^2 V_{tb}m_W m_t(s+m_t^2+(s-m_t^2)\cos\theta_W)} \tag{2.70}$$

If the top spin $\hat{\mathbf{s}}$ is measured in the direction perpendicular to the production plane, the corresponding asymmetries are

$$\begin{aligned} A_{bu\to td} &= \frac{N(\mathbf{s}_\perp=1)-N(\mathbf{s}_\perp=-1)}{N(\mathbf{s}_\perp=1)+N(\mathbf{s}_\perp=-1)} \\ &= -\mathrm{Im}C_{tW}\frac{\sqrt{2}\pi v^2\sqrt{s}((s-m_t^2+2m_W^2)\sqrt{s-m_t^2+m_W^2}-2m_W(s-m_t^2+m_W^2))}{\Lambda^2 V_{tb}(s-m_t^2)^2} \end{aligned} \tag{2.71}$$

$$\begin{aligned} A_{b\bar{d}\to t\bar{u}} &= \frac{N(\mathbf{s}_\perp=1)-N(\mathbf{s}_\perp=-1)}{N(\mathbf{s}_\perp=1)+N(\mathbf{s}_\perp=-1)} \\ &= -\mathrm{Im}C_{tW}\frac{\sqrt{2}\pi v^2\sqrt{s}((s-m_t^2+4m_W^2)\sqrt{s-m_t^2+mW^2}-(3s-3m_t^2+4m_W^2)m_W)}{\Lambda^2 V_{tb}((s-m_t^2)(s+2m_W^2)-m_W^2(2s+2m_W^2-m_t^2)\ln\frac{s-m_t^2+m_W^2}{m_W^2})} \end{aligned} \tag{2.72}$$

In Wt associated production channel $gb\to Wt$, the chromo-electric dipole moment operator

$$O_{tG} = (\bar{q}\sigma^{\mu\nu}\lambda^A t)\tilde{\phi}G^A_{\mu\nu} \tag{2.73}$$

will also contribute. We find

$$
\begin{aligned}
&A_{gb\to Wt} = \frac{N(\mathbf{s}_\perp = 1) - N(\mathbf{s}_\perp = -1)}{N(\mathbf{s}_\perp = 1) + N(\mathbf{s}_\perp = -1)} \\
=&\mathrm{Im}C_{tW}\frac{v^2\sqrt{2s}m_W\lambda}{2\Lambda^2 V_{tb}} \\
&\times\left(\sqrt{\lambda}((2m_W^2-3m_t^2)s - 7(m_t^2+2m_W^2)(m_t^2-m_W^2)) - 2(m_t^2+2m_W^2)(\lambda+4sm_t^2+(m_t^2-m_W^2)^2)\log y\right)^{-1} \\
&-\mathrm{Im}C_{tG}\frac{2\sqrt{2}vm_t^2 s^{3/2}}{g_s\Lambda^2(s+m_t^2-m_W^2+\sqrt{\lambda})^3 y^2} \\
&\times\left\{\left[(7m_t^2-8m_W^2)\lambda + 4sm_t^2(11m_t^2-15m_W^2) - 4m_t^2(m_t^2-m_W^2)^2\right]\left(\sqrt{\lambda}+s+m_t^2-m_W^2\right)\right. \\
&\left.-8y\left[2(m_t^2-2m_W^2)(m_t^2-m_W^2)+s(3m_t^2-4m_W^2)\right]\left[\lambda+(s+m_t^2-m_W^2)\sqrt{\lambda}+2sm_t^2\right]\right\} \\
&\times\left(\sqrt{\lambda}\left(s(2m_W^2-3m_t^2) - 7(m_t^2+2m_W^2)(m_t^2-m_W^2)\right) - 2(m_t^2+2m_W^2)(\lambda+4sm_t^2+(m_t^2-m_W^2)^2)\log y\right)^{-1}
\end{aligned}
\tag{2.74}
$$

where

$$
\lambda = s^2 + m_t^4 + m_W^4 - 2sm_t^2 - 2sm_W^2 - 2m_t^2 m_W^2 \tag{2.75}
$$

and

$$
y = \sqrt{\frac{s+m_t^2-m_W^2-\sqrt{\lambda}}{s+m_t^2-m_W^2+\sqrt{\lambda}}} \tag{2.76}
$$

In practice there is no way to measure the top spin directly, so we need to use the momentum of the decay products as the spin analyzer. The positron has a spin analyzing power $\alpha_{e^+} = 1$. It can be shown that, if the top production process is followed by a semileptonic decay, one can replace the top spin in the triple-product T by the positron three-momentum, and the corresponding asymmetry will be decreased by a factor of 1/2. For example, in the s-channel process, consider

$$
T = (\mathbf{p}_u \times \mathbf{p}_{\bar{d}}) \cdot \mathbf{p}_{e^+} \tag{2.77}
$$

We find

$$
\begin{aligned}
A_{u\bar{d}\to t\bar{b}} &= \frac{N(T>0) - N(T<0)}{N(T>0) + N(T<0)} \\
&= -\mathrm{Im}C_{tW}\frac{3\pi v^2\sqrt{s}(s-m_t^2)}{4\sqrt{2}\Lambda^2 V_{tb} m_W(2s+m_t^2)}
\end{aligned}
\tag{2.78}
$$

which is exactly half of Eq. (2.68), as expected. Similarly, for t-channel and $gb \to tW$ channel, the results in Eqs. (2.71), (2.72) and (2.74) should also be reduced by a factor of 1/2. Note that although the CP-odd

operator has effects on both production and decay processes, this asymmetry only reflects its effect on the production, because the decay process is only used as the spin analyzer, and the analyzing power $\alpha_{e^+} = 1$ is not affected by the CP-odd effect.

We can also reverse the procedure and construct a CP-odd observable that only reflects the CP-odd effect in the decay process. In single top production, the top spin in its rest frame is always in the direction of the d or $\bar{d}$ quark [36]. Although this gets modified by the operator O_{tW} in the production vertex as is shown in Eqs. (2.36), (2.37), the direction in which the top spin deviates is independent of the decay process, and thus the leading order effect gets averaged out as one considers the asymmetries. Therefore the d or $\bar{d}$ three-momentum can be used to replace the top spin in Eq. (2.63):

$$T = (\mathbf{p}_b \times \mathbf{p}_{e^+}) \cdot \mathbf{p}_{d,\bar{d}} \tag{2.79}$$

and the asymmetry becomes

$$\begin{aligned} A_{t\to Wb} &= \frac{N(T>0) - N(T<0)}{N(T>0) + N(T<0)} \\ &= \mathrm{Im}C_{tW} \frac{3\pi v^2 (m_t^2 - m_W^2)}{4\sqrt{2}\Lambda^2 V_{tb}(m_t^2 + 2m_W^2)} \end{aligned} \tag{2.80}$$

which agrees with Eq. (2.64).

2.4.3 CP-Violation in Top Pair Production

The CP-violation effects in top pair production and decay have been considered in the literature before. Refs. [54, 55] have considered the CP-violation effect in the multi-Higgs doublet extensions of the SM. The effect of the top quark "chromoelectric" dipole moment, which corresponds the operator O_{tG} with an imaginary coefficient, can be found in Refs. [56, 57, 58], where [58] has also considered the other two operators, $O_{\tilde{G}}$ and O_{tW}. An analysis of the lepton transverse energy asymmetry at the Tevatron can be found in Ref. [59]. A recent numerical study of the ATLAS sensitivity to the complex phase of the Wtb anomalous couplings can be found in Ref. [23]. The CP-violation effects of the top quark at linear colliders and photon colliders are discussed in Refs. [14, 60, 9].

In the top pair production processes, there are three operators that will contribute to CP violating

observables:

$$\begin{aligned} O_{tG} &= (\bar{q}\sigma^{\mu\nu}\lambda^A t)\tilde{\phi}G^A_{\mu\nu} \\ O_{\tilde{G}} &= f_{ABC}\tilde{G}^{A\nu}_{\mu}G^{B\rho}_{\nu}G^{C\mu}_{\rho} \\ O_{\phi\tilde{G}} &= \frac{1}{2}(\phi^+\phi)\tilde{G}^A_{\mu\nu}G^{A\mu\nu} \end{aligned} \tag{2.81}$$

where $\tilde{G}_{\mu\nu} = \epsilon_{\mu\nu\rho\sigma}G^{\rho\sigma}$. The first one contributes to both $gg \to t\bar{t}$ and $q\bar{q} \to t\bar{t}$ channels, while the last two contribute only to the $gg \to t\bar{t}$ channel.

A natural choice of the CP-odd observable is the triple-product considered in single top production. One could define similar quantities such as

$$T = (\mathbf{p}_g \times \mathbf{p}_g) \cdot \mathbf{s}_t \tag{2.82}$$

However this quantity doesn't result in any asymmetry, because the three CP-odd operators are P-odd but C-even. For both $gg \to t\bar{t}$ and $q\bar{q} \to t\bar{t}$ channels, under PT_N symmetry the initial and final state do not change, except that the spins of t and $\bar{t}$ are flipped. This means that T defined in Eq. (2.82) is PT_N-odd and therefore the C-even operators cannot result in non-zero expectation values for T. We will need the spin information of both t and $\bar{t}$ to observe CP-violation effect.

Here we define our CP-odd observables in a different way than the usual CP-odd triple product in most of the literature. In the top quark semileptonic decay, the amplitude contains a factor which is the inner product of the top spin and the lepton spin [56], and therefore we can use the spin projection operator to project the top spin on to the direction of the lepton three-momentum and ignore the other two decay products, in order to reduce the problem to a 2 to 2 scattering problem.

Consider the quark channel process $q\bar{q} \to t\bar{t}$ followed by the semileptonic decays of both t and $\bar{t}$ quarks. We choose the coordinate axes such that in the CM frame, the top quark momentum is in the z-direction, the q and $\bar{q}$ momenta are in xz plane, and the angle between the q and t momenta is θ. Let $\hat{\mathbf{p}}_{e^+} = (\sin\alpha_1\cos\beta_1, \sin\alpha_1\sin\beta_1, \cos\alpha_1)$ be the unit vector of the positron three-momentum in the top rest frame, $\hat{\mathbf{p}}_e = (\sin\alpha_2\cos\beta_2, \sin\alpha_2\sin\beta_2, \cos\alpha_2)$ be the unit vector of the electron three-momentum in the anti-top rest frame, and $\mathbf{v} = (\cos\theta, 0, \sqrt{1-\beta^2}\sin\theta)$. Define the following triple-product:

$$T = (\hat{\mathbf{p}}_{e^+} \times \hat{\mathbf{p}}_e) \cdot \mathbf{v} \tag{2.83}$$

we find that the the contribution from O_{tG} can be written as:

$$\frac{d\sigma}{d\cos\theta d\cos\alpha_1 d\beta_1 d\cos\alpha_2 d\beta_2} = -\mathrm{Im}C_{tG}\frac{g_s^3 v\beta^2\sin\theta}{23328\sqrt{2}\pi^3\Lambda^2\sqrt{s}}T \tag{2.84}$$

Clearly T leads to an asymmetry:

$$\begin{aligned} A_{q\bar{q}\to t\bar{t}} &= \frac{N(T>0)-N(T<0)}{N(T>0)+N(T<0)} \\ &= -\mathrm{Im}C_{tG}\frac{\pi\sqrt{s}v\sqrt{1-\beta^2}}{2\sqrt{2}g_s\Lambda^2\beta(3-\beta^2)}\left(K\left(\frac{\beta^2}{\beta^2-1}\right)-(1-2\beta^2)E\left(\frac{\beta^2}{\beta^2-1}\right)\right) \end{aligned} \tag{2.85}$$

where

$$K(k^2) = \int_0^{\pi/2}\frac{d\theta}{\sqrt{1-k^2\sin^2\theta}} \tag{2.86}$$

and

$$E(k^2) = \int_0^{\pi/2}\sqrt{1-k^2\sin^2\theta}d\theta \tag{2.87}$$

are the complete elliptic integral of the first and the second kind. The SM has no contribution to this asymmetry because T is parity-odd while the strong interaction is parity-even.

Now consider the gluon channel $gg \to t\bar{t}$. We use the same coordinate system, i.e. top quark momentum is in the z-direction and gluon momenta are in the xz plane. $\hat{\mathbf{p}}_{e^+}$ ($\hat{\mathbf{p}}_e$) is the unit vector in the direction of the momentum of the positron (electron) in the top (anti-top) rest frame. Define two triple-products T_z and T_x:

$$T_z = (\hat{\mathbf{p}}_{e^+}\times\hat{\mathbf{p}}_e)\cdot\hat{\mathbf{z}} \tag{2.88}$$

$$T_x = (\hat{\mathbf{p}}_{e^+}\times\hat{\mathbf{p}}_e)\cdot\hat{\mathbf{x}} \tag{2.89}$$

The cross-section due to the CP-odd operators is

$$\frac{d\sigma}{d\cos\theta d\cos\alpha_1 d\beta_1 d\cos\alpha_2 d\beta_2} = \mathrm{Im}C_{tG}(f_{tG}^z T_z + f_{tG}^x T_x) + C_{\tilde{G}}(f_{\tilde{G}}^z T_z + f_{\tilde{G}}^x T_x) + C_{\phi\tilde{G}}f_{\phi\tilde{G}}^z T_z \tag{2.90}$$

where

$$
\begin{aligned}
f^z_{tG} &= -\frac{g_s^3 v\beta^2}{248832\sqrt{2}\pi^3\Lambda^2\sqrt{s}(1-\beta^2\cos^2\theta)^2}\sqrt{1-\beta^2} \\
&\quad \left(9\beta^4\cos^6\theta + (7\beta^2-18\beta^4)\cos^4\theta + (18\beta^4-25\beta^2+16)\cos^2\theta + 7(2\beta^2-3)\right) \qquad (2.91)\\
f^x_{tG} &= \frac{g_s^3 v\beta^2}{248832\sqrt{2}\pi^3\Lambda^2\sqrt{s}(1-\beta^2\cos^2\theta)^2} \\
&\quad \left(9\beta^4\cos^4\theta + (7\beta^2-9\beta^4)\cos^2\theta - (23\beta^2-16)\right)\sin\theta\cos\theta \qquad (2.92)\\
f^z_{\tilde{G}} &= \frac{3g_s^3\beta^2(1-\beta^2)\cos^2\theta}{165888\pi^3\Lambda^2(1-\beta^2\cos^2\theta)} \qquad (2.93)\\
f^x_{\tilde{G}} &= -\frac{3g_s^3\beta^2\sqrt{1-\beta^2}\sin\theta\cos\theta}{165888\pi^3\Lambda^2(1-\beta^2\cos^2\theta)} \qquad (2.94)\\
f^z_{\phi\tilde{G}} &= -\frac{g_s^2 s\beta^2(1-\beta^2)}{165888\pi^3\Lambda^2(s-m_h^2)(1-\beta^2\cos^2\theta)} \qquad (2.95)
\end{aligned}
$$

In general, any quantity that has the form $T(\hat{\mathbf{a}}) = (\hat{\mathbf{p}}_{e^+}\times\hat{\mathbf{p}}_e)\cdot\hat{\mathbf{a}}$ may lead to an asymmetry. Using the following property of $T(\hat{\mathbf{a}})$:

$$\int \mathrm{d}\Omega_{e^+}\mathrm{d}\Omega_e T(\hat{\mathbf{a}})\mathrm{sign}\left(T(\hat{\mathbf{b}})\right) = 2\pi^3\left(\hat{\mathbf{a}}\cdot\hat{\mathbf{b}}\right) \qquad (2.96)$$

we find the asymmetry of $T(\hat{\mathbf{a}})$ is

$$
\begin{aligned}
&\frac{d\sigma(T(\hat{\mathbf{a}})>0)}{d\cos\theta} - \frac{d\sigma(T(\hat{\mathbf{a}})<0)}{d\cos\theta} \\
&= 2\pi^3\left[\mathrm{Im}C_{tG}(f^z_{tG}a_z + f^x_{tG}a_x) + C_{\tilde{G}}(f^z_{\tilde{G}}a_z + f^x_{\tilde{G}}a_x) + C_{\phi\tilde{G}}f^z_{\phi\tilde{G}}a_z\right] \qquad (2.97)
\end{aligned}
$$

2.5 Conclusions

We have considered the effects of dimension-six operators in top quark production and decay processes in hadron colliders. The analysis is linear in the coefficients of these operators, therefore the deviation from the SM is the interference terms between the SM and the new operators. In general, integrating out heavy particles leads not to just one but to several operators whose coefficients are related. Therefore it is necessary to consider all dimension-six operators simultaneously. Fortunately, although the total number of these operators is large, we found that there are only 15 operators that can have significant interference terms. In addition, for each decay or production process, only a few of them will contribute. This is one of the advantages of the effective field theory approach: although we don't have any knowledge of the new physics beyond the SM, by making use of power counting and symmetries, the number of parameters required to describe the new physics can be largely reduced.

We have obtained the deviation from the SM caused by these operators. This allows us to constrain

the new physics in a systematic way. For example, we can measure (or put bounds on) the operator O_{tW} by measuring the W boson helicity fraction $F_{L,R,0}$ and the analyzing power $\alpha_{b,\nu}$, and then use the s- and t-channel single top production to put bounds on $O_{\phi q}^{(3)}$ and $O_{qq}^{(1,3)}$. The operator O_{tG} can be constrained from the Wt associated production and the gluon channel $t\bar{t}$ production, while the latter process also constrains O_G and $O_{\phi G}$. Finally, the quark channel $t\bar{t}$ production can be used to put bounds on the four linear combinations of the four-quark operators.

The CP-violation effects in top quark physics are of particular interest. We have calculated the spin asymmetries caused by the 4 CP-odd operators. The observation of these asymmetries can be evidence of physics beyond the SM. In the single top production, these are the spin asymmetries in the direction perpendicular to the production plane. One could use the top decay process as a spin analyzer to study the asymmetry in the top production process, or vice versa. In $t\bar{t}$ production, we showed that both the top quark spin and anti-top quark spin are required to construct CP-odd observables.

Chapter 3

PEWM vs W-Helicity Measurements[1]

In Chapter 2 we have considered the effects of dimension-six operators on top-quark production and decay. The top quark also plays an important role as a virtual particle in precision electroweak physics. Indeed, the correct range for the top-quark mass was anticipated by precision electroweak studies. Now that the top-quark mass is accurately known from direct measurements, we can ask what the PEWM have to say about the presence of dimension-six operators in loop diagrams involving the top quark. As we have explained in Chapter 1, the effective field theory is a renormalizable theory in the modern sense, and is able to calculate radiative corrections involving effective interactions. Therefore this is a well-defined question with an unambiguous answer.

In this Chapter, we will focus on just one dimension-six operator that affects the top quark,

$$O_{tW} = (\bar{q}\sigma^{\mu\nu}\tau^I t)\tilde{\phi}W^I_{\mu\nu}, \tag{3.1}$$

We chose this operator because as we have shown in Eq. (2.14), it is the only one which contributes to the leading correction to the branching ratio of the top quark to W bosons of zero helicity.[2] Thus this operator can already be bounded from present data.

The remainder of this Chapter is organized as follows. In Section 3.1, we extract bounds on this operator from W-helicity fraction measurements. In Section 3.2, we calculate the contribution of this operator to precision electroweak data via a top-quark loop and compare the resulting bound on this operator with the bound obtained from W-helicity measurements. In Section 3.3, we perform a more general analysis, assuming that new physics is oblique. The conclusion is present in Section 3.4.

[1] The work presented in this Chapter is published in Ref. [61].

[2] Two other operators contribute to the leading correction to the branching ratio of the top quark to W bosons of positive helicity [22, 62].

3.1 Constraints from W-helicity Fraction

When the Higgs field acquires a vacuum-expectation value, the dimension-six operator O_{tW} yields the effective interactions [10]

$$\begin{aligned}\mathcal{L}_{eff} &= \mathcal{L}_{SM} + \frac{C_{tW}}{\Lambda^2}\Big[(v(\bar{b}\sigma^{\mu\nu}(1+\gamma_5)t)\partial_\mu W^-_\nu + h.c.) \\ &\quad +\sqrt{2}c_W v(\bar{t}\sigma^{\mu\nu}t)\partial_\mu Z_\nu + \sqrt{2}s_W v(\bar{t}\sigma^{\mu\nu}t)\partial_\mu A_\nu - \sqrt{2}igv(\bar{t}\sigma^{\mu\nu}t)W^+_\mu W^-_\nu + \cdots\Big] \end{aligned} \tag{3.2}$$

where C_{tW} is a dimensionless coefficient, $v \approx 246$ GeV is the Higgs vacuum expectation value, and s_W, c_W are the sine and cosine of the weak mixing angle. The first term in the effective interactions modifies the top-quark branching ratios to zero-helicity, negative-helicity, and positive-helicity W bosons (see Fig. 3.1), as is given in Eq. (2.14)

$$f_0 = \frac{m_t^2}{m_t^2+2m_W^2} - \frac{4\sqrt{2}C_{tW}v^2}{\Lambda^2}\frac{m_t m_W(m_t^2-m_W^2)}{(m_t^2+2m_W^2)^2} \tag{3.3}$$

$$f_- = \frac{2m_W^2}{m_t^2+2m_W^2} + \frac{4\sqrt{2}C_{tW}v^2}{\Lambda^2}\frac{m_t m_W(m_t^2-m_W^2)}{(m_t^2+2m_W^2)^2} \tag{3.4}$$

$$f_+ = 0 \tag{3.5}$$

where we have neglected the bottom-quark mass throughout, which is an excellent approximation for the operator O_{tW} (but not for the other two operators mentioned in a previous footnote [22, 62]).

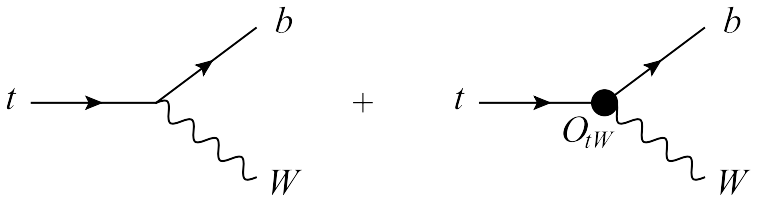

Figure 3.1: The dimension-six operator O_{tW} contributes to the top-quark decay process through a correction to the Wtb vertex.

We compare with recent data from the CDF [63] and D0 [64] collaborations, which report a measurement of f_0 (with the constraint $f_+ = 0$ imposed):

$$f_0 = 0.62 \pm 0.11\,(\text{stat}) \pm 0.06\,(\text{syst}) \quad (\text{CDF})\,, \tag{3.6}$$

$$f_0 = 0.735 \pm 0.051\,(\text{stat}) \pm 0.051\,(\text{syst}) \quad (\text{D0})\,. \tag{3.7}$$

These measurements are consistent with the SM prediction, at NNLO in QCD [65],

$$f_0 = 0.687(5) \tag{3.8}$$

where the uncertainty is primarily from the uncertainty in the top-quark mass. Because we are using an effective-field-theory approach, we can consistently include both QCD radiative corrections and the correction due to the dimension-six operator. Comparing with data yields the constraints

$$\frac{C_{tW}}{\Lambda^2} = 1.10 \pm 2.06 \text{ TeV}^{-2} \quad \text{(CDF)} , \tag{3.9}$$

$$\frac{C_{tW}}{\Lambda^2} = -0.79 \pm 1.19 \text{ TeV}^{-2} \quad \text{(D0)} . \tag{3.10}$$

The NLO QCD correction to the second term in Eq. (3.3) is also known [66]. It increases the value of C_{tW}/Λ^2 by about 1%, much less than the uncertainty in this quantity.

3.2 Constraints from PEWM

We now turn to the effect of O_{tW} on precision electroweak measurements via a top-quark loop, as shown in Fig. 3.2.[3] Since this loop only affects the electroweak-gauge-boson self energies, we may be able to use the well-known S, T, U formalism to characterize it [67, 68, 69]. The idea is to Taylor-expand the four self-energies Π_{WW}, Π_{ZZ}, $\Pi_{\gamma\gamma}$ and $\Pi_{\gamma Z}$ (which only include the new physics contributions), to the leading order of q^2. Requiring the photon to be massless, $\Pi_{\gamma\gamma}$ and $\Pi_{\gamma Z}$ must be zero at $q^2 = 0$, so there will be six non-zero coefficients. Three of them are absorbed in the definition of g, g' and v. This leaves three independent parameters.

Following Ref. [69], we define these oblique parameters in terms of self energies and derivatives of self energies at $q^2 = 0$,

$$\hat{S} = -\frac{c_W}{s_W}\Pi'_{30}(0) = c_W^2\Pi'_{ZZ}(0) - \frac{c_W}{s_W}(c_W^2 - s_W^2)\Pi'_{\gamma Z}(0) - c_W^2\Pi'_{\gamma\gamma}(0) \tag{3.11}$$

$$\hat{T} = -\frac{\Pi_{33}(0) - \Pi_{11}(0)}{m_W^2} = \frac{1}{m_W^2}\left[\Pi_{WW}(0) - c_W^2\Pi_{ZZ}(0)\right] \tag{3.12}$$

$$\hat{U} = \Pi'_{33}(0) - \Pi'_{11}(0) = -\Pi'_{WW}(0) + c_W^2\Pi'_{ZZ}(0) + 2c_W s_W\Pi'_{\gamma Z}(0) + s_W^2\Pi'_{\gamma\gamma}(0) . \tag{3.13}$$

The contribution of the operator O_{tW} to the oblique parameters, via Fig. 3.2, is calculated in dimensional

[3] There is also a diagram contributing to the W-boson self energy, with a top-quark loop, constructed from the contact interaction given by the last term in Eq. (3.2). Since this interaction is antisymmetric in μ, ν, this diagram does not contribute to the self energy.

regularization to be

$$\hat{S} = N_c \frac{g C_{tW}}{4\pi^2} \frac{\sqrt{2} v m_t}{4\Lambda^2} \frac{5}{3} \left(\frac{1}{\epsilon} - \gamma + \ln 4\pi - \ln \frac{m_t^2}{\mu^2} \right) \tag{3.14}$$

$$\hat{T} = 0 \tag{3.15}$$

$$\hat{U} = N_c \frac{g C_{tW}}{4\pi^2} \frac{\sqrt{2} v m_t}{4\Lambda^2} \tag{3.16}$$

where $N_c = 3$ is the number of colors and μ is the 't Hooft mass.

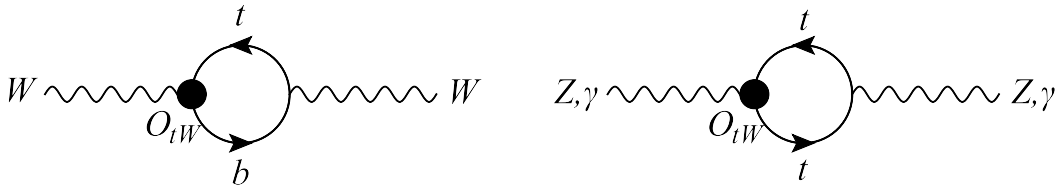

Figure 3.2: The dimension-six operator O_{tW} contributes to the electroweak-gauge-boson self energies via loop diagrams.

The contribution of O_{tW} to the $\hat{S}$ parameter is ultraviolet divergent. However, there is another dimension-six operator,

$$O_{WB} = (\phi^\dagger \tau^I \phi) W^I_{\mu\nu} B^{\mu\nu} \ , \tag{3.17}$$

($B^{\mu\nu}$ is the $U(1)_Y$ field-strength tensor) that contributes to the $\hat{S}$ parameter at tree level, as shown in Fig. 3.3. This operator must be included for consistency, since it also contributes to the $\hat{S}$ parameter at order $1/\Lambda^2$. We find

$$\hat{S} = \frac{C^0_{WB} v^2}{\Lambda^2} \frac{c_W}{s_W} \tag{3.18}$$

where C^0_{WB} is the bare coefficient of the operator. This coefficient is renormalized by the one-loop contribution of the operator O_{tW} in Eq. (3.14). In the $\overline{\rm MS}$ scheme, the total contribution to the $\hat{S}$ parameter is

$$\hat{S} = \frac{C_{WB}(\mu) v^2}{\Lambda^2} \frac{c_W}{s_W} - N_c \frac{g C_{tW}}{4\pi^2} \frac{\sqrt{2} v m_t}{4\Lambda^2} \frac{5}{3} \ln \frac{m_t^2}{\mu^2} \tag{3.19}$$

which is finite and unambiguous. This is an example of the renormalizability of an effective field theory in the modern sense. Although an effective field theory is not renormalizable in the old-fashioned sense, it is renormalizable at any order in $1/\Lambda$, provided that all the pertinent operators are included [3].

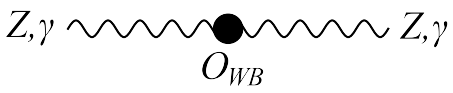

Figure 3.3: The operator O_{WB} contributes to the electroweak-gauge-boson self energies at tree level.

Although the result for the $\hat{S}$ parameter is finite and unambiguous, it cannot be used to constrain the coefficient C_{tW}, because of the tree-level contribution from the operator O_{WB}. A measurement of the $\hat{S}$ parameter constrains only the linear combination of C_{WB} and C_{tW} contained in Eq. (3.19). For the choice $\mu = m_t$, a measurement of the $\hat{S}$ parameter constrains only $C_{WB}(m_t)$.

There is no contribution to the $\hat{T}$ parameter from the operator O_{tW} [see Eq. (3.15)]. Even if there were a contribution, there is also a tree-level contribution from the operator $O_\phi^{(3)} = (\phi^\dagger D^\mu \phi)[(D_\mu \phi)^\dagger \phi]$ that would mask the one-loop contribution from O_{tW}. A top-quark model that gives a nonvanishing contribution to the $\hat{T}$ parameter is discussed in Ref. [70].

There is no tree-level contribution to the $\hat{U}$ parameter, defined by Eq. (3.13), at order $1/\Lambda^2$, so the one-loop contribution from the operator O_{tW}, Eq. (3.16), is the sole contribution at this order. The one-loop result is finite, as guaranteed by the renormalizability of the effective field theory in the modern sense.

The value of the $\hat{U}$ parameter may be obtained from Ref. [71]. In Ref. [71], the U parameter is defined as

$$\begin{aligned}\alpha U =& 4s_W^2 \left[\frac{\Pi_{11}(m_W^2) - \Pi_{11}(0)}{m_W^2} - \frac{\Pi_{33}(m_Z^2) - \Pi_{33}(0)}{m_Z^2}\right] \\ =& 4s_W^2 \left[\frac{\Pi_{WW}(m_W^2) - \Pi_{WW}(0)}{m_W^2} - \frac{c_W^2(\Pi_{ZZ}(m_Z^2) - \Pi_{ZZ}(0)) + 2s_W c_W \Pi_{\gamma Z}(m_Z^2) + s_W^2 \Pi_{\gamma\gamma}(m_Z^2)}{m_Z^2}\right]\end{aligned} \tag{3.20}$$

(α is the fine structure constant) which apparently differs from the definition of $\hat{U}$ in Eq. (3.13). However, Ref. [71] tacitly assumes that the gauge boson self energies are linear in q^2, in which case the two definitions of U are equivalent up to normalization: $\hat{U} = -\alpha U/4s_W^2$. Nevertheless, we must also check whether our calculation of the contribution to the self-energy function from O_{tW} is approximately linear in q^2. Since the constraint on the U parameter comes dominantly from the measurement of the W-boson mass [71], it suffices to show that the linear approximation is valid in predicting the value of W-boson mass.

In the $\hat{S}, \hat{T}, \hat{U}$ formalism, the W-boson mass can be expressed as [68]

$$\begin{aligned} m_W^2 &= m_W^2(\mathrm{SM})\left(1 - \frac{2s_W^2}{c_W^2 - s_W^2}\hat{S} + \frac{c_W^2}{c_W^2 - s_W^2}\hat{T} - \hat{U}\right) \\ &= m_W^2(\mathrm{SM}) + \frac{c_W^2}{c_W^2 - s_W^2}\Pi_{WW}(0) + m_W^2 \Pi'_{WW}(0) \\ &\quad - \frac{c_W^4}{c_W^2 - s_W^2}\left[\Pi_{ZZ}(0) + m_Z^2 \Pi'_{ZZ}(0)\right] + \frac{s_W^2 c_W^2}{c_W^2 - s_W^2} m_Z^2 \Pi'_{\gamma\gamma}(0), \end{aligned} \tag{3.21}$$

where the definitions of $\hat{S}, \hat{T}, \hat{U}$ in Eqs. (3.11-3.13) are used, and $m_W(\mathrm{SM})$ is the value of the W-boson mass calculated as accurately as possible in the SM.

The exact formula for m_W, without assuming a linear dependence of the self energies on q^2, is

$$m_W^2 = m_W^2(\mathrm{SM}) + \Pi_{WW}(m_W^2) + \frac{s_W^2}{c_W^2 - s_W^2}\Pi_{WW}(0) - \frac{c_W^4}{c_W^2 - s_W^2}\Pi_{ZZ}(m_Z^2) + \frac{s_W^2 c_W^2}{c_W^2 - s_W^2} m_Z^2 \Pi'_{\gamma\gamma}(0) \ . \quad (3.22)$$

Comparing Eqs. (3.21) and (3.22), we find that the error introduced by the linear approximation is

$$\delta m_W^2 = -\left[\Pi_{WW}(m_W^2) - \Pi_{WW}(0) - m_W^2 \Pi'_{WW}(0)\right] + \frac{c_W^4}{c_W^2 - s_W^2}\left[\Pi_{ZZ}(m_Z^2) - \Pi_{ZZ}(0) - m_Z^2 \Pi'_{ZZ}(0)\right] \ . \quad (3.23)$$

For the operator O_{tW}, we find

$$\begin{aligned} \delta m_W^2 &= -N_c \frac{g C_{tW}}{4\pi^2} \frac{\sqrt{2} v m_t}{\Lambda^2} m_W^2 \left\{ \frac{3 - 8 s_W^2}{3(1 - 2 s_W^2)} c_W^2 \left(1 - \frac{\sqrt{4m_t^2 - m_Z^2}}{m_Z} \arctan \frac{m_Z}{\sqrt{4m_t^2 - m_Z^2}} \right) \right. \\ &\quad \left. + \frac{1}{2}\left[\frac{m_t^2}{m_W^2} + \left(\frac{m_t^2}{m_W^2} - 1 \right)^2 \ln\left(1 - \frac{m_W^2}{m_t^2} \right) \right] - \frac{3}{4} \right\} \\ &= 0.47 \ \mathrm{GeV}^2 \frac{C_{tW}}{\Lambda^2} \mathrm{TeV}^2 \ . \end{aligned} \quad (3.24)$$

Using the world-average W-boson mass, $m_W = 80.399 \pm 0.023$ GeV, the uncertainty in m_W^2 is $\delta m_W^2 \approx 4$ GeV^2. As we will see shortly, the value of C_{tW}/Λ^2 extracted from precision electroweak data is of order 1 TeV^{-2}, so the error introduced by the linear approximation, Eq. (3.24), is an order of magnitude less than the experimental uncertainty in m_W^2. Thus the linear approximation is excellent, and we may use the U parameter to bound C_{tW}/Λ^2. The linear approximation is valid because the expansion parameter for the contribution of the operator O_{tW} to the self energies (Fig. 3.2) is q^2/m_t^2, and this parameter is sufficiently small for the values $q^2 = m_W^2, m_Z^2$ needed in Eq. (3.23).

The value of the U parameter is [71]

$$U = 0.06 \pm 0.10 \quad (3.25)$$

for $m_t = 173.0$ GeV and $m_h = 117$ GeV, although there is very little dependence on the Higgs mass. This corresponds to

$$\hat{U} = (-5.0 \pm 8.4) \times 10^{-4} \quad (3.26)$$

Using Eq. (3.16), we find the constraint

$$\frac{C_{tW}}{\Lambda^2} = -0.7 \pm 1.1 \ \mathrm{TeV}^{-2} \quad (3.27)$$

which is slightly stronger than the constraint from the measurement of top-quark decay, Eqs. (3.9) and (3.10).

3.3 A More General Analysis with All Oblique Parameters Included

Thus far we have assumed that O_{tW}, O_{WB}, and $O_\phi^{(3)}$ are the only nonvanishing dimension-six operators. We can relax this assumption by including, along with O_{tW}, all dimension-six operators that contribute to the gauge-boson self energies at tree level, which includes O_{WB} and $O_\phi^{(3)}$. These are [72]

$$O_{WB} = (\phi^\dagger \tau^I \phi) W^I_{\mu\nu} B^{\mu\nu} \,, \qquad O_\phi^{(3)} = (\phi^\dagger D^\mu \phi)[(D_\mu \phi)^\dagger \phi] \,, \tag{3.28}$$

$$O_{DB} = \tfrac{1}{2}(\partial_\rho B_{\mu\nu})(\partial^\rho B^{\mu\nu}) \,, \qquad O_{DW} = \frac{1}{2}(D_\rho W^I_{\mu\nu})(D^\rho W^{I\mu\nu}) \,. \tag{3.29}$$

Such operators originate whenever heavy fields directly couple only to the SM gauge fields and the Higgs doublet. Such operators are sometimes referred to as "universal."

Once these operators are included, the self energies are no longer approximately linear functions of q^2, since O_{DB} and O_{DW} generate terms proportional to q^4. Therefore we need four additional oblique parameters, which correspond to the second order derivatives of the four self energies with respect to q^2. Along with $\hat{S}, \hat{T}, \hat{U}$, we will use the four additional oblique parameters defined in Ref. [69]:

$$V = -\frac{m_W^2}{2}(\Pi''_{33}(0) - \Pi''_{11}(0)) = \frac{m_W^2}{2}\left[\Pi''_{WW}(0) - c_W^2 \Pi''_{ZZ}(0) - 2c_W s_W \Pi''_{\gamma Z}(0) - s_W^2 \Pi''_{\gamma\gamma}(0)\right] \tag{3.30}$$

$$W = -\frac{m_W^2}{2}\Pi''_{33}(0) = -\frac{m_W^2}{2}\left[c_W^2 \Pi''_{ZZ}(0) + 2c_W s_W \Pi''_{\gamma Z}(0) + s_W^2 \Pi''_{\gamma\gamma}(0)\right] \tag{3.31}$$

$$X = -\frac{m_W^2}{2}\Pi''_{30}(0) = \frac{m_W^2}{2}\left[c_W s_W \Pi''_{ZZ}(0) - (c_W^2 - s_W^2)\Pi''_{\gamma Z}(0) - c_W s_W \Pi''_{\gamma\gamma}(0)\right] \tag{3.32}$$

$$Y = -\frac{m_W^2}{2}\Pi''_{00}(0) = -\frac{m_W^2}{2}\left[s_W^2 \Pi''_{ZZ}(0) - 2c_W s_W \Pi''_{\gamma Z}(0) + c_W^2 \Pi''_{\gamma\gamma}(0)\right] \tag{3.33}$$

At tree level, four of the seven oblique parameters receive a contribution from a dimension-six operator:

$$\hat{S} = C_{WB}\frac{c_W}{s_W}\frac{v^2}{\Lambda^2}, \tag{3.34}$$

$$\hat{T} = -C_{\phi}^{(3)}\frac{v^2}{2\Lambda^2}, \tag{3.35}$$

$$W = -2C_{DW}\frac{m_W^2}{\Lambda^2}, \tag{3.36}$$

$$Y = -2C_{DB}\frac{m_W^2}{\Lambda^2}. \tag{3.37}$$

The other three oblique parameters, $\hat{U}$, V, and X, are zero at tree level. Thus the contribution to these parameters from O_{tW} at one loop (Fig, 3.2) must be finite, as guaranteed by the renormalizability of the effective field theory in the modern sense. We find

$$\hat{U} = N_c\frac{gC_{tW}}{4\pi^2}\frac{\sqrt{2}vm_t}{4\Lambda^2}, \tag{3.38}$$

$$V = -N_c\frac{gC_{tW}}{4\pi^2}\frac{\sqrt{2}vm_t}{\Lambda^2}\frac{m_W^2}{12m_t^2}, \tag{3.39}$$

$$X = N_c\frac{gC_{tW}}{4\pi^2}\frac{\sqrt{2}vm_t}{\Lambda^2}\frac{5m_Z^2}{72m_t^2}s_W c_W. \tag{3.40}$$

where the result for $\hat{U}$ was already given in Eq. (3.16). The one-loop contribution to the parameter Y vanishes, and the one-loop contribution to the W parameter is $-V$ [Eq. (3.39)].

In order to obtain constraints on $\hat{U}$, V and X, we did a global fit using most major precision electroweak measurements. These include the Z-pole data, the W-boson mass and width, DIS and atomic parity violation, and fermion pair production at LEP 2. The data and corresponding SM predictions can be found in [71, 73, 74, 75]. The corrections to these observables from the seven oblique parameters can be derived from the "star" formalism described in Ref. [68]. We will present the details of this formalism in Chapter 3. We calculated the total χ^2 as a function of the oblique parameters. The central value for the fit is given by minimizing χ^2, and the one-sigma bound is given by $\chi^2 - \chi^2_{\rm min} = 1$. We let $\hat{S}$, $\hat{T}$, W and Y freely float and put constraints on the $\hat{U}$, V and X parameters. We find three statistically independent combinations:

$$0.46\hat{U} - 0.46V + 0.76X = -0.0013 \pm 0.0007, \tag{3.41}$$

$$0.54\hat{U} - 0.54V - 0.65X = 0.0000 \pm 0.0017, \tag{3.42}$$

$$0.71\hat{U} + 0.71V = -0.009 \pm 0.030. \tag{3.43}$$

The most stringent constrain, Eq. (3.41), corresponds to $\hat{U} - V + \frac{2s_W c_W}{c_W^2 - s_W^2}X$, which appears in the theoretical

value of the W-boson mass:

$$m_W^2 = m_W^2(\mathrm{SM})\left[1 - \frac{1}{c_W^2 - s_W^2}\left(2s_W^2\hat{S} - c_W^2\hat{T} - s_W^2 W - s_W^2 Y\right) - \left(\hat{U} - V + \frac{2s_W c_W}{c_W^2 - s_W^2}X\right)\right]. \tag{3.44}$$

Combining Eqs. (3.38-3.41) yields the constraint

$$\frac{C_{tW}}{\Lambda^2} = -3.4 \pm 2.0 \text{ TeV}^{-2}. \tag{3.45}$$

Including Eqs. (3.42) and (3.43) gives a slightly better constraint,

$$\frac{C_{tW}}{\Lambda^2} = -2.8 \pm 1.8 \text{ TeV}^{-2}. \tag{3.46}$$

This constraint is weaker than the one given in Eq. (3.27), but it is still comparable in precision to the constraints from direct measurements, Eqs. (3.9) and (3.10). It applies in more general situations than Eq. (3.27), as we only assume that the new physics is oblique (aside from O_{tW}). If this assumption were not valid, and additional operators were present at low energies, our analysis could be extended to include them. The central value of C_{tW} in Eq. (3.46) is nonzero at 1.5σ, which indicates that the precision electroweak data have a slight preference for the presence of physics beyond the standard model.

Constraints on the operator O_{tW} may also be gleaned from B physics. This operator affects the branching ratio for $\bar{B} \to X_s\gamma$, which is a loop-induced process. It was found in Ref. [76] that the contribution from O_{tW} is ultraviolet divergent. Thus there must be a tree-level contribution from another dimension-six operator, which masks the contribution from O_{tW}. The operator O_{tW} also affects $B - \bar{B}$ mixing, and it was found in Ref. [77] that the contribution is ultraviolet finite, despite the fact that there are other dimension-six operators that contribute to this process at tree level. Focusing only on O_{tW}, the constraint

$$\frac{C_{tW}}{\Lambda^2} = -0.06 \pm 1.57 \text{ TeV}^{-2}. \tag{3.47}$$

was obtained, which is comparable with the bounds from precision electroweak data [Eq. (3.27)] and top-quark decay [Eqs. (3.9) and (3.10)].

3.4 Conclusions

We found that the indirect measurement of the coefficient of the operator O_{tW} from precision electroweak data is comparable in precision to the direct measurement from the branching ratio of top quarks to W

bosons of zero helicity. The indirect measurement will become more accurate with more precise electroweak measurements, in particular of the W-boson mass. The direct measurement will become more accurate with more data from the Tevatron and the Large Hadron Collider. The direct measurement has the advantage that is affected, at order $1/\Lambda^2$, only by the operator O_{tW}. In contrast, there are nine operators that contribute to precision electroweak data at order $1/\Lambda^2$, of which O_{tW} is just one. In Chapter 4, we will present a global analysis of constraints on these dimension-six operators from PEWM.

Chapter 4

A Global Analysis for PEWM

Any operator that generates anomalous interaction among top quark and a electroweak gauge boson can potentially affect the precision electroweak data. These operators modify the SM $W\bar{t}b$, $Z\bar{t}t$ and $\gamma\bar{t}t$ vertices, and therefore contribute to the self-energies of the electroweak bosons, via top-quark loop. There are 9 such operators at dimension-6:

$$O_{\phi q}^{(3)} = i(\phi^\dagger \tau^I D_\mu \phi)(\bar{q}\gamma^\mu \tau^I q), \tag{4.1}$$

$$O_{\phi q}^{(1)} = i(\phi^\dagger D_\mu \phi)(\bar{q}\gamma^\mu q), \tag{4.2}$$

$$O_{\phi t} = i(\phi^\dagger D_\mu \phi)(\bar{t}\gamma^\mu t), \tag{4.3}$$

$$O_{\phi b} = i(\phi^\dagger D_\mu \phi)(\bar{b}\gamma^\mu b), \tag{4.4}$$

$$O_{\phi\phi} = i(\tilde{\phi}^\dagger D_\mu \phi)(\bar{t}\gamma^\mu b), \tag{4.5}$$

$$O_{tW} = (\bar{q}\sigma^{\mu\nu}\tau^I t)\tilde{\phi} W_{\mu\nu}^I, \tag{4.6}$$

$$O_{bW} = (\bar{q}\sigma^{\mu\nu}\tau^I b)\phi W_{\mu\nu}^I, \tag{4.7}$$

$$O_{tB} = (\bar{q}\sigma^{\mu\nu} t)\tilde{\phi} B_{\mu\nu}, \tag{4.8}$$

$$O_{bB} = (\bar{q}\sigma^{\mu\nu} b)\phi B_{\mu\nu}, \tag{4.9}$$

The contribution from these operators to the vertices can be found in [10].

Naively, from dimensional analysis we may expect that the effects of these operators are suppressed by E^2/Λ^2 where E is the energy scale of the process. However, this is not the case for the operators listed above in Eqs. (4.1)-(4.9). These anomalous couplings violate the $SU(2)_L$ symmetry, so they are related to the Higgs VEV v, which is the electroweak symmetry breaking scale. Instead of E^2/Λ^2, these anomalous vertices scale as v^2/Λ^2, and is independent of the energy scale of the process. This can be seen in [10], where the relation between the anomalous couplings and the dimension-six operators are given.

The consequence of this is that the effects of new physics will not increase as much with energy at a collider experiment as we might have expected. On the other hand, the effect will not disappear in the

low energy limit. Therefore an important question is whether it is possible to extract better bounds from PEWM for these operators, than from the measurements performed at the high-energy colliders.

Most of the operators listed above do not directly contribute to PEWM at tree-level. Their corrections to the W, Z and γ self-energies occur at loop-level, so they are suppressed by $1/(4\pi)^2$. However, the electroweak measurements have a much cleaner background than hadron colliders, and therefore are performed with a much higher level of precision. In addition, the large mass of the top quark can also lead to an enhancement of the loop-level contribution. As a result, the constraints on top quark obtained from PEWM may be comparable with those obtained from collider experiments. This is exactly what we have seen in Chapter 3, where the bounds on operator O_{tW} are extracted from both PEWM and W-helicity measurements, and are found to be comparable.

The easiest way to put constraints on these operators is to simply extend the analysis in Chapter 3 to include these operators. However, as we will see, this approach is not appropriate for all 9 operators. In addition, by calculating the $\hat{U}$ parameter, one can only put constraint on one special linear combination of the operators. The PEWM itself, on the other hand, contains much more information.

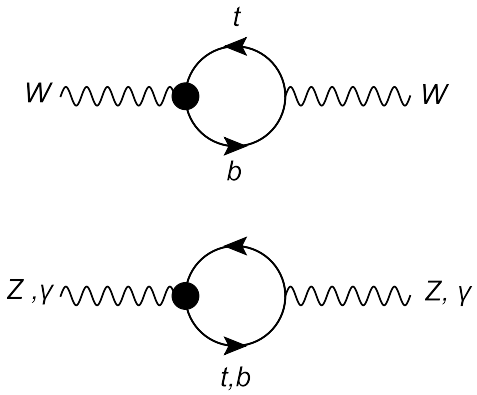

Figure 4.1: Corrections to gauge boson self-energy. The black dots indicate the dimension-six vertex.

Consider the gauge boson self-energies modified by these operators, through the loop diagrams shown in Figure 4.1.[1] Here one should assume that the coefficients C_i are real because an imaginary part of C_i violates CP and will not contribute to any self-energy. We list the leading order contribution of the 9 dimension-six operators to the gauge boson self-energies in Appendix B. These expressions in general contain ultraviolet divergences. However, not all of these divergences have physical effects, because self-energies are not directly observable. Since all divergent terms are either constant or proportional to q^2 (q is the momentum of the gauge boson), they can contribute at most to the three oblique parameters $\hat{S}$, $\hat{T}$ and $\hat{U}$. In fact, we find that

[1]There is also a diagram contributing to the W-boson self-energy, with a top-quark loop, constructed from the contact interaction given by O_{tW} and O_{bW}. Since this interaction is antisymmetric in μ, ν, this diagram does not contribute to the self-energy.

the $\hat{S}$ and $\hat{T}$ parameters are divergent. As we have discussed in Chapter 3, these divergences are properly absorbed by including

$$O_{WB} = (\phi^\dagger \tau^I \phi) W^I_{\mu\nu} B^{\mu\nu}, \tag{4.10}$$

$$O^{(3)}_\phi = (\phi^\dagger D^\mu \phi)[(D_\mu \phi)^\dagger \phi]. \tag{4.11}$$

in the analysis.

On the other hand, the $\hat{U}$ parameter is always finite, because there is no dimension-six operator that can be used to absorb the divergence. It is straightforward to calculate the $\hat{U}$ and compare it with data. However, the constraints on $\hat{S}$, $\hat{T}$ and $\hat{U}$ parameters are obtained by assuming a linear q^2 dependence of the self-energies. While this assumption is reasonable for the operator O_{tW}, as is explicitly shown in Eq. (3.24), it is too crude after including all 9 operators. Once loop-level contributions are included, the self-energies will contain terms like $\ln q^2$ and $q^2 \ln q^2$. Especially, in a diagram with a bottom quark loop, the self-energies can have very different q^2 dependence in the regions $q^2 < 4m_b^2$ and $q^2 > 4m_b^2$. An example is shown in Figure 4.2. Since the PEWM include data measured at both $q^2 = 0$ and $q^2 \geq m_Z^2$, it is not reasonable to use a bound obtained by assuming a linear q^2 dependence. In addition, obtaining bounds from the $\hat{U}$ parameter does not make full use of the q^2 dependence of the self-energies. When the linear q^2 dependence is subtracted into $\hat{S}$ and $\hat{T}$, the residual q^2 dependence can still affect the PEWM. In fact, PEWM contains more than a hundred of observables measured at different values of q^2. This allows a more detailed determination of these operators.

Therefore we should abandon the $\hat{S}$, $\hat{T}$ and $\hat{U}$ parameters, and explicitly calculate the effects of these operators on all electroweak measurements. We then compare the results with data and perform a global fit to obtain one-sigma bounds on the coefficients of these operators. In order to be specific, we assume that these operators are the only new physics effects in the theory.

This Chapter is organized as follows. In Section 4.1, we show all major precision electroweak measurements which we will use to obtain bounds. In Section 4.2, we calculate the corrections on all observables from these operators, and perform the global fit. We present our conclusion in Section 4.3. Finally, the self-energy corrections from each operator are shown in Appendix B, and some numerical details of the global fit are given in Appendix C.

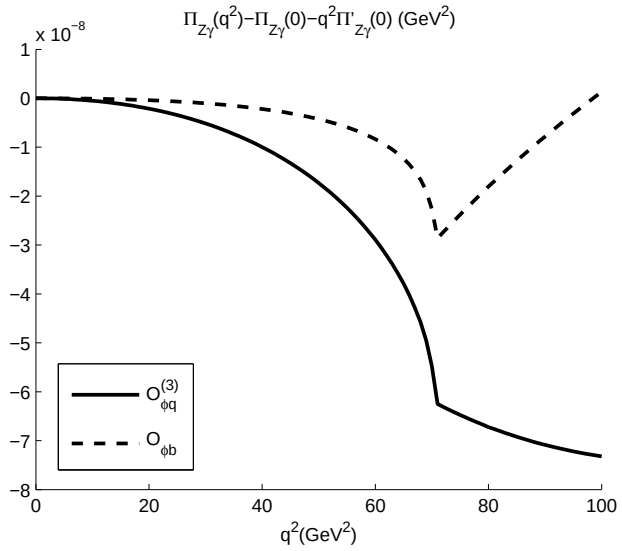

Figure 4.2: The q^2 dependence of $\Pi_{Z\gamma}$. The contributions from the operators $O^{(3)}_{\phi q}$ and $O_{\phi b}$ are shown for illustration. A linear part in q^2 is subtracted so that $\Pi_{\gamma Z}(0) = \Pi'_{\gamma Z}(0) = 0$.

4.1 Experiments

The measurements we use to constrain the coefficients of the operators are listed in Table 4.1. Detailed descriptions for individual experiments can be found in the corresponding references.

For a given observable X, the prediction of the effective field theory can be written as

$$X_{\rm th} = X_{\rm SM} + \sum_i C_i X_i^{\rm dim6}, \tag{4.12}$$

where $X_{\rm th}$ is the prediciton in the presence of the operators. $X_{\rm SM}$ is the Standard Model prediction, and $\sum_i C_i X_i^{\rm dim6}$ are the corrections from the new operators. Since only dimension-six operators are included, higher-order terms in C_i/Λ^2 must be dropped.

The SM predictions are computed to the required accuracy, and can be found in the literature shown in Table 4.1. The three most precisely measured electroweak sector observables, α, G_F, and m_Z, are taken to be the input parameters, from which the SM gauge couplings and the Higgs vev are inferred. In addition, the following input parameters are used:

$$m_{\rm Higgs} = 90^{+27}_{-22}\ {\rm GeV}, \quad m_t = 173.2 \pm 1.3\ {\rm GeV}, \quad \alpha_s(m_Z) = 0.1183 \pm 0.0015, \tag{4.13}$$

except for LEP2. The sensitivities of the SM predictions for the fermion pair production and W pair production cross sections at LEP2 are negligible compared to the experimental errors [79]. Therefore, we

	Notation	Measurement	Reference
Z-pole	Γ_Z	Total Z width	[71, 73]
	$\sigma_{\rm had}$	Hadronic cross section	
	$R_f(f=e,\mu,\tau,b,c)$	Ratios of decay rates	
	$A_{FB}^{0,f}(f=e,\mu,\tau,b,c,s)$	Forward-backward asymmetries	
	$\bar{s}_l^2$	Hadronic charge asymmetry	
	$A_f(f=e,\mu,\tau,b,c,s)$	Polarized asymmetries	
Fermion pair production at LEP2	$\sigma_f(f=q,\mu,\tau,e)$	Total cross sections for $e^+e^-\to f\bar{f}$	[74]
	$A_{FB}^f(f=\mu,\tau)$	Forward-backward asymmetries for $e^+e^-\to f\bar{f}$	
W mass and decay rate	m_W	W mass from LEP and Tevatron	[71]
	Γ_W	W width from Tevatron	
DIS and atomic parity violation	$Q_W(Cs)$	Weak charge in Cs	[71]
	$Q_W(Tl)$	Weak charge in Tl	
	$Q_W(e)$	Weak charge of the electron	
	g_L^2, g_R^2	ν_μ-nucleon scattering from NuTeV	
	$g_V^{\nu e}, g_A^{\nu e}$	ν-e scattering from CHARM II	
W pair production	σ_W	Total cross section for $e^+e^-\to W^+W^-$	[78]

Table 4.1: Relevant measurements. The total cross section for $e^+e^-\to e^+e^-$ is divergent. We use the cross section in the angular range $\cos\theta\in[-0.9,0.9]$ instead.

use the SM prediction given in the corresponding references.

The corrections from the dimension-six operators include:

- The tree-level contribution from O_{WB} and $O_\phi^{(3)}$.
- The tree-level correction to the $Zb\bar{b}$ couplings from $O_{\phi q}^{(3)}$, $O_{\phi q}^{(1)}$ and $O_{\phi b}$.
- The loop-level contribution from all 9 operators in Eqs. (4.1)-(4.9) to the self-energies.

Once the self-energies are given, the corrections $X_i^{\rm dim6}$ to all the experiments can be obtained from the tree-level formulae for each observable. This will be discussed in the next Section.

Given these results, we can calculate the total χ^2 as a function of C_i:

$$\chi^2=\sum_X\frac{(X_{\rm th}-X_{\rm exp})^2}{\sigma_X^2}=\sum_X\frac{(X_{\rm SM}-X_{\rm exp}+\sum_i C_iX_i^{\rm dim6})^2}{\sigma_X^2},\tag{4.14}$$

where $X_{\rm exp}$ is the experimental value for observable X and σ_X is the total error which consists of both experimental and theoretical uncertainties. The χ^2 is a quadratic function of C_i. The fit for the coefficients of the new operators is given by minimizing χ^2. The one-sigma bounds on the coefficients are given by $\chi^2-\chi^2_{\rm min}=1$.

Eq. (4.14) needs to be modified to account for the correlations between different measurements. There are two sets of data for which the correlations between measurements cannot be neglected. These are the correlations between Z-pole observables [73], and the experimental error correlations for the hadronic total

cross sections at LEP2 [74]. To include correlations, Eq. (4.14) should be modified to

$$\chi^2 = \sum_{p,q}(X^p_{\rm SM} - X^p_{\rm exp} + \sum_i C_i X_i^{p,\rm dim6})(\sigma^2)^{-1}_{pq}(X^q_{\rm SM} - X^q_{\rm exp} + \sum_i C_i X_i^{q,\rm dim6}) \tag{4.15}$$

where $X^{p,q}$ denotes different observables. The error matrix σ^2 is related to the error σ_p and the correlation matrix ρ_{pq} by

$$\sigma^2_{pq} = \sigma_p \rho_{pq} \sigma_q \tag{4.16}$$

The correlations for theoretical and experimental errors should be taken into account separately.

4.2 Calculations

In the presence of the new operators, the corrections to the self-energies of W, Z and γ can be written as

$$\Pi_{XY} = \sum_i C_i \Pi_{XY\,i}, \tag{4.17}$$

where Π_{XY} only includes the contributions from the new operators. $(XY) = (ZZ)$, (WW), $(\gamma\gamma)$, (γZ).

For the operators in Eqs. (4.1)-(4.9), the $\Pi_{XY\,i}$'s are given in Appendix B. We also include O_{WB} and $O^{(3)}_\phi$ in our calculation, so that the divergences can be absorbed. For these two operators, the contributions at tree-level are:

$$\Pi_{WW} = 0, \tag{4.18}$$

$$\Pi_{ZZ} = C_{WB}\frac{2v^2}{\Lambda^2}s_W c_W q^2 + C^{(3)}_\phi \frac{v^2}{2\Lambda^2} m_Z^2, \tag{4.19}$$

$$\Pi_{\gamma\gamma} = -C_{WB}\frac{2v^2}{\Lambda^2}s_W c_W q^2, \tag{4.20}$$

$$\Pi_{\gamma Z} = -C_{WB}\frac{v^2}{\Lambda^2}(c_W^2 - s_W^2) q^2, \tag{4.21}$$

where $s_W = \sin\theta_W$ and $c_W = \cos\theta_W$ with the weak angle θ_W.

In this Section, we discuss the effect of self-energy corrections on each experiment. We will show how to obtain the $C_i X_i^{\rm dim6}$ term in Eq. (4.14). We first illustrate the idea in an example.

For processes involving light fermions as external particles, Peskin and Takeuchi have shown in Ref. [68] that the corrections of the gauge boson self-energies can be incorporated by a change in the coupling constants and gauge boson parameters. For example, for electromagnetic interactions, the fine structure constant α

should be replaced by

$$\alpha_*(q^2) = \alpha_0(1 + \Pi'_{\gamma\gamma}(q^2)), \tag{4.22}$$

where α_0 is the SM value, i.e. the value that appears as parameters in the SM Lagrangian.[2]

Note that α_0 is different from the value of α measured in the experiment. Therefore, the self-energy corrections affect the theoretical predictions in two different ways, which we will call direct correction and indirect correction respectively. The direct correction is simply described by Eq. (4.22). Any observable in an electromagnetic process is affected by a change in α. The indirect correction arise from the fact that we take α as one of the input parameters. The SM value α_0 is then shifted from the measured α, which can be obtained by substituting $q^2 = 0$ (α is measured at $q^2 = 0$) into Eq. (4.22):

$$\alpha = \alpha_0(1 + \Pi'_{\gamma\gamma}(0)). \tag{4.23}$$

Therefore any observable that depends on α as an input parameter is affected by Eq. (4.23). We can now eliminate α_0 by combining Eq. (4.22) and (4.23), to obtain

$$\alpha_*(q^2) = \alpha \left[1 + \Pi'_{\gamma\gamma}(q^2) - \Pi'_{\gamma\gamma}(0)\right], \tag{4.24}$$

which can be used to calculate the corrections on any electromagnetic observable.

This is the basic idea of our calculation. We will show the direct correction and indirect correction to all parameters in Section 4.2.1 and 4.2.2, respectively, and combine them to calculate the total effects on all electroweak measurements, except for the cross section of the W pair production. The W pair production at LEP2 only has a low statistics in the measurements, and thus we will only consider the tree-level contribution, i.e. the contribution from O_{WB} and $O_\phi^{(3)}$.

4.2.1 Direct Correction

In the SM, the matrix elements of the charged- and neutral-current interactions mediated by electroweak gauge bosons can be written as

$$\mathcal{M}_{\rm NC} = e^2 \frac{QQ'}{q^2} + \frac{e^2}{s_W^2 c_W^2}(I_3 - s_W^2 Q)\frac{1}{q^2 - m_Z^2}(I'_3 - s_W^2 Q'), \tag{4.25}$$

$$\mathcal{M}_{\rm CC} = \frac{e^2}{2s_W^2} I_+ \frac{1}{q^2 - m_W^2} I_-. \tag{4.26}$$

[2]The running of α_0 is a higher order effect. As we will see, because we are only focusing on the contribution from dimension-six operators, the running only leads to effects of order $1/(4\pi)^2\Lambda^2$ and thus can be neglected.

Peskin and Takeuchi have shown in Ref. [68] that the modification of the gauge boson self-energies can be included by writing

$$\mathcal{M}_{\rm NC} = e_*^2 \frac{QQ'}{q^2} + \frac{e_*^2}{s_{W*}^2 c_{W*}^2}(I_3 - s_{W*}^2 Q)\frac{Z_{Z*}}{q^2 - m_{Z*}^2}(I_3' - s_{W*}^2 Q'), \tag{4.27}$$

$$\mathcal{M}_{\rm CC} = \frac{e_*^2}{2s_{W*}^2} I_+ \frac{Z_{W*}}{q^2 - m_{W*}^2} I_-, \tag{4.28}$$

where the starred quantities are functions of q^2:

$$\begin{aligned}
m_{W*}^2(q^2) &= (1 - Z_W)q^2 + Z_W\left(m_{W0}^2 + \Pi_{WW}(q^2)\right), && (4.29)\\
m_{Z*}^2(q^2) &= (1 - Z_Z)q^2 + Z_Z\left(m_{Z0}^2 + \Pi_{ZZ}(q^2)\right), && (4.30)\\
Z_W &= 1 + \frac{d}{dq^2}\Pi_{WW}(q^2)|_{q^2=m_W^2}, && (4.31)\\
Z_Z &= 1 + \frac{d}{dq^2}\Pi_{ZZ}(q^2)|_{q^2=m_Z^2}, && (4.32)\\
Z_{W*}(q^2) &= 1 + \frac{d}{dq^2}\Pi_{WW}(q^2)|_{q^2=m_W^2} - \Pi'_{\gamma\gamma}(q^2) - \frac{c_W}{s_W}\Pi'_{\gamma Z}(q^2), && (4.33)\\
Z_{Z*}(q^2) &= 1 + \frac{d}{dq^2}\Pi_{ZZ}(q^2)|_{q^2=m_Z^2} - \Pi'_{\gamma\gamma}(q^2) - \frac{c_W^2 - s_W^2}{s_W c_W}\Pi'_{\gamma Z}(q^2), && (4.34)\\
s_{W*}^2(q^2) &= s_{W0}^2 - s_W c_W \Pi'_{\gamma Z}(q^2), && (4.35)\\
e_*^2(q^2) &= e_0^2 + e^2\Pi'_{\gamma\gamma}(q^2), && (4.36)
\end{aligned}$$

where $\Pi'_{XY}(q^2)$ is defined as

$$\Pi'_{XY}(q^2) = \left(\Pi_{XY}(q^2) - \Pi_{XY}(0)\right)/q^2. \tag{4.37}$$

The subscript 0 denotes the SM value, i.e. the value derived from the SM parameters. For example,

$$m_{W0}^2 = \frac{e_0^2}{s_{W0}^2}\frac{v^2}{4}, \quad m_{Z0}^2 = \frac{e_0^2}{s_{W0}^2 c_{W0}^2}\frac{v^2}{4}. \tag{4.38}$$

Since the Π_{XY}'s are already of order C/Λ^2, we do not distinguish the subscript 0 and $*$ if a term is already of order $1/\Lambda^2$, because their difference only leads to terms that are of order $1/\Lambda^4$. For example, for the e^2 in the last term of Eq. (4.36), the difference between e_0^2 and $e_*^2(q^2)$ is a C^2/Λ^4 order contribution. Thus we will simply omit the subscript at this order.

Eqs. (4.27) and (4.28) have exactly the same form as the tree-level SM amplitudes, except that all the coupling constants and gauge-boson parameters are replaced by starred parameters. This shows that the oblique corrections affect electroweak interaction observables only via the starred parameters. In other words, given an observable in terms of bare parameters at tree-level, we only need to replace the bare parameters

with their starred counterparts evaluated at the appropriate momentum to incorporate the corrections from the self-energy diagrams. For example, at tree-level the left-right asymmetry A_e at the Z-pole is given by

$$A_e(m_Z^2) = \frac{2\left(1-4s_{W0}^2\right)}{1+\left(1-4s_{W0}^2\right)^2}. \tag{4.39}$$

This is modified to

$$A_e(m_Z^2) = \frac{2\left(1-4s_{W*}^2(m_Z^2)\right)}{1+\left(1-4s_{W*}^2(m_Z^2)\right)^2} \tag{4.40}$$

after the self-energy corrections are included. Similarly, the Z to e^+e^- partial width is now corrected to

$$\Gamma_{e^+e^-} = \frac{e_*^2(m_Z^2)Z_{Z*}(m_Z^2)m_Z}{192\pi s_{W*}^2(m_Z^2)c_{W*}^2(m_Z^2)}\left(\left(1-4s_{W*}^2(m_Z^2)\right)^2+1\right). \tag{4.41}$$

Note that these corrections come from a change of the SM parameters, i.e. the quantities with a subscript 0, such as e_0 and s_{W0}. Therefore these are direct corrections.

For low energy measurements, it is more convenient to write

$$\mathcal{M}_{\rm NC} = -4\sqrt{2}G_{F0}\left(1-\frac{1}{m_Z^2}\Pi_{ZZ}(0)\right)\left(I_3-s_{W*}^2(0)Q\right)\left(I_3'-s_{W*}^2(0)Q'\right), \tag{4.42}$$

$$\mathcal{M}_{\rm CC} = -2\sqrt{2}G_{F0}\left(1-\frac{1}{m_W^2}\Pi_{WW}(0)\right)I_+I_-, \tag{4.43}$$

where

$$G_{F0} = \frac{1}{\sqrt{2}v^2} \tag{4.44}$$

is the SM value of the Fermi constant. The direct corrections to any low energy observables are thus incorporated by replacing s_{W0} by $s_{W*}(0)$ and including an overall factor of $(1-\Pi_{ZZ}(0)/m_Z^2)$ (or $(1-\Pi_{WW}(0)/m_W^2)$) for neutral-current (or charged-current) observables.

4.2.2 Indirect Correction

The indirect corrections arise from the shifts in the input parameters. The SM parameters (g, g', v) are not directly measured. Instead, we derive them from the most precisely measured observables (α, m_Z, G_F). When calculating the SM predictions for these observables, the SM relations between (g, g', v) and (α, m_Z, G_F) are used. When we include the new operators, the SM relations are altered. This corresponds to a correction to all three input parameters.

To consider the indirect corrections, we use (α_0, m_{Z0}, G_{F0}) to denote the SM values for the three input

parameters. The relation between α and α_0 can be read off from Eqs. (4.27) and (4.36):

$$\alpha = \frac{e_*^2(0)}{4\pi} = \alpha_0(1 + \Pi'_{\gamma\gamma}(0)). \tag{4.45}$$

The Z mass m_Z can be obtained by solving $m_{Z*}^2(m_Z^2) = m_Z^2$, this gives

$$m_Z^2 = m_{Z0}^2 + \Pi_{ZZ}(m_Z^2). \tag{4.46}$$

The Fermi constant can be read off from Eq. (4.43):

$$G_F = G_{F0}\left(1 - \frac{1}{m_W^2}\Pi_{WW}(0)\right). \tag{4.47}$$

We will also need

$$\begin{aligned} s_{W0}^2 &= \frac{1}{2}\left(1 - \sqrt{1 - \frac{4\pi\alpha_0}{\sqrt{2}G_{F0}m_{Z0}^2}}\right) \\ &= \frac{1}{2}\left(1 - \sqrt{1 - \frac{4\pi\alpha}{\sqrt{2}G_F m_Z^2}}\right)\left[1 - \frac{c_W^2}{c_W^2 - s_W^2}\left(\Pi'_{\gamma\gamma}(0) + \frac{1}{m_W^2}\Pi_{WW}(0) - \frac{1}{m_Z^2}\Pi_{ZZ}(m_Z^2)\right)\right]. \end{aligned} \tag{4.48}$$

Combining Eq. (4.29)-(4.36) with Eq. (4.45)-(4.48) to eliminate α_0, m_{Z0}, G_{F0} and s_{W0}, we conclude that, for $q^2 > 0$, the total effect of direct and indirect corrections can be incorporated by making the following replacement to the bare parameters in the tree-level expressions for any observable:

$$\alpha \to \alpha + \delta\alpha = \alpha\left(1 + \Pi'_{\gamma\gamma}(q^2) - \Pi'_{\gamma\gamma}(0)\right) \times \begin{cases} 1 & \text{for interactions mediated by photon} \\ Z_{Z*}(q^2) & \text{for interactions mediated by } Z \text{ boson} \\ Z_{W*}(q^2) & \text{for interactions mediated by } W \text{ boson} \end{cases}, \tag{4.49}$$

$$m_Z^2 \to m_Z^2 + \delta m_Z^2 = m_Z^2 - \Pi_{ZZ}(m_Z^2) + \Pi_{ZZ}(q^2) - (q^2 - m_Z^2)\frac{d}{dq^2}\Pi_{ZZ}(q^2)|_{q^2=m_Z^2}, \tag{4.50}$$

$$s_W^2 \to s_W^2 + \delta s_W^2 = s_W^2\left[1 - \frac{c_W}{s_W}\Pi'_{\gamma Z}(q^2) - \frac{c_W^2}{c_W^2 - s_W^2}\left(\Pi'_{\gamma\gamma}(0) + \frac{1}{m_W^2}\Pi_{WW}(0) - \frac{1}{m_Z^2}\Pi_{ZZ}(m_Z^2)\right)\right]. \tag{4.51}$$

For any observable measured at the Z-pole or above, we can write it at tree-level in terms of α, m_Z^2 and s_W^2:

$$X_{\rm th}^{\rm tree} = X_{\rm th}^{\rm tree}(\alpha, m_Z^2, s_W^2). \tag{4.52}$$

Therefore the contribution from the self-energy corrections can be written as

$$\delta X = C_i X_i^{\rm dim6} = \frac{\partial X_{\rm th}^{\rm tree}}{\partial \alpha}\delta\alpha + \frac{\partial X_{\rm th}^{\rm tree}}{\partial m_Z^2}\delta m_Z^2 + \frac{\partial X_{\rm th}^{\rm tree}}{\partial s_W^2}\delta s_W^2. \tag{4.53}$$

Note that Eq. (4.52) is a tree-level relation, and we will not use it to compute the entire theoretical prediction. Instead, we use Eq. (4.53) to find the corrections which arise from the dimension-six operators. Since these are already small corrections, the tree-level calculation is enough. We then add them to the full SM predictions, which are provided in the references shown in Table 4.1.

If the observables depend on the $Zb\bar{b}$ couplings, we will need to add to the r.h.s of Eq. (4.53) the following terms:

$$-\frac{v^2}{2\Lambda^2}\left(C_{\phi q}^{(3)} + C_{\phi q}^{(1)} + C_{\phi b}\right)\frac{\partial X_{\rm th}^{\rm tree}}{\partial g_V^b} - \frac{v^2}{2\Lambda^2}\left(C_{\phi q}^{(3)} + C_{\phi q}^{(1)} - C_{\phi b}\right)\frac{\partial X_{\rm th}^{\rm tree}}{\partial g_A^b}. \tag{4.54}$$

This accounts for the tree-level correction to the $Zb\bar{b}$ couplings from $C_{\phi q}^{(3)}$, $C_{\phi q}^{(1)}$ and $C_{\phi b}$.

For low energy measurements, we can now write

$$\mathcal{M}_{\rm NC} = -4\sqrt{2}G_F\rho_*(0)\left(I_3 - s_{W*}^2(0)Q\right)\left(I_3' - s_{W*}^2(0)Q'\right), \tag{4.55}$$

$$\mathcal{M}_{\rm CC} = -2\sqrt{2}G_F I_+ I_-, \tag{4.56}$$

where

$$\rho_*(0) = 1 - \frac{1}{m_Z^2}\Pi_{ZZ}(0) + \frac{1}{m_W^2}\Pi_{WW}(0). \tag{4.57}$$

The results of DIS and atomic parity violation experiments are usually expressed in terms of the effective couplings in the neutral-current interactions. The corrections to these results can thus be obtained by replacing s_W^2 by

$$s_W^2\left[1 - \frac{c_W}{s_W}\Pi_{\gamma Z}'(0) - \frac{c_W^2}{c_W^2 - s_W^2}\left(\Pi_{\gamma\gamma}'(0) + \frac{1}{m_W^2}\Pi_{WW}(0) - \frac{1}{m_Z^2}\Pi_{ZZ}(m_Z^2)\right)\right] \tag{4.58}$$

and including an overall factor of $\rho_*(0)$ to the couplings.

4.2.3 Observables

Now we proceed to consider the correction to each observable. We will give the tree-level expressions for each observable, and then use Eq. (4.53) to find the corrections that arise from the new operators.

Z-pole observables

The $e^+e^- \to f\bar{f}$ was studied around the Z-pole at SLC and LEP1. At tree-level, the measured cross sections and asymmetries can be derived from two quantities: the partial width of $Z \to f\bar{f}$, Γ_{ff}, and the polarized asymmetry A_f. The expressions are

$$\Gamma_{ff} = \frac{\alpha m_Z}{12 s_W^2 c_W^2} \left({g_V^f}^2 + {g_A^f}^2 \right), \tag{4.59}$$

$$A_f = \frac{2 g_V^f g_A^f}{{g_V^f}^2 + {g_A^f}^2}, \tag{4.60}$$

where the Z-fermion couplings g_V^f and g_A^f are given by

$$\begin{array}{ccc} f & g_V^f & g_A^f \\ \nu_e, \nu_\mu, \nu_\tau & +\frac{1}{2} & +\frac{1}{2} \\ e, \mu, \tau & -\frac{1}{2} + 2s_W^2 & -\frac{1}{2} \\ u, c, t & +\frac{1}{2} - \frac{4}{3} s_W^2 & +\frac{1}{2} \\ d, s, b & -\frac{1}{2} + \frac{2}{3} s_W^2 & -\frac{1}{2} \end{array} \tag{4.61}$$

The Z-pole observables include:

- Total width

$$\Gamma_Z = \sum_f \Gamma_{ff}. \tag{4.62}$$

- Total hadronic cross-section

$$\sigma_h^0 = \frac{12\pi}{m_Z^2} \frac{\Gamma_{ee} \Gamma_{\text{had}}}{\Gamma_Z^2}. \tag{4.63}$$

- Ratios of decay rates

$$R_f = \begin{cases} \frac{\Gamma_{\text{had}}}{\Gamma_{ff}} & \text{for } f = e, \mu, \tau \\ \frac{\Gamma_{ff}}{\Gamma_{\text{had}}} & \text{for } f = b, c \end{cases}. \tag{4.64}$$

- Forward-backward asymmetries

$$A_{FB}^{0,f} = \frac{3}{4} A_e A_f, \quad f = e, \mu, \tau, b, c, s. \tag{4.65}$$

- Hadronic charge asymmetry

$$\bar{s}_l^2 = s_W^2. \tag{4.66}$$

- Polarized asymmetries

$$A_f, \quad f = e, \mu, \tau, b, c, s. \tag{4.67}$$

With these tree-level expressions, we can apply Eq. (4.53) to derive the correction from the new operators. For example, for the ratio R_b, we find

$$\begin{aligned}\delta R_b = &-24\frac{16s_W^4 - 36s_W^2 + 9}{(88s_W^4 - 84s_W^2 + 45)^2}\left[\frac{c_W}{s_W}\Pi'_{\gamma Z}(m_Z^2) + \frac{c_W^2}{c_W^2 - s_W^2}\left(\Pi'_{\gamma\gamma}(0) + \frac{1}{m_W^2}\Pi_{WW}(0) - \frac{1}{m_Z^2}\Pi_{ZZ}(m_Z^2)\right)\right] \\ &-24\frac{v^2}{\Lambda^2}\left(C_{\phi q}^{(3)} + C_{\phi q}^{(1)}\right)\frac{40s_W^6 - 96s_W^4 + 72s_W^2 - 27}{(88s_W^4 - 84s_W^2 + 45)^2} - 48\frac{v^2}{\Lambda^2}C_{\phi b}\frac{20s_W^4 - 18s_W^2 + 9}{(88s_W^4 - 84s_W^2 + 45)^2}.\end{aligned} \tag{4.68}$$

This is a leading order result. Using the expressions for the Π_{XY}'s given in Appendix B, this can be written in the form of $C_i X_i^{\rm dim6}$.

Fermion pair production at LEP2

The observables are the total cross-sections and forward-backward asymmetries for fermion pair production, measured at different center of mass energies. The matrix element for $e^+e^- \to f\bar{f}$ ($f \neq e$) is given by

$$\begin{aligned}\mathcal{M} &= \frac{4\pi\alpha}{(p+p')^2 - m_Z^2 + i\Gamma_Z m_Z}\frac{1}{4c_W^2 s_W^2}\bar{v}(p')\gamma^\mu\left(g_V^e - g_A^e\gamma^5\right)u(p)\bar{u}(k)\gamma_\mu\left(g_V^f - g_A^f\gamma^5\right)v(k') \\ &\quad -\frac{4\pi\alpha Q}{(p+p')^2}\bar{v}(p')\gamma^\mu u(p)\bar{u}(k)\gamma_\mu v(k'),\end{aligned} \tag{4.69}$$

where p, p' are the momenta of the incoming e^+e^-, and k, k' are the momenta of the outgoing fermions. The cross-sections and forward-backward asymmetries can be calculated from $\mathcal{M}$, and Eq. (4.53) can be applied to obtain the corrections from the operators.

For $f = e$, there are additional contributions from the t-channel diagrams. The matrix element is

$$\begin{aligned}\mathcal{M} &= \frac{4\pi\alpha}{(p+p')^2 - m_Z^2 + i\Gamma_Z m_Z}\frac{1}{4c_W^2 s_W^2}\bar{v}(p')\gamma^\mu\left(g_V^e - g_A^e\gamma^5\right)u(p)\bar{u}(k)\gamma_\mu\left(g_V^e - g_A^e\gamma^5\right)v(k') \\ &\quad -\frac{4\pi\alpha}{(p-k)^2 - m_Z^2 + i\Gamma_Z m_Z}\frac{1}{4c_W^2 s_W^2}\bar{u}(k)\gamma^\mu\left(g_V^e - g_A^e\gamma^5\right)u(p)\bar{v}(p')\gamma_\mu\left(g_V^e - g_A^e\gamma^5\right)v(k') \\ &\quad +\frac{4\pi\alpha}{(p+p')^2}\bar{v}(p')\gamma^\mu u(p)\bar{u}(k)\gamma_\mu v(k') - \frac{4\pi\alpha}{(p-k)^2}\bar{u}(k)\gamma^\mu u(p)\bar{v}(p')\gamma_\mu v(k').\end{aligned} \tag{4.70}$$

W mass and width

The W mass is measured both at Tevatron and LEP2. For the tree-level expression of m_W, we first solve $m_{W*}(m_W^2) = m_W^2$, which gives

$$m_W^2 = m_{W0}^2 + \Pi_{WW}(m_W^2). \tag{4.71}$$

Combining Eq. (4.38), (4.46) and (4.48) with Eq. (4.71), we find that the correction to the W mass is

$$\delta m_W^2 = \Pi_{WW}(m_W^2) + \frac{s_W^2}{c_W^2 - s_W^2}\Pi_{WW}(0) - \frac{c_W^4}{c_W^2 - s_W^2}\Pi_{ZZ}(m_Z^2) + \frac{s_W^2 c_W^2}{c_W^2 - s_w^2} m_Z^2 \Pi'_{\gamma\gamma}(0). \tag{4.72}$$

The W width is measured at Tevatron. The tree level expression is

$$\Gamma_W = \frac{3\alpha m_W}{4 s_W^2}. \tag{4.73}$$

The correction can be calculated using Eq. (4.53).

DIS and atomic parity violation

These are experiments performed at $q^2 \approx 0$. These low energy observables are usually expressed in terms of the effective couplings g_V^f and g_A^f, which depend on s_W^2. For the tree-level expressions, we will also include the factor $\rho_*(0)$, which is 1 in the SM, and takes the value of Eq. (4.57) in the presence of new operators:

$$\rho_*(0) = 1 + \delta\rho(0) = 1 - \frac{1}{m_Z^2}\Pi_{ZZ}(0) + \frac{1}{m_W^2}\Pi_{WW}(0). \tag{4.74}$$

The correction to an observable X is then given by

$$\delta X = C_i X_i^{\text{dim6}} = \left.\frac{\partial X_{\text{th}}^{\text{tree}}}{\partial s_W^2}\right|_{\rho_*(0)=1} \delta s_W^2(0) + \left.\frac{\partial X_{\text{th}}^{\text{tree}}}{\partial \rho_*(0)}\right|_{\rho_*(0)=1} \delta\rho(0). \tag{4.75}$$

The observables include:

- The weak charges for Cs and Tl, measured in the atomic parity violations. The weak charge is given by

$$Q_W(Z,N) = -2\left[(2Z+N)C_{1u} + (Z+2N)C_{1d}\right], \tag{4.76}$$

  where Z and N are the proton number and the neutron number of the atom. The tree-level expressions for C_{1u} and C_{1d} are

$$C_{1u} = 2\rho_*(0) g_A^e g_V^u, \quad C_{1d} = 2\rho_*(0) g_A^e g_V^d. \tag{4.77}$$

- The weak charge of the electron, $Q_W(e)$, measured in the polarized Møller scattering:

$$Q_W(e) = -2C_{2e} = -4\rho_*(0) g_A^e g_V^e. \tag{4.78}$$

- The effective couplings g_L and g_R for ν-nucleon scattering, measured at NuTeV. These are defined as

$$g_L^2 = g_{L,\text{eff}}^{u2} + g_{L,\text{eff}}^{d2}, \quad g_R^2 = g_{R,\text{eff}}^{u2} + g_{R,\text{eff}}^{d2}. \tag{4.79}$$

  where $g^u_{L,\text{eff}}$, $g^u_{R,\text{eff}}$, $g^d_{L,\text{eff}}$ and $g^d_{R,\text{eff}}$ are the effective couplings between the Z boson and the up and down quarks. The tree-level expressions are

$$g^u_{L,\text{eff}} = \rho_*(0)\frac{g_V^u + g_A^u}{2}, \quad g^d_{L,\text{eff}} = \rho_*(0)\frac{g_V^d + g_A^d}{2}, \tag{4.80}$$

$$g^u_{R,\text{eff}} = \rho_*(0)\frac{g_V^u - g_A^u}{2}, \quad g^d_{R,\text{eff}} = \rho_*(0)\frac{g_V^d - g_A^d}{2}. \tag{4.81}$$

$$\tag{4.82}$$

- The effective couplings $g_V^{\nu e}$ and $g_A^{\nu e}$ for ν-e scattering, measured at CHARM II. The expressions are

$$g_V^{\nu e} = \rho_*(0) g_V^e, \quad g_A^{\nu e} = \rho_*(0) g_A^e. \tag{4.83}$$

W pair production

This is the total cross section σ_W for $e^+e^- \to W^+W^-$ at LEP2.

So far we have been using the approach of Peskin and Takeuchi to study the effects of new operators. However, this approach only applies for processes involving light fermions as external particles, and cannot be used to study the W pair production. Due to the low statistics in the measurements, the constraints from W pair production are weak compared to other electroweak observables. Therefore we will ignore all loop effects, and only focus on the effects of operators O_{WB} and $O_\phi^{(3)}$.

Using Eq. (4.18)-(4.21) and Eq. (4.48), we have

$$s^2_{W0} = \frac{1}{2}\left(1 - \sqrt{1 - \frac{4\pi\alpha}{\sqrt{2}G_F m_Z^2}}\right)\left[1 + \frac{c_W^2}{c_W^2 - s_W^2}\left(4C_{WB}\frac{v^2}{\Lambda^2}s_W c_W + \frac{1}{2}C_\phi^{(3)}\frac{v^2}{\Lambda^2}\right)\right]. \tag{4.84}$$

Note that Eq. (4.48) only has to do with the indirect corrections, so it is still valid.

The operator O_{WB} changes the mixing of W^3 and B boson. We then define s_{W*} and c_{W*} as the new mixing angle,

$$s_{W*} = s_{W0} - C_{WB}\frac{v^2}{\Lambda^2}s_W^2 c_W, \quad c_{W*} = \sqrt{1 - s^2_{W*}}, \tag{4.85}$$

so that the W^+W^-Z and $W^+W^-\gamma$ vertices from the kinetic term $-\frac{1}{4}W^I_{\mu\nu}W^{I\mu\nu}$ have the same form as in the SM. Note that this definition of s_{W*} is different from the one in Eq. (4.35) which was only valid for light

fermions. In this way, the operators O_{WB} and $O_\phi^{(3)}$ have the following effects:

- The SM $Zf\bar{f}$ vertices are modified to:

$$\mathcal{L}_{Zf\bar{f}} = \frac{e}{s_{W*}c_{W*}}\left(1 + C_{WB}\frac{v^2}{\Lambda^2}\frac{s_W}{c_W}\right) Z_\mu \bar{f}\gamma^\mu \left(T^3 P_L - s_{W*}^2\left(1 + C_{WB}\frac{v^2}{\Lambda^2}\frac{c_W}{s_W}\right)Q_f\right) f, \tag{4.86}$$

  where $P_L = (1-\gamma^5)/2$.

- The SM W^+W^-Z and $W^+W^-\gamma$ vertices are modified. The contribution comes from O_{WB}:

$$O_{WB} \to -igC_{WB}\frac{v^2}{\Lambda^2}c_W A^{\mu\nu}W_\mu^+ W_\nu^- + igC_{WB}\frac{v^2}{\Lambda^2}s_W Z^{\mu\nu}W_\mu^+ W_\nu^-. \tag{4.87}$$

- The W mass is changed to:

$$m_W^2 = m_Z^2\left(\frac{1}{2}\left(1 + \sqrt{1 - \frac{4\pi\alpha}{\sqrt{2}G_F m_Z^2}}\right) - 2C_{WB}\frac{v^2}{\Lambda^2}\frac{s_W c_W^3}{c_W^2 - s_W^2} - \frac{1}{2}C_\phi^{(3)}\frac{v^2}{\Lambda^2}\frac{c_W^4}{c_W^2 - s_W^2}\right). \tag{4.88}$$

Using these results we can write down the matrix element. The process has a t-channel contribution $\mathcal{M}_t$ and s-channel contributions $\mathcal{M}_\gamma$ and $\mathcal{M}_Z$, which come from photon and Z boson exchange. They are given by

$$\mathcal{M}_t = -i\frac{e^2}{2s_{W*}^2}\bar{v}(p')\gamma^\mu\frac{1}{\not{k} - \not{p}'}\gamma^\nu P_L u(p)\epsilon_\mu^{*\lambda_1}\epsilon_\nu^{*\lambda_2}, \tag{4.89}$$

$$\mathcal{M}_\gamma = -ie^2\bar{v}(p')\gamma_\rho u(p)\frac{1}{q^2}\times \left[(g^{\mu\nu}(k'-k)^\rho - g^{\nu\rho}(q+k')^\mu + g^{\mu\rho}(q+k)^\nu) + C_{WB}\frac{v^2}{\Lambda^2}\frac{c_W}{s_W}\left(g^{\mu\rho}q^\nu - g^{\nu\rho}q^\mu\right)\right]\epsilon_\mu^{*\lambda_1}\epsilon_\nu^{*\lambda_2}, \tag{4.90}$$

$$\mathcal{M}_Z = -i\frac{e^2}{s_{W*}^2}\left(1 + C_{WB}\frac{v^2}{\Lambda^2}\frac{s_W}{c_W}\right)\bar{v}(p')\gamma_\rho\left[\frac{1}{2}P_L - \left(1 + C_{WB}\frac{v^2}{\Lambda^2}\frac{c_W}{s_W}\right)s_{W*}^2\right]u(p)\frac{1}{q^2 - m_Z^2}\times \left[(g^{\mu\nu}(k'-k)^\rho - g^{\nu\rho}(q+k')^\mu + g^{\mu\rho}(q+k)^\nu) - C_{WB}\frac{v^2}{\Lambda^2}\frac{s_W}{c_W}\left(g^{\mu\rho}q^\nu - g^{\nu\rho}q^\mu\right)\right]\epsilon_\mu^{*\lambda_1}\epsilon_\nu^{*\lambda_2}. \tag{4.91}$$

where p, p' are the momenta of the incoming e^+e^-, k, k' are the momenta of the outgoing W^+W^-, and $\epsilon_\mu^{*\lambda_1}$, $\epsilon_\nu^{*\lambda_2}$ are the polarization vectors of the W^+W^-. $q = p + p'$. The cross section can be calculated from the matrix element. The correction due to O_{WB} and $O_\phi^{(3)}$ is obtained by taking the linear part in C_{WB} and $C_\phi^{(3)}$. Higher order terms in C/Λ^2 are neglected.

4.2.4 Total χ^2

In the calculation of χ^2, we choose the $\overline{\rm MS}$ scheme, with the renormalization scale $M^2 = m_Z^2$. We find that the contribution from the operator $O_{\phi\phi}$ is suppressed by the bottom quark mass, as can be seen from Eq. (B.17). Therefore we neglect this operator. The contributions from operators O_{bW} and O_{bB} also have a factor of m_b. However, their effects can still be large, because the expressions contain the function $b_0(m_b^2, m_b^2, q^2)$, and its derivative with respect to q^2 is inversely proportional to m_b^2:

$$\frac{d}{dq^2} b_0(m_b^2, m_b^2, q^2)\bigg|_{q^2=0} = -\frac{1}{6m_b^2}. \tag{4.92}$$

and so their contributions to, for example, s_W, may not be suppressed by m_b. Therefore, we will consider 10 operators:

$$O_{WB},\ O_\phi^{(3)},\ O_{\phi q}^{(3)},\ O_{\phi q}^{(1)},\ O_{\phi t},\ O_{\phi b},\ O_{tW},\ O_{bW},\ O_{tB},\ O_{bB}. \tag{4.93}$$

On the other hand, the operator $O_{\phi\phi}$ can be bounded from the $b \to s\gamma$ decay [32]

$$\left|\frac{C_{\phi\phi}}{\Lambda^2}\right| < 0.13\ \text{TeV}^{-2}. \tag{4.94}$$

Using Eq. (4.14), χ^2 can be written as a quadratic function of C_i:

$$\chi^2 = \chi^2_{\rm min} + (C_i - \hat{C}_i) M_{ij} (C_j - \hat{C}_j). \tag{4.95}$$

Here $\chi^2_{\rm min}$ is the minimum χ^2 in the presence of the new operators. $\hat{C}_i$ corresponds to the best fit value for C_i.

In our calculation, we used the following input parameters:

$$\alpha(m_Z^2) = 1/128.91, \qquad G_F = 1.166364 \times 10^{-5}\ \text{GeV}^{-2}, \qquad m_Z = 91.1876\ \text{GeV},$$
$$m_t = 172.9\ \text{GeV}, \qquad m_b = 4.79\ \text{GeV}. \tag{4.96}$$

We find $\chi^2_{\rm min} = 78.40$, the $\chi^2_{\rm min}$ per degree of freedom is 0.78, compared with the SM value 0.82. The matrix M_{ij} and the best fit values $\hat{C}_i$ are given in Appendix C.

4.2.5 A Global Fit

The one-sigma bounds on the operators are given by $\chi^2 - \chi^2_{\text{min}} = 1$. By diagonalizing the matrix M_{ij}, we find 10 linear combinations of C_i that are statistically independent. Their best fit values and one-sigma bounds are given by:

$$\begin{pmatrix}
-0.961 & -0.273 & +0.029 & -0.004 & +0.024 & +0.000 & +0.012 & -0.000 & +0.015 & +0.001 \\
-0.064 & +0.159 & -0.701 & -0.680 & -0.015 & +0.130 & +0.001 & -0.000 & +0.001 & +0.000 \\
+0.267 & -0.940 & -0.063 & -0.182 & +0.088 & +0.002 & -0.022 & +0.002 & -0.005 & -0.001 \\
+0.008 & -0.019 & +0.095 & +0.086 & +0.004 & +0.991 & +0.019 & -0.001 & +0.000 & +0.000 \\
+0.016 & +0.036 & +0.241 & -0.249 & +0.223 & -0.019 & +0.903 & -0.071 & +0.079 & +0.041 \\
-0.005 & +0.121 & +0.402 & -0.401 & +0.670 & +0.004 & -0.403 & +0.048 & +0.221 & -0.004 \\
-0.016 & +0.030 & +0.136 & -0.136 & +0.126 & -0.000 & -0.002 & +0.139 & -0.935 & -0.229 \\
-0.004 & +0.008 & +0.035 & -0.034 & +0.039 & +0.001 & -0.094 & -0.745 & -0.244 & +0.610 \\
-0.001 & +0.001 & -0.004 & +0.004 & +0.007 & -0.000 & +0.025 & +0.646 & -0.090 & +0.757 \\
-0.001 & +0.001 & +0.505 & -0.505 & -0.689 & -0.000 & -0.108 & +0.014 & +0.054 & +0.009
\end{pmatrix}$$

$$\times \frac{1}{\Lambda^2} \begin{pmatrix} C_{WB} \\ C_{\phi}^{(3)} \\ C_{\phi q}^{(3)} \\ C_{\phi q}^{(1)} \\ C_{\phi t} \\ C_{\phi b} \\ C_{tW} \\ C_{bW} \\ C_{tB} \\ C_{bB} \end{pmatrix} = \begin{pmatrix} -0.0004 & \pm 0.0029 \\ -0.013 & \pm 0.014 \\ +0.011 & \pm 0.023 \\ -0.59 & \pm 0.27 \\ -0.05 & \pm 1.17 \\ +2.86 & \pm 2.14 \\ -1.7 & \pm 11.9 \\ -8.7 & \pm 21.2 \\ +102.4 & \pm 50.4 \\ -1.10\text{e}{+3} & \pm 1.41\text{e}{+3} \end{pmatrix} \text{TeV}^{-2}. \quad (4.97)$$

where the 10 by 10 matrix in the l.h.s is orthogonal. We can see that in the first row and the third row, the first two components are much larger than the other components. This means that these two rows approximately correspond to constraints on the coefficients C_{WB} and $C_{\phi}^{(3)}$, or equivalently, the S and T parameters. Since we are interested in the other 8 operators, we can let C_{WB} and $C_{\phi}^{(3)}$ freely flow (or in other words, assume that C_{WB} and $C_{\phi}^{(3)}$ always take the values that minimize the χ^2). In this way, we find

the following constraints on the 8 operators:

$$\begin{pmatrix} -0.702 & -0.701 & -0.000 & +0.128 & -0.003 & +0.000 & -0.000 & -0.000 \\ +0.094 & +0.087 & +0.002 & +0.992 & +0.019 & -0.001 & +0.001 & +0.000 \\ -0.244 & +0.251 & -0.228 & +0.019 & -0.901 & +0.071 & -0.080 & -0.041 \\ +0.405 & -0.404 & +0.675 & +0.004 & -0.408 & +0.049 & +0.218 & -0.005 \\ -0.136 & +0.136 & -0.126 & +0.000 & +0.002 & -0.138 & +0.936 & +0.229 \\ -0.035 & +0.034 & -0.039 & -0.001 & +0.094 & +0.745 & +0.244 & -0.610 \\ -0.004 & +0.004 & +0.007 & -0.000 & +0.025 & +0.646 & -0.090 & +0.757 \\ -0.505 & +0.505 & +0.689 & +0.000 & +0.108 & -0.014 & -0.054 & -0.009 \end{pmatrix}$$

$$\times \frac{1}{\Lambda^2} \begin{pmatrix} C_{\phi q}^{(3)} \\ C_{\phi q}^{(1)} \\ C_{\phi t} \\ C_{\phi b} \\ C_{tW} \\ C_{bW} \\ C_{tB} \\ C_{bB} \end{pmatrix} = \begin{pmatrix} -0.011 & \pm 0.014 \\ -0.59 & \pm 0.27 \\ +0.04 & \pm 1.17 \\ +2.84 & \pm 2.12 \\ +1.7 & \pm 11.9 \\ +8.7 & \pm 21.2 \\ +102.4 & \pm 50.4 \\ +1.10\text{e}{+3} & \pm 1.41\text{e}{+3} \end{pmatrix} \text{TeV}^{-2}. \tag{4.98}$$

This is the main result of this analysis.

We can see that the first row is approximately a constraint on $(O_{\phi q}^{(3)} + O_{\phi q}^{(1)})/\sqrt{2}$, which corresponds to the left-handed $Zb\bar{b}$ coupling, while the second row corresponds to a constraint on $O_{\phi b}$, which is the right-handed $Zb\bar{b}$ coupling. These are the tightest bounds, since the contribution arises at tree-level. The other constraints are mainly from loop-level effects. The third row is approximately a bound on C_{tW}. This can be compared with the bound obtained from direct measurement of W-helicity fraction at the Tevatron, i.e. Eqs. (3.9, 3.10). The results are of the same order.

4.3 Conclusions

In this Chapter, we have studied the effects of non-standard top quark couplings in the precision electroweak measurements. The top quark plays a role as a virtual particle in these measurements. Our study is based on an effective field theory approach, which allows us to calculate the self-energies of the electroweak gauge bosons at loop-level.

We have examined the effects of 8 dimension-six operators which generate non-standard couplings between electroweak gauge bosons and the third generation quarks. These operators mainly contribute through loop corrections to the gauge boson self-energies, but some of them also have a tree-level contribution to the $Zb\bar{b}$ couplings. We have also included the operators O_{WB} and $O_{\phi}^{(3)}$, in order to deal with the divergences that appear in our calculation.

We have calculated the total χ^2 and performed a global fit including these 10 operators. We float C_{WB} and $C_{\phi}^{(3)}$, and thus obtain bounds on the 8 dimension-six operators. The result is shown in Eq. (4.98). The two tightest bounds are from tree-level contribution to the $Zb\bar{b}$ couplings, g_L^b and g_R^b, and the other bounds are from loop-level contribution. The best bound from loop-level contribution constrains $\frac{C}{\Lambda^2}$ to be of order 1 TeV^{-2} which implies that Λ is of order 1 TeV if one makes the assumption that the coupling constant C is of order one. This can be compared with the bound obtained from direct measurement at the Tevatron. In addition, our results also include bounds on operators that cannot be constrained in high-energy collider experiments.

Using Eq. (4.95), one can also put constraints on a subset of these operators. For example, the one-sigma bound on the coefficient C_i, assuming only one coefficient deviates from its best fit value, is given by $\hat{C}_i \pm M_{ii}^{-1/2}$, where M_{ii} is the diagonal element of the matrix M and is not summed over i. However, some linear combinations of C_i are only weakly bounded. These weak bounds can not be completely trusted, because the linear analysis is not applicable if the coefficients are large.

Appendix A

Proof that Odd-Dimensional Operators Violate Lepton and/or Baryon Number Conservation

If an effective operator conserves baryon and lepton number, the fermion fields must be paired up to form terms such as $\bar{f}_L f_R$, $\bar{f}_L \gamma^\mu f_L$, $\bar{f}_L \sigma^{\mu\nu} f_R$, *etc.*, where f_L, f_R are the left-handed and right-handed fermions. There is no need to put in γ_5, because f_L and f_R are eigenstates of γ_5. These fermion fields, combined with other Standard Model fields, are the basic "building blocks" of any operator. We put these terms in the first column of Table A.1.

An effective operator will be composed of some combination of the operators in Table A.1. Each of these terms may have some Lorentz indices and some SU(2) fundamental representation indices, but the operator must be invariant under both the Lorentz and SU(2) groups. Therefore, the total number of the Lorentz indices in the operator must be an even number because we need either two vectors to form a scalar or four vectors to form a pseudoscalar. Similarly, the total number of the SU(2) fundamental representation indices in the operator must be even because we need two such indices to form an SU(2) singlet or triplet. These numbers are shown in the second and third columns of Table A.1. Note that in the SM, f_L is an SU(2) doublet but f_R is a singlet.

The dimension of each of the "building blocks" is shown in the fourth column of Table A.1. The sum of these numbers is the dimension of the operator, which we denote by D. If we add the first three numbers in each row of Table A.1, the result is always an even number, so the sum of these numbers for any given lepton- and baryon-number-conserving operator must be even as well. Note also that the sum of the last row in the Table is D plus an even number. We conclude that D, the dimension of the operator, must be an even number.

	Lorentz indices	SU(2) indices	Dimension	Total
$\bar{f}_L f_R$, $\bar{f}_R f_L$	0	1	3	4
$\bar{f}_L \gamma^\mu f_L$	1	2	3	6
$\bar{f}_R \gamma^\mu f_R$	1	0	3	4
$\bar{f}_L \sigma^{\mu\nu} f_R$, $\bar{f}_R \sigma^{\mu\nu} f_L$	2	1	3	4
ϕ, $\tilde{\phi}$	0	1	1	2
D^μ	1	0	1	2
$B^{\mu\nu}$, $G^{\mu\nu}$, $W^{I\mu\nu}$	2	0	2	4
Effective operator	even	even	D	D+even number

Table A.1: The numbers of Lorentz and SU(2) indices, and the dimensions, of the fields and the operator.

Appendix B

Dimension-six Corrections to Gauge Boson Self-Energies

Here we give Π_{XY} for all 9 operators. The following expressions are obtained assuming only one operator is present at a time. The coefficient C_i is set to one.

- $O_{\phi q}^{(3)}$

$$\begin{aligned}
\Pi_{WW} &= -N_c \frac{g^2}{4\pi^2}\frac{v^2}{\Lambda^2}\left[\left(\frac{1}{6}q^2 - \frac{1}{4}(m_t^2+m_b^2)\right)E\right. \\
&\quad \left. -q^2 b_2(m_t^2,m_b^2,q^2) + \frac{1}{2}\left(m_b^2 b_1(m_t^2,m_b^2,q^2) + m_t^2 b_1(m_b^2,m_t^2,q^2)\right)\right] \qquad \text{(B.1)} \\
\Pi_{ZZ} &= -N_c \frac{g^2}{\cos^2\theta_W}\frac{1}{4\pi^2}\frac{v^2}{\Lambda^2}\left[\left(\frac{1}{6}(1-\sin^2\theta_W)q^2 - \frac{1}{4}(m_t^2+m_b^2)\right)E\right. \\
&\quad -q^2\left(\left(\frac{1}{2}-\frac{2}{3}\sin^2\theta_W\right)b_2(m_t^2,m_t^2,q^2) + \left(\frac{1}{2}-\frac{1}{3}\sin^2\theta_W\right)b_2(m_b^2,m_b^2,q^2)\right) \\
&\quad \left. +\frac{1}{4}\left(m_t^2 b_0(m_t^2,m_t^2,q^2) + m_b^2 b_0(m_b^2,m_b^2,q^2)\right)\right] \qquad \text{(B.2)} \\
\Pi_{\gamma\gamma} &= 0 \qquad \text{(B.3)} \\
\Pi_{\gamma Z} &= -N_c g^2 \frac{\sin\theta_W}{\cos\theta_W}\frac{1}{8\pi^2}\frac{v^2}{\Lambda^2}\left[\frac{1}{6}E - \frac{2}{3}b_2(m_t^2,m_t^2,q^2) - \frac{1}{3}b_2(m_b^2,m_b^2,q^2)\right]q^2 \qquad \text{(B.4)}
\end{aligned}$$

- $O_{\phi q}^{(1)}$

$$\begin{aligned}
\Pi_{WW} &= 0 \qquad \text{(B.5)} \\
\Pi_{ZZ} &= N_c \frac{g^2}{\cos^2\theta_W}\frac{1}{4\pi^2}\frac{v^2}{\Lambda^2}\left[-\left(\frac{1}{4}m_t^2 - \frac{1}{4}m_b^2 + \frac{1}{18}q^2\sin^2\theta_W\right)E\right. \\
&\quad -q^2\left(\left(\frac{1}{2}-\frac{2}{3}\sin^2\theta_W\right)b_2(m_t^2,m_t^2,q^2) - \left(\frac{1}{2}-\frac{1}{3}\sin^2\theta_W\right)b_2(m_b^2,m_b^2,q^2)\right) \\
&\quad \left. +\frac{1}{4}\left(m_t^2 b_0(m_t^2,m_t^2,q^2) - m_b^2 b_0(m_b^2,m_b^2,q^2)\right)\right] \qquad \text{(B.6)} \\
\Pi_{\gamma\gamma} &= 0 \qquad \text{(B.7)} \\
\Pi_{\gamma Z} &= N_c g^2 \frac{\sin\theta_W}{\cos\theta_W}\frac{1}{8\pi^2}\frac{v^2}{\Lambda^2}\left[\frac{1}{18}E - \frac{2}{3}b_2(m_t^2,m_t^2,q^2) + \frac{1}{3}b_2(m_b^2,m_b^2,q^2)\right]q^2 \qquad \text{(B.8)}
\end{aligned}$$

- $O_{\phi t}$

$$\Pi_{WW} = 0 \tag{B.9}$$

$$\Pi_{ZZ} = N_c \frac{g^2}{\cos^2\theta_W}\frac{1}{4\pi^2}\frac{v^2}{\Lambda^2}\left[\left(\frac{1}{4}m_t^2 - \frac{1}{9}q^2\sin^2\theta_W\right)E - \left(\frac{1}{4}m_t^2 b_0(m_t^2,m_t^2,q^2) - \frac{2}{3}q^2\sin^2\theta_W b_2(m_t^2,m_t^2,q^2)\right)\right] \tag{B.10}$$

$$\Pi_{\gamma\gamma} = 0 \tag{B.11}$$

$$\Pi_{\gamma Z} = N_c g^2 \frac{\sin\theta_W}{\cos\theta_W}\frac{1}{12\pi^2}\frac{v^2}{\Lambda^2}\left(\frac{1}{6}E - b_2(m_t^2,m_t^2,q^2)\right)q^2 \tag{B.12}$$

- $O_{\phi b}$

$$\Pi_{WW} = 0 \tag{B.13}$$

$$\Pi_{ZZ} = N_c \frac{g^2}{\cos^2\theta_W}\frac{1}{4\pi^2}\frac{v^2}{\Lambda^2}\left[-\left(\frac{1}{4}m_b^2 - \frac{1}{18}q^2\sin^2\theta_W\right)E + \left(\frac{1}{4}m_b^2 b_0(m_b^2,m_b^2,q^2) - \frac{1}{3}q^2\sin^2\theta_W b_2(m_b^2,m_b^2,q^2)\right)\right] \tag{B.14}$$

$$\Pi_{\gamma\gamma} = 0 \tag{B.15}$$

$$\Pi_{\gamma Z} = -N_c g^2 \frac{\sin\theta_W}{\cos\theta_W}\frac{1}{24\pi^2}\frac{v^2}{\Lambda^2}\left(\frac{1}{6}E - b_2(m_b^2,m_b^2,q^2)\right)q^2 \tag{B.16}$$

- $O_{\phi\phi}$

$$\Pi_{WW} = -N_c g^2 \frac{1}{16\pi^2}\frac{v^2}{\Lambda^2}m_t m_b\left(E - b_0(m_t^2,m_b^2,q^2)\right) \tag{B.17}$$

$$\Pi_{ZZ} = 0 \tag{B.18}$$

$$\Pi_{\gamma\gamma} = 0 \tag{B.19}$$

$$\Pi_{\gamma Z} = 0 \tag{B.20}$$

- O_{tW}

$$\Pi_{WW} = -N_c g \frac{\sqrt{2}}{4\pi^2}\frac{v m_t}{\Lambda^2}\left(\frac{1}{2}E - b_1(m_b^2,m_t^2,q^2)\right)q^2 \tag{B.21}$$

$$\Pi_{ZZ} = -N_c g \frac{\sqrt{2}}{4\pi^2}\frac{v m_t}{\Lambda^2}\left(\frac{1}{2} - \frac{4}{3}\sin^2\theta_W\right)\left(E - b_0(m_t^2,m_t^2,q^2)\right)q^2 \tag{B.22}$$

$$\Pi_{\gamma\gamma} = -N_c g \frac{\sqrt{2}}{4\pi^2}\frac{v m_t}{\Lambda^2}\frac{4}{3}\sin^2\theta_W\left(E - b_0(m_t^2,m_t^2,q^2)\right)q^2 \tag{B.23}$$

$$\Pi_{\gamma Z} = -N_c g \frac{\sqrt{2}}{4\pi^2}\frac{v m_t}{\Lambda^2}\frac{\sin\theta_W}{\cos\theta_W}\left(\frac{11}{12} - \frac{4}{3}\sin^2\theta_W\right)\left(E - b_0(m_t^2,m_t^2,q^2)\right)q^2 \tag{B.24}$$

- O_{bW}

$$\Pi_{WW} = -N_c g \frac{\sqrt{2}}{4\pi^2} \frac{v m_b}{\Lambda^2} \left(\frac{1}{2} E - b_1(m_t^2, m_b^2, q^2) \right) q^2 \tag{B.25}$$

$$\Pi_{ZZ} = -N_c g \frac{\sqrt{2}}{4\pi^2} \frac{v m_b}{\Lambda^2} \left(\frac{1}{2} - \frac{2}{3} \sin^2\theta_W \right) \left(E - b_0(m_b^2, m_b^2, q^2) \right) q^2 \tag{B.26}$$

$$\Pi_{\gamma\gamma} = -N_c g \frac{\sqrt{2}}{4\pi^2} \frac{v m_b}{\Lambda^2} \frac{2}{3} \sin^2\theta_W \left(E - b_0(m_b^2, m_b^2, q^2) \right) q^2 \tag{B.27}$$

$$\Pi_{\gamma Z} = -N_c g \frac{\sqrt{2}}{4\pi^2} \frac{v m_b}{\Lambda^2} \frac{\sin\theta_W}{\cos\theta_W} \left(\frac{7}{12} - \frac{2}{3} \sin^2\theta_W \right) \left(E - b_0(m_b^2, m_b^2, q^2) \right) q^2 \tag{B.28}$$

- O_{tB}

$$\Pi_{WW} = 0 \tag{B.29}$$

$$\Pi_{ZZ} = N_c g \frac{\sqrt{2}}{4\pi^2} \frac{v m_t}{\Lambda^2} \frac{\sin\theta_W}{\cos\theta_W} \left(\frac{1}{2} - \frac{4}{3} \sin^2\theta_W \right) \left(E - b_0(m_t^2, m_t^2, q^2) \right) q^2 \tag{B.30}$$

$$\Pi_{\gamma\gamma} = -N_c g \frac{\sqrt{2}}{4\pi^2} \frac{v m_t}{\Lambda^2} \frac{4}{3} \sin\theta_W \cos\theta_W \left(E - b_0(m_t^2, m_t^2, q^2) \right) q^2 \tag{B.31}$$

$$\Pi_{\gamma Z} = -N_c g \frac{\sqrt{2}}{4\pi^2} \frac{v m_t}{\Lambda^2} \left(\frac{1}{4} - \frac{4}{3} \sin^2\theta_W \right) \left(E - b_0(m_t^2, m_t^2, q^2) \right) q^2 \tag{B.32}$$

- O_{bB}

$$\Pi_{WW} = 0 \tag{B.33}$$

$$\Pi_{ZZ} = -N_c g \frac{\sqrt{2}}{4\pi^2} \frac{v m_b}{\Lambda^2} \frac{\sin\theta_W}{\cos\theta_W} \left(\frac{1}{2} - \frac{2}{3} \sin^2\theta_W \right) \left(E - b_0(m_b^2, m_b^2, q^2) \right) q^2 \tag{B.34}$$

$$\Pi_{\gamma\gamma} = N_c g \frac{\sqrt{2}}{4\pi^2} \frac{v m_b}{\Lambda^2} \frac{2}{3} \sin\theta_W \cos\theta_W \left(E - b_0(m_b^2, m_b^2, q^2) \right) q^2 \tag{B.35}$$

$$\Pi_{\gamma Z} = N_c g \frac{\sqrt{2}}{4\pi^2} \frac{v m_b}{\Lambda^2} \left(\frac{1}{4} - \frac{2}{3} \sin^2\theta_W \right) \left(E - b_0(m_b^2, m_b^2, q^2) \right) q^2 \tag{B.36}$$

Here θ_W is the weak angle, $N_c = 3$ is the number of colors. $E = \frac{2}{4-d} - \gamma + \ln 4\pi$, and the functions b_i are given by

$$b_0(m_1^2, m_2^2, q^2) = \int_0^1 \ln \frac{(1-x)m_1^2 + x m_2^2 - x(1-x)q^2}{M^2} dx, \tag{B.37}$$

$$b_1(m_1^2, m_2^2, q^2) = \int_0^1 x \ln \frac{(1-x)m_1^2 + x m_2^2 - x(1-x)q^2}{M^2} dx, \tag{B.38}$$

$$b_2(m_1^2, m_2^2, q^2) = \int_0^1 x(1-x) \ln \frac{(1-x)m_1^2 + x m_2^2 - x(1-x)q^2}{M^2} dx, \tag{B.39}$$

where M is the 't Hooft mass. They have the following analytical expressions:

$$b_0(m_1^2, m_2^2, q^2) = -2 + \log\frac{m_1 m_2}{M^2} + \frac{m_1^2 - m_2^2}{q^2}\log\left(\frac{m_1}{m_2}\right) + \frac{1}{q^2}\sqrt{|(m_1+m_2)^2 - q^2||(m_1-m_2)^2 - q^2|}f(m_1^2, m_2^2, q^2), \tag{B.40}$$

where

$$f(m_1^2, m_2^2, q^2) = \begin{cases} \log\frac{\sqrt{(m_1+m_2)^2-q^2}-\sqrt{(m_1-m_2)^2-q^2}}{\sqrt{(m_1+m_2)^2-q^2}+\sqrt{(m_1-m_2)^2-q^2}} & q^2 \le (m_1-m_2)^2 \\ 2\arctan\sqrt{\frac{q^2-(m_1-m_2)^2}{(m_1+m_2)^2-q^2}} & (m_1-m_2)^2 < q^2 < (m_1+m_2)^2 \\ \log\frac{\sqrt{q^2-(m_1-m_2)^2}+\sqrt{q^2-(m_1+m_2)^2}}{\sqrt{q^2-(m_1-m_2)^2}-\sqrt{q^2-(m_1+m_2)^2}} & q^2 \ge (m_1+m_2)^2 \end{cases}, \tag{B.41}$$

and

$$b_1(m_1^2, m_2^2, q^2) = -\frac{1}{2}\left[\frac{m_1^2}{q^2}\left(\log\frac{m_1^2}{M^2} - 1\right) - \frac{m_2^2}{q^2}\left(\log\frac{m_2^2}{M^2} - 1\right)\right] + \frac{1}{2}\frac{m_1^2 - m_2^2 + q^2}{q^2}b_0(m_1, m_2, q), \tag{B.42}$$

$$b_2(m_1^2, m_2^2, q^2) = \frac{1}{18} + \frac{1}{6}\left[\frac{m_1^2(2m_1^2 - 2m_2^2 - q^2)}{(q^2)^2}\log\frac{m_1^2}{M^2} + \frac{m_2^2(2m_2^2 - 2m_1^2 - q^2)}{(q^2)^2}\log\frac{m_2^2}{M^2}\right] - \frac{1}{3}\left(\frac{m_1^2 - m_2^2}{q^2}\right)^2 - \frac{1}{6}\left[2\left(\frac{m_1^2 - m_2^2}{q^2}\right)^2 - \left(\frac{m_1^2 + m_2^2 + q^2}{q^2}\right)\right]b_0(m_1, m_2, q). \tag{B.43}$$

Appendix C

Matrix M_{ij} and the Best Fit Values $\hat{C}_i$

The matrix M_{ij} and the best fit values $\hat{C}_i$ in Eq. (4.95) are given by

$$M = \frac{(1\ \mathrm{TeV}^4)}{\Lambda^4} \times 10^{-2} \times$$

	C_{WB}	$C_\phi^{(3)}$	$C_{\phi q}^{(3)}$	$C_{\phi q}^{(1)}$	$C_{\phi t}$	$C_{\phi b}$	C_{tW}	C_{bW}	C_{tB}	C_{bB}
O_{WB}	$+1.10e7$	$+3.06e6$	$-3.16e5$	$+5.47e4$	$-2.70e5$	$-6.16e3$	$-1.35e5$	$+3.11e3$	$-1.71e5$	$-1.40e4$
$O_\phi^{(3)}$	$+3.06e6$	$+1.06e6$	$-1.40e5$	$-1.03e4$	$-9.49e4$	$+9.46e3$	$-3.39e4$	$+4.04e2$	$-4.77e4$	$-3.85e3$
$O_{\phi q}^{(3)}$	$-3.16e5$	$-1.40e5$	$+2.58e5$	$+2.40e5$	$+1.28e4$	$-4.55e4$	$+3.99e3$	$-4.49e1$	$+4.96e3$	$+4.35e2$
$O_{\phi q}^{(1)}$	$+5.47e4$	$-1.03e4$	$+2.40e5$	$+2.39e5$	$+1.16e3$	$-4.42e4$	$-1.28e2$	$+3.21e0$	$-8.20e2$	$-3.34e1$
$O_{\phi t}$	$-2.70e5$	$-9.49e4$	$+1.28e4$	$+1.16e3$	$+8.49e3$	$-9.17e2$	$+2.98e3$	$-3.34e1$	$+4.21e3$	$+3.40e2$
$O_{\phi b}$	$-6.16e3$	$+9.46e3$	$-4.55e4$	$-4.42e4$	$-9.17e2$	$+9.83e3$	$+1.13e2$	$-1.46e1$	$+9.24e1$	$+3.20e0$
O_{tW}	$-1.35e5$	$-3.39e4$	$+3.99e3$	$-1.28e2$	$+2.98e3$	$+1.13e2$	$+1.78e3$	$-5.16e1$	$+2.11e3$	$+1.76e2$
O_{bW}	$+3.11e3$	$+4.04e2$	$-4.49e1$	$+3.21e0$	$-3.34e1$	$-1.46e1$	$-5.16e1$	$+2.49e0$	$-4.89e1$	$-4.42e0$
O_{tB}	$-1.71e5$	$-4.77e4$	$+4.96e3$	$-8.20e2$	$+4.21e3$	$+9.24e1$	$+2.11e3$	$-4.89e1$	$+2.67e3$	$+2.19e2$
O_{bB}	$-1.40e4$	$-3.85e3$	$+4.35e2$	$-3.34e1$	$+3.40e2$	$+3.20e0$	$+1.76e2$	$-4.42e0$	$+2.19e2$	$+1.82e1$

(C.1)

and

C_i	C_{WB}	$C_\phi^{(3)}$	$C_{\phi q}^{(3)}$	$C_{\phi q}^{(1)}$	$C_{\phi t}$	$C_{\phi b}$	C_{tW}	C_{bW}	C_{tB}	C_{bB}
$\hat{C}_i$	$+0.74$	-1.12	-556	$+556$	$+761$	-0.60	$+121$	$+57.2$	-64.5	$+62.8$

(C.2)

The numerical values of $\hat{C}_i$ depends on both the experimental values and the SM predictions. The matrix M is symmetric and positive definite, and its value only depends on the errors of different measurements. If any of the SM input parameters changes, the best values $\hat{C}_i$ will be affected, but the matrix M will not. The sizes of the one-sigma bounds on the operators only depend on matrix M.

References

[1] S. Weinberg, Physica A **96**, 327 (1979).

[2] S. Weinberg, Rev. Mod. Phys. **52**, 515 (1980) [Science **210**, 1212 (1980)].

[3] J. Gomis and S. Weinberg, Nucl. Phys. B **469**, 473 (1996) [arXiv:hep-th/9510087].

[4] H. Georgi, Ann. Rev. Nucl. Part. Sci. **43**, 209-252 (1993).

[5] S. Weinberg, Phys. Rev. Lett. **43**, 1566 (1979).

[6] W. Buchmuller and D. Wyler, Nucl. Phys. B **268**, 621 (1986).

[7] C. N. Leung, S. T. Love and S. Rao, Z. Phys. C **31**, 433 (1986).

[8] C. Arzt, M. B. Einhorn and J. Wudka, Nucl. Phys. B **433**, 41 (1995) [arXiv:hep-ph/9405214].

[9] B. Grzadkowski, Z. Hioki, K. Ohkuma and J. Wudka, Nucl. Phys. B **689**, 108 (2004) [arXiv:hep-ph/0310159].

[10] J. A. Aguilar-Saavedra, Nucl. Phys. B **812**, 181 (2009) [arXiv:0811.3842 [hep-ph]].

[11] B. Grzadkowski, M. Iskrzynski, M. Misiak and J. Rosiek, JHEP **1010**, 085 (2010) [arXiv:1008.4884 [hep-ph]].

[12] J. A. Aguilar-Saavedra, Nucl. Phys. **B843**, 638-672 (2011). [arXiv:1008.3562 [hep-ph]].

[13] C. Zhang, S. Willenbrock, Phys. Rev. **D83**, 034006 (2011). [arXiv:1008.3869 [hep-ph]].

[14] G. A. Ladinsky and C. P. Yuan, Phys. Rev. D **49**, 4415 (1994) [arXiv:hep-ph/9211272].

[15] L. Brzezinski, B. Grzadkowski and Z. Hioki, Int. J. Mod. Phys. A **14**, 1261 (1999) [arXiv:hep-ph/9710358];

B. Grzadkowski and Z. Hioki, Phys. Rev. D **61**, 014013 (1999) [arXiv:hep-ph/9805318]; Phys. Lett. B **476**, 87 (2000) [arXiv:hep-ph/9911505].

[16] B. Grzadkowski, Acta Phys. Polon. B **27**, 921 (1996) [arXiv:hep-ph/9511279];

B. Grzadkowski, Z. Hioki and M. Szafranski, Phys. Rev. D **58**, 035002 (1998) [arXiv:hep-ph/9712357].

[17] B. Grzadkowski, Z. Hioki, K. Ohkuma and J. Wudka, Phys. Lett. B **593**, 189 (2004) [arXiv:hep-ph/0403174]; JHEP **0511**, 029 (2005) [arXiv:hep-ph/0508183].

[18] D. Atwood, S. Bar-Shalom, G. Eilam and A. Soni, Phys. Rept. **347**, 1 (2001) [arXiv:hep-ph/0006032].

[19] C. Amsler *et al.* [Particle Data Group], Phys. Lett. B **667**, 1 (2008).

[20] G. L. Kane, G. A. Ladinsky and C. P. Yuan, Phys. Rev. D **45**, 124 (1992).

[21] C. Zhang and S. Willenbrock, to appear in the Proceedings of the International Workshop on Top Quark Physics (top2010), Bruges, Belgium, May 31–June 4, 2010, arXiv:1008.3155 [hep-ph].

[22] J. A. Aguilar-Saavedra, J. Carvalho, N. F. Castro, F. Veloso and A. Onofre, Eur. Phys. J. C **50**, 519 (2007) [arXiv:hep-ph/0605190].

[23] J. A. Aguilar-Saavedra, J. Carvalho, N. F. Castro, A. Onofre and F. Veloso, Eur. Phys. J. C **53**, 689 (2008) [arXiv:0705.3041 [hep-ph]].

[24] M. Jezabek and J. H. Kuhn, Phys. Lett. B **329**, 317 (1994) [arXiv:hep-ph/9403366].

[25] M. Jezabek, Nucl. Phys. Proc. Suppl. **37B**, 197 (1994) [arXiv:hep-ph/9406411].

[26] B. Grzadkowski and Z. Hioki, Phys. Lett. B **557**, 55 (2003) [arXiv:hep-ph/0208079].

[27] S. Cortese and R. Petronzio, Phys. Lett. B **253**, 494 (1991).

[28] S. S. D. Willenbrock and D. A. Dicus, Phys. Rev. D **34**, 155 (1986).

[29] C. P. Yuan, Phys. Rev. D **41**, 42 (1990).

[30] R. K. Ellis and S. J. Parke, Phys. Rev. D **46**, 3785 (1992).

[31] A. Heinson, A. S. Belyaev and E. E. Boos, Phys. Rev. D **56**, 3114 (1997) [arXiv:hep-ph/9612424].

[32] Q. H. Cao, J. Wudka and C. P. Yuan, Phys. Lett. B **658**, 50 (2007) [arXiv:0704.2809 [hep-ph]].

[33] E. Boos, L. Dudko and T. Ohl, Eur. Phys. J. C **11**, 473 (1999) [arXiv:hep-ph/9903215].

[34] C. R. Chen, F. Larios and C. P. Yuan, Phys. Lett. B **631**, 126 (2005) [AIP Conf. Proc. **792**, 591 (2005)] [arXiv:hep-ph/0503040].

[35] J. A. Aguilar-Saavedra, Nucl. Phys. B **804**, 160 (2008) [arXiv:0803.3810 [hep-ph]].

[36] G. Mahlon and S. J. Parke, Phys. Rev. D **55**, 7249 (1997) [arXiv:hep-ph/9611367].

[37] P. L. Cho and E. H. Simmons, Phys. Rev. D **51**, 2360 (1995) [arXiv:hep-ph/9408206].

[38] K. Kumar, T. M. P. Tait and R. Vega-Morales, JHEP **0905**, 022 (2009) [arXiv:0901.3808 [hep-ph]].

[39] B. Lillie, J. Shu and T. M. P. Tait, JHEP **0804**, 087 (2008) [arXiv:0712.3057 [hep-ph]].

[40] A. V. Manohar and M. B. Wise, Phys. Lett. B **636**, 107 (2006) [arXiv:hep-ph/0601212].

[41] T. Aaltonen *et al.* [CDF Collaboration], Phys. Rev. Lett. **101**, 202001 (2008) [arXiv:0806.2472 [hep-ex]].

[42] G. Stricker *et al.* , CDF note **9724** (2009).

[43] The CDF Collaboration, CDF note **10224** (2010).

[44] V. M. Abazov *et al.* [D0 Collaboration], Phys. Rev. Lett. **100**, 142002 (2008) [arXiv:0712.0851 [hep-ex]].

[45] The D0 Collaboration, D0 Note **6062**-CONF (2010)

[46] J. H. Kuhn and G. Rodrigo, Phys. Rev. Lett. **81**, 49 (1998) [arXiv:hep-ph/9802268].

[47] J. H. Kuhn and G. Rodrigo, Phys. Rev. D **59**, 054017 (1999) [arXiv:hep-ph/9807420].

[48] M. T. Bowen, S. D. Ellis and D. Rainwater, Phys. Rev. D **73**, 014008 (2006) [arXiv:hep-ph/0509267].

[49] L. G. Almeida, G. F. Sterman and W. Vogelsang, Phys. Rev. D **78**, 014008 (2008) [arXiv:0805.1885 [hep-ph]].

[50] T. Aaltonen *et al.* , CDF note **9448** (2009).

[51] S. L. Glashow, J. Iliopoulos and L. Maiani, Phys. Rev. D **2**, 1285 (1970).

[52] G. Eilam, J. L. Hewett and A. Soni, Phys. Rev. D **44**, 1473 (1991) [Erratum-ibid. D **59**, 039901 (1999)].

[53] B. Grzadkowski, J. F. Gunion and P. Krawczyk, Phys. Lett. B **268**, 106 (1991).

[54] W. Bernreuther and A. Brandenburg, Phys. Rev. D **49**, 4481 (1994) [arXiv:hep-ph/9312210].

[55] G. Valencia and Y. Wang, Phys. Rev. D **73**, 053009 (2006) [arXiv:hep-ph/0512127].

[56] D. Atwood, A. Aeppli and A. Soni, Phys. Rev. Lett. **69**, 2754 (1992).

[57] O. Antipin and G. Valencia, Phys. Rev. D **79**, 013013 (2009) [arXiv:0807.1295 [hep-ph]].

[58] A. Brandenburg and J. P. Ma, Phys. Lett. B **298**, 211 (1993).

[59] B. Grzadkowski, B. Lampe and K. J. Abraham, Phys. Lett. B **415**, 193 (1997) [arXiv:hep-ph/9706489].

[60] D. Chang, W. Y. Keung and I. Phillips, Nucl. Phys. B **408**, 286 (1993) [Erratum-ibid. B **429**, 255 (1994)] [arXiv:hep-ph/9301259];

B. Grzadkowski and Z. Hioki, Nucl. Phys. B **484**, 17 (1997) [arXiv:hep-ph/9604301]; Phys. Lett. B **391**, 172 (1997) [arXiv:hep-ph/9608306];

J. M. Yang and B. L. Young, Phys. Rev. D **56**, 5907 (1997) [arXiv:hep-ph/9703463];

M. S. Baek, S. Y. Choi and C. S. Kim, Phys. Rev. D **56**, 6835 (1997) [arXiv:hep-ph/9704312];

A. Bartl, E. Christova, T. Gajdosik and W. Majerotto, Phys. Rev. D **58**, 074007 (1998) [arXiv:hep-ph/9802352].

[61] N. Greiner, S. Willenbrock, C. Zhang, Phys. Lett. **B704**, 218-222 (2011). [arXiv:1104.3122 [hep-ph]].

[62] J. A. Aguilar-Saavedra, PoS **ICHEP2010**, 378 (2010) [arXiv:1008.3225 [hep-ph]].

[63] [CDF Collaboration], CDF note 10333.

[64] V. M. Abazov *et al.* [D0 Collaboration], Phys. Rev. D **83**, 032009 (2011) [arXiv:1011.6549 [hep-ex]].

[65] A. Czarnecki, J. G. Korner and J. H. Piclum, Phys. Rev. D **81**, 111503 (2010) [arXiv:1005.2625 [hep-ph]].

[66] J. Drobnak, S. Fajfer and J. F. Kamenik, Phys. Rev. D **82**, 114008 (2010) [arXiv:1010.2402 [hep-ph]].

[67] M. E. Peskin and T. Takeuchi, Phys. Rev. Lett. **65**, 964 (1990).

[68] M. E. Peskin and T. Takeuchi, Phys. Rev. D **46**, 381 (1992).

[69] R. Barbieri, A. Pomarol, R. Rattazzi and A. Strumia, Nucl. Phys. B **703**, 127 (2004) [arXiv:hep-ph/0405040].

[70] A. Pomarol and J. Serra, Phys. Rev. D **78**, 074026 (2008) [arXiv:0806.3247 [hep-ph]].

[71] K. Nakamura *et al.* [Particle Data Group], J. Phys. G **37**, 075021 (2010), Section 10.7.

[72] B. Grinstein and M. B. Wise, Phys. Lett. B **265**, 326 (1991).

[73] [ALEPH Collaboration and DELPHI Collaboration and L3 Collaboration and OPAL Collaboration and SLD Collaboration and LEP Electroweak Working Group and SLD Electroweak Group and SLD Heavy Flavour Group], Phys. Rept. **427**, 257 (2006) [arXiv:hep-ex/0509008];

[74] J. Alcaraz *et al.* [ALEPH Collaboration and DELPHI Collaboration and L3 Collaboration and OPAL Collaboration and LEP Electroweak Working Group], arXiv:hep-ex/0612034.

[75] S. Schael *et al.* [ALEPH Collaboration], Eur. Phys. J. C **49**, 411 (2007) [arXiv:hep-ex/0609051].

[76] B. Grzadkowski and M. Misiak, Phys. Rev. D **78**, 077501 (2008) [arXiv:0802.1413 [hep-ph]].

[77] J. Drobnak, S. Fajfer and J. F. Kamenik, arXiv:1102.4347 [hep-ph].

[78] P. Achard *et al.* [L3 Collaboration], Phys. Lett. B **600**, 22 (2004) [arXiv:hep-ex/0409016].

[79] Z. Han and W. Skiba, Phys. Rev. D **71**, 075009 (2005) [arXiv:hep-ph/0412166].